Supplementary Material (ESI) for New Journal of Chemistry

SUPPORTING INFORMATION

Reversible Constitutional Switching between Macrocycles and Polymers Induced by Shape Change in a Dynamic Covalent System

Sébastien Ulrich, Eric Buhler, and Jean-Marie Lehn*

S. Ulrich, Pr. J.-M. Lehn
Laboratoire de Chimie Supramoléculaire
Institut de Science et d'Ingénierie Supramoléculaires (ISIS)
8 allée Gaspard Monge, 67083 Strasbourg (France)
Fax: (+33) 390-245-140
E-mail: lehn@isis.u-strasbg.fr

Pr. E. Buhler
Laboratoire Matière et Systèmes Complexes (MSC), UMR CNRS 7057
Université Paris Diderot-Paris 7
Bâtiment Condorcet, 75205 Paris cedex 13 (France)

2D NMR analyses of **1-Me**:

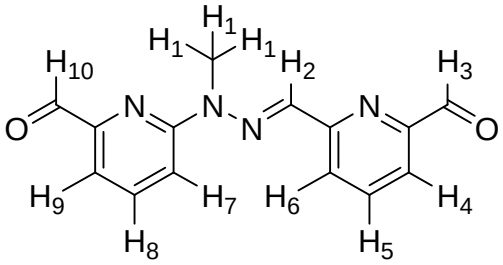

HSQC (500 MHz, $CDCl_3$*/CD_3CN: 6/4):

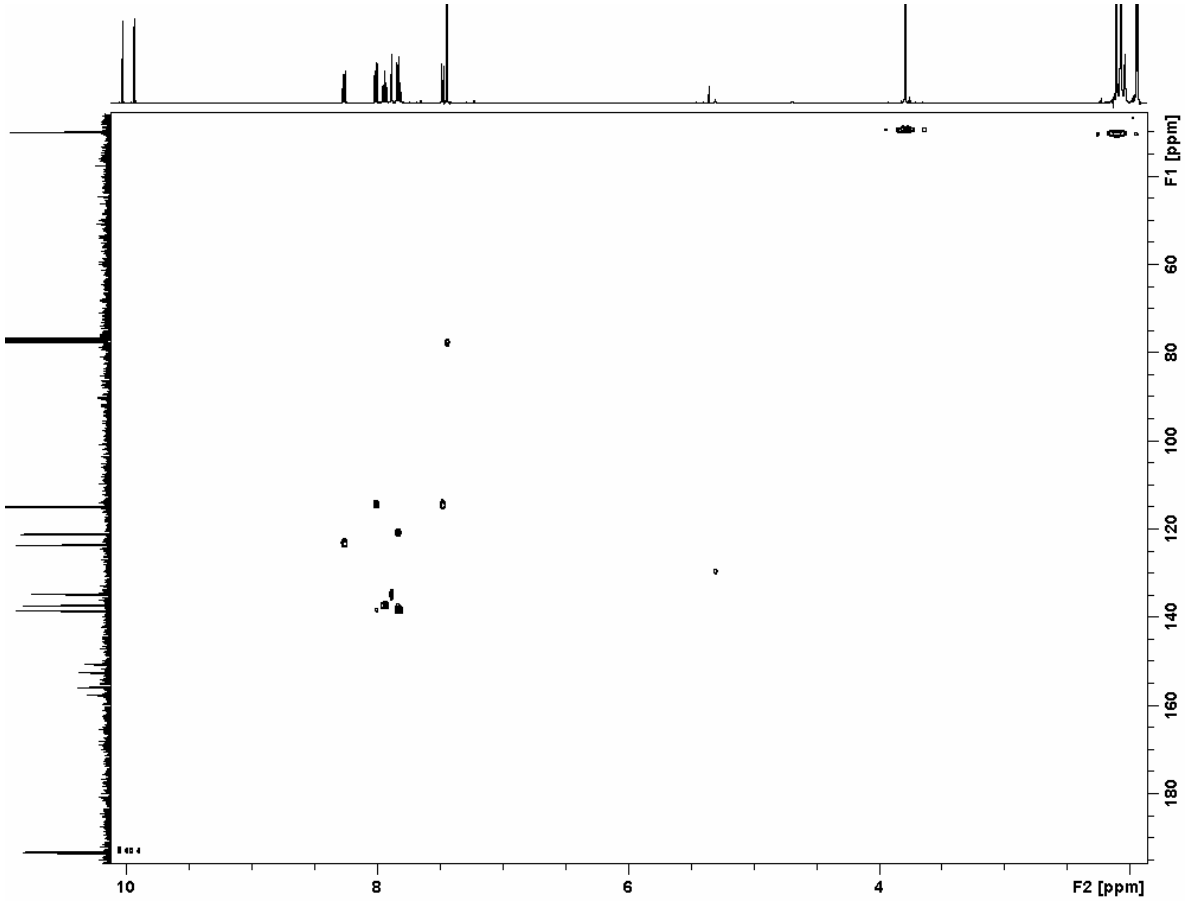

HMBC (500 MHz, $CDCl_3$*/CD_3CN: 6/4):

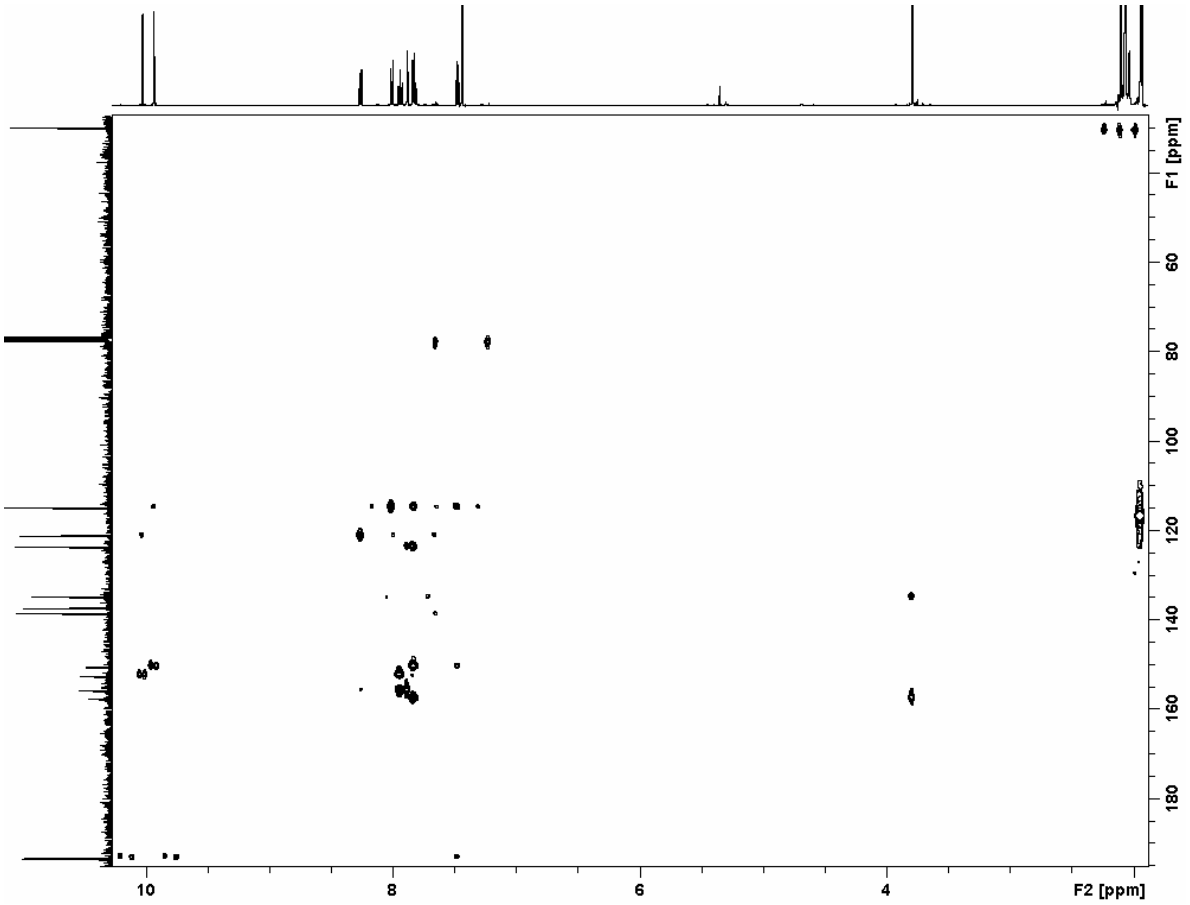

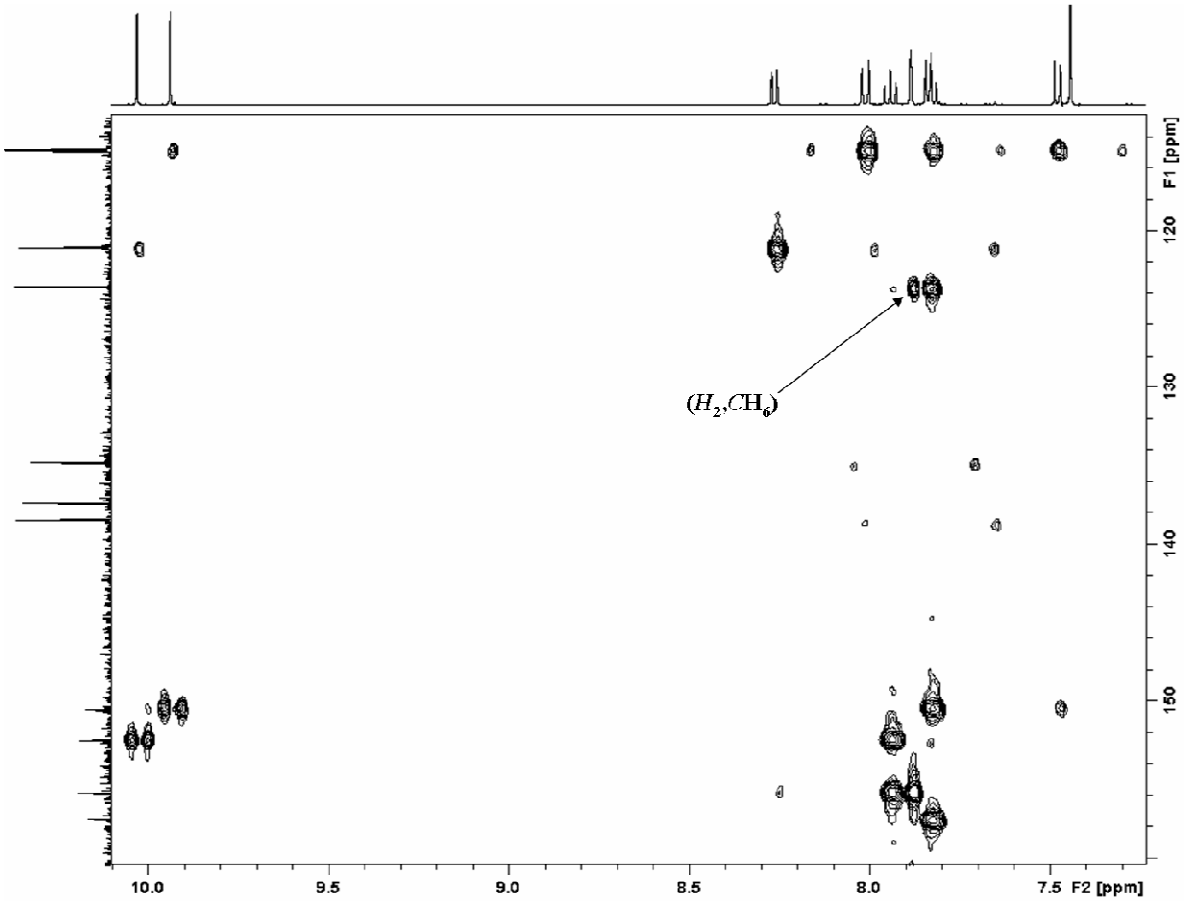

COSY (500 MHz, $CDCl_3$*/CD_3CN: 6/4):

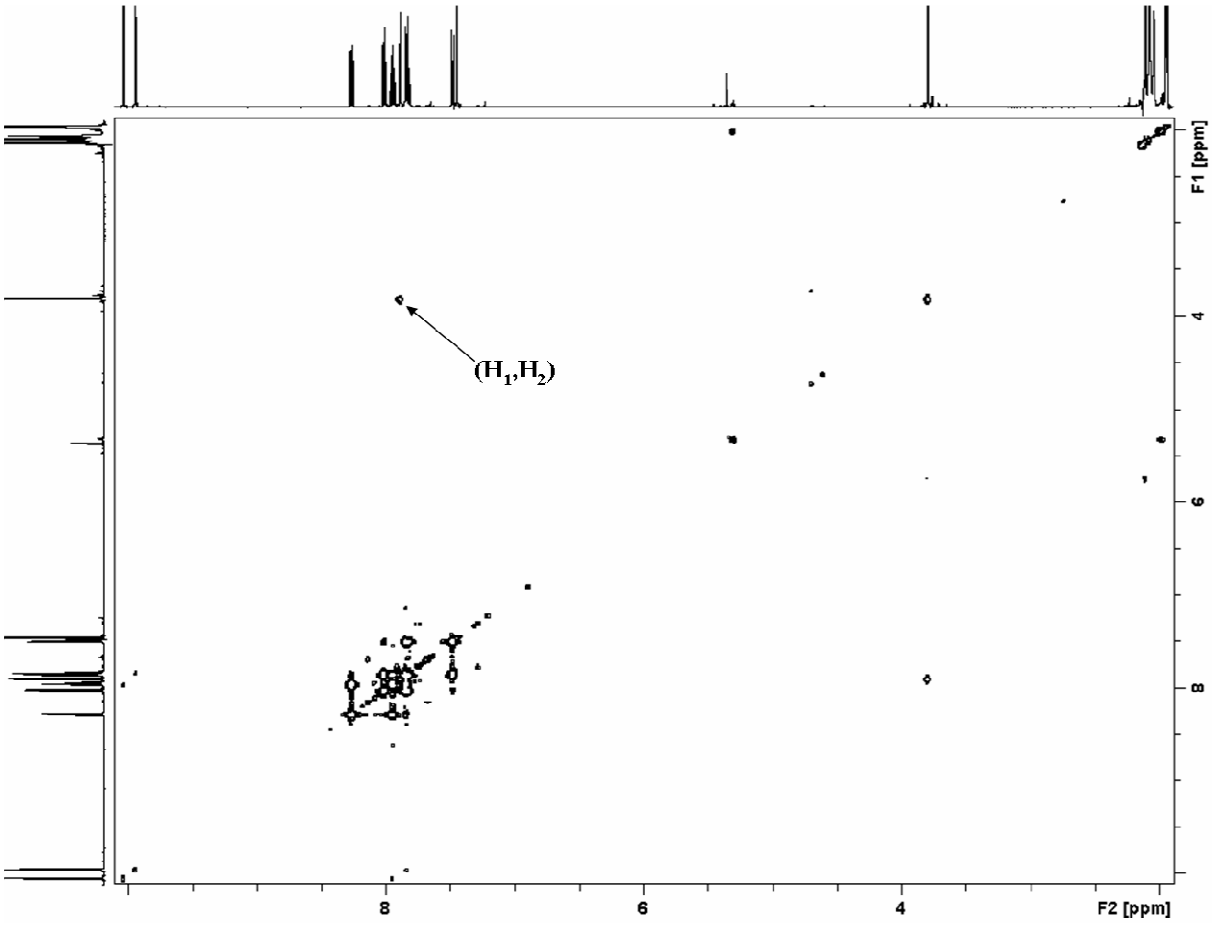

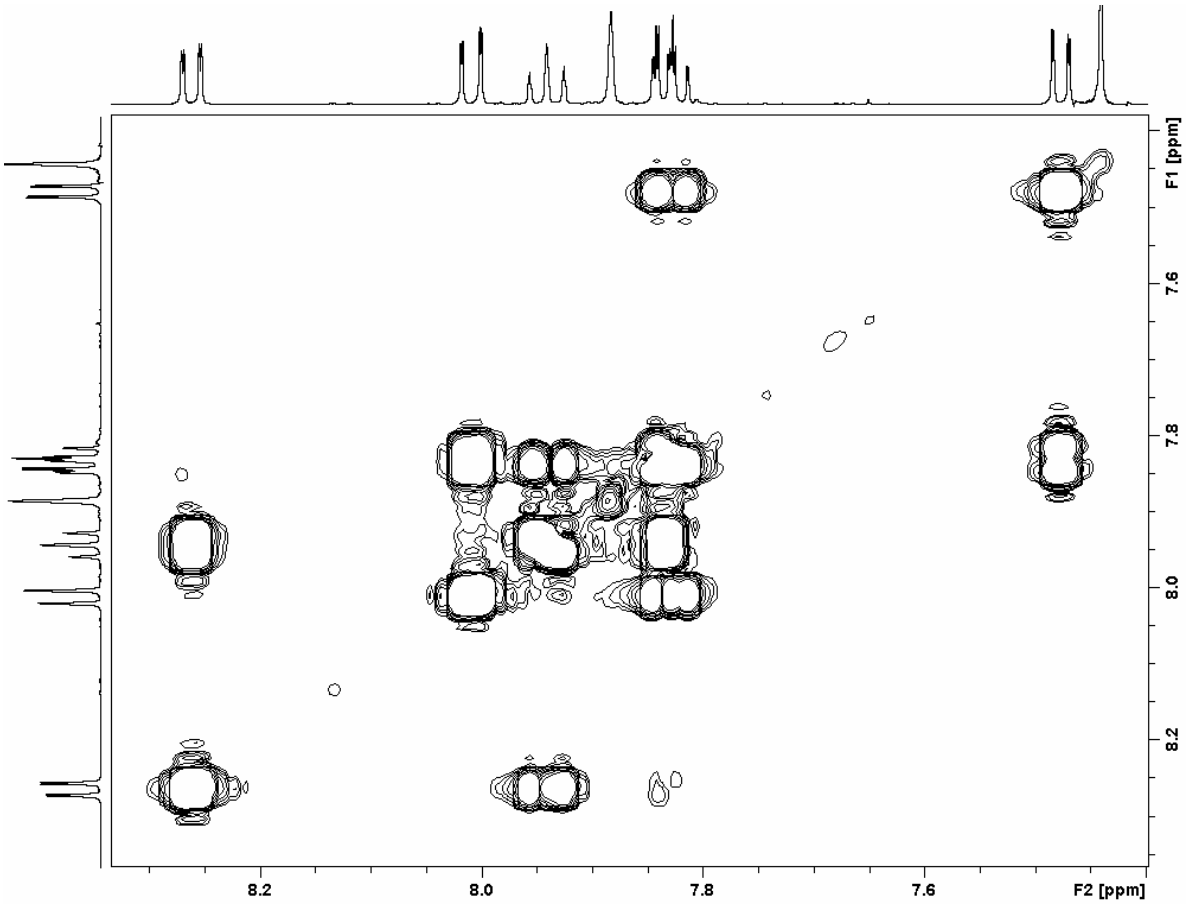

ROESY (500 MHz, $CDCl_3$*/CD_3CN: 6/4):

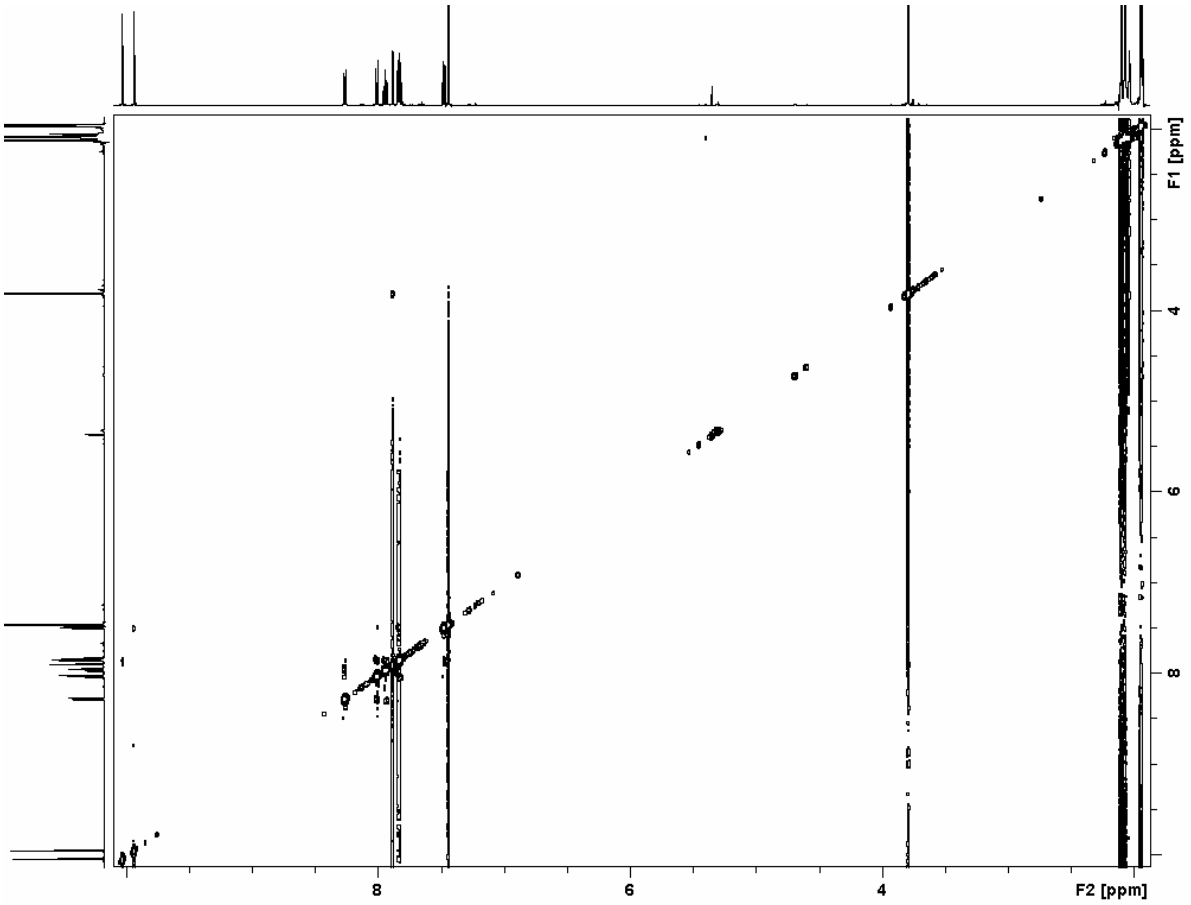

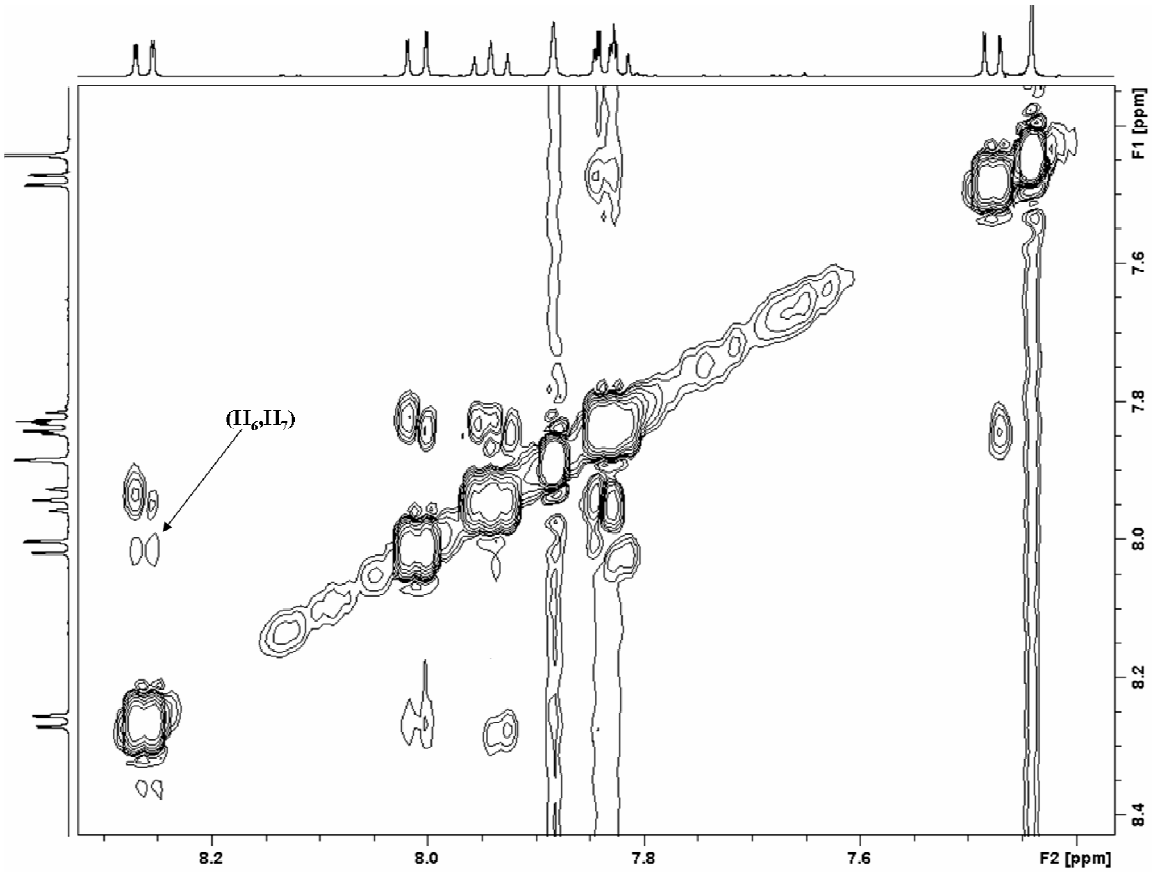

2D NMR analyses of **2**:

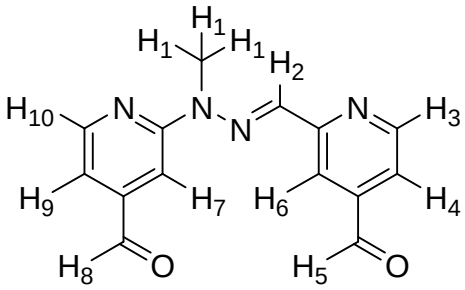

HSQC (500 MHz, $CDCl_3$*/CD_3CN: 6/4):

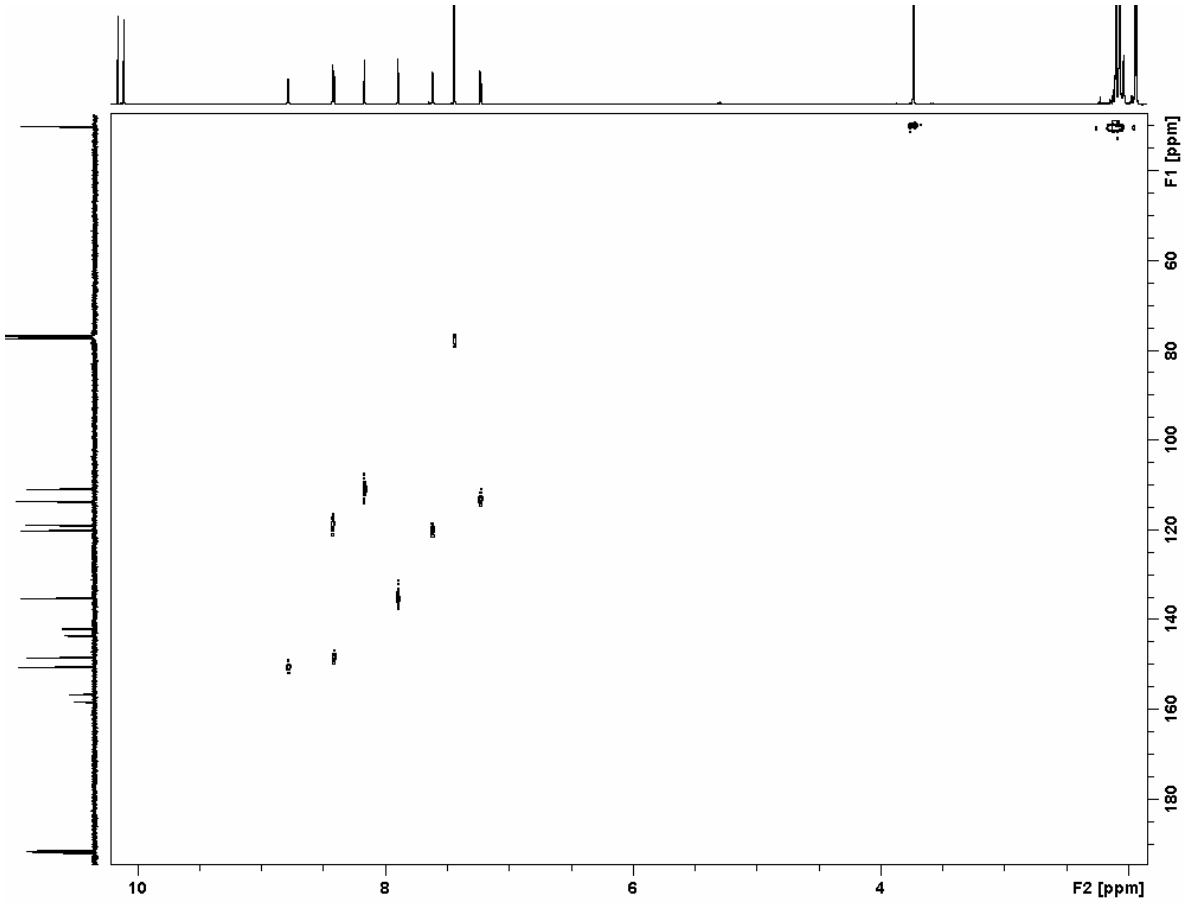

HMBC (500 MHz, $CDCl_3$*/CD_3CN: 6/4):

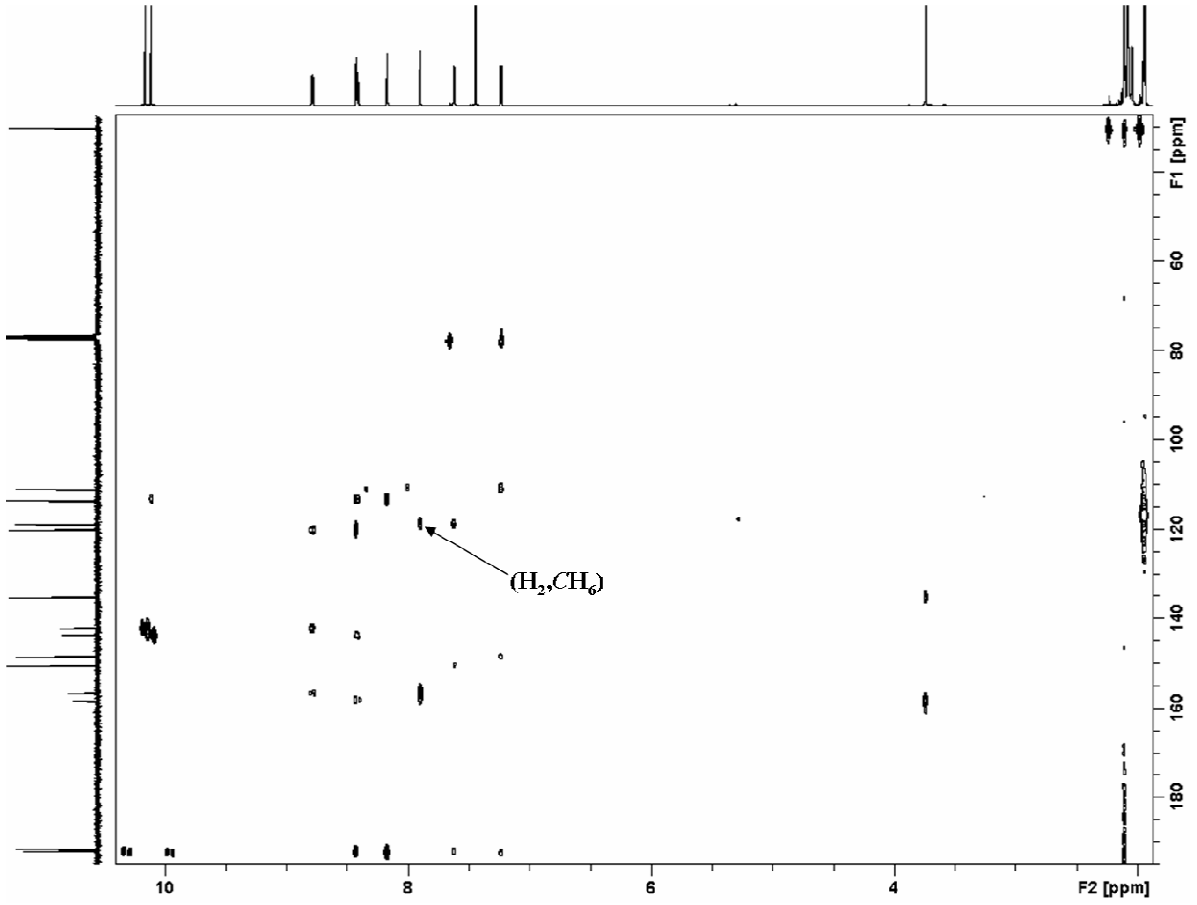

COSY (500 MHz, $CDCl_3$*/CD_3CN: 6/4):

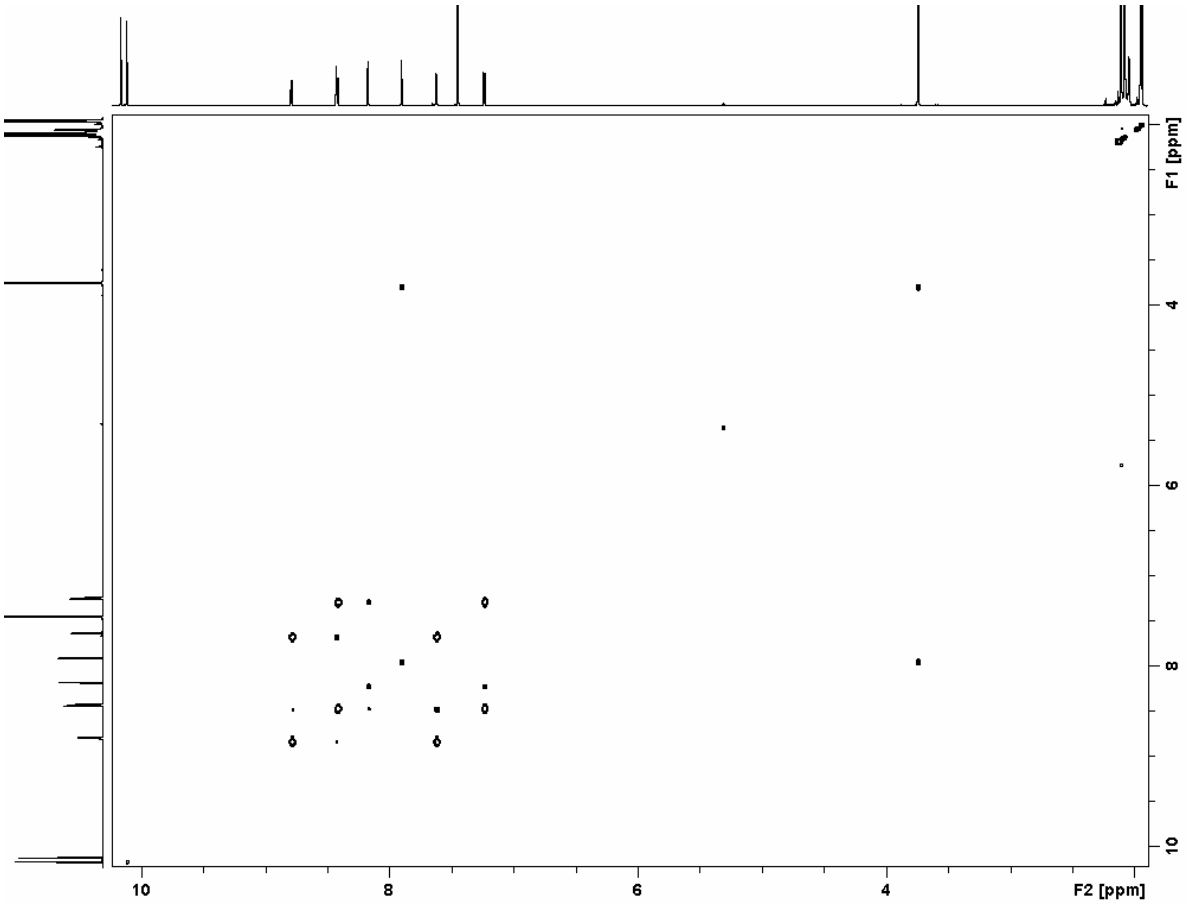

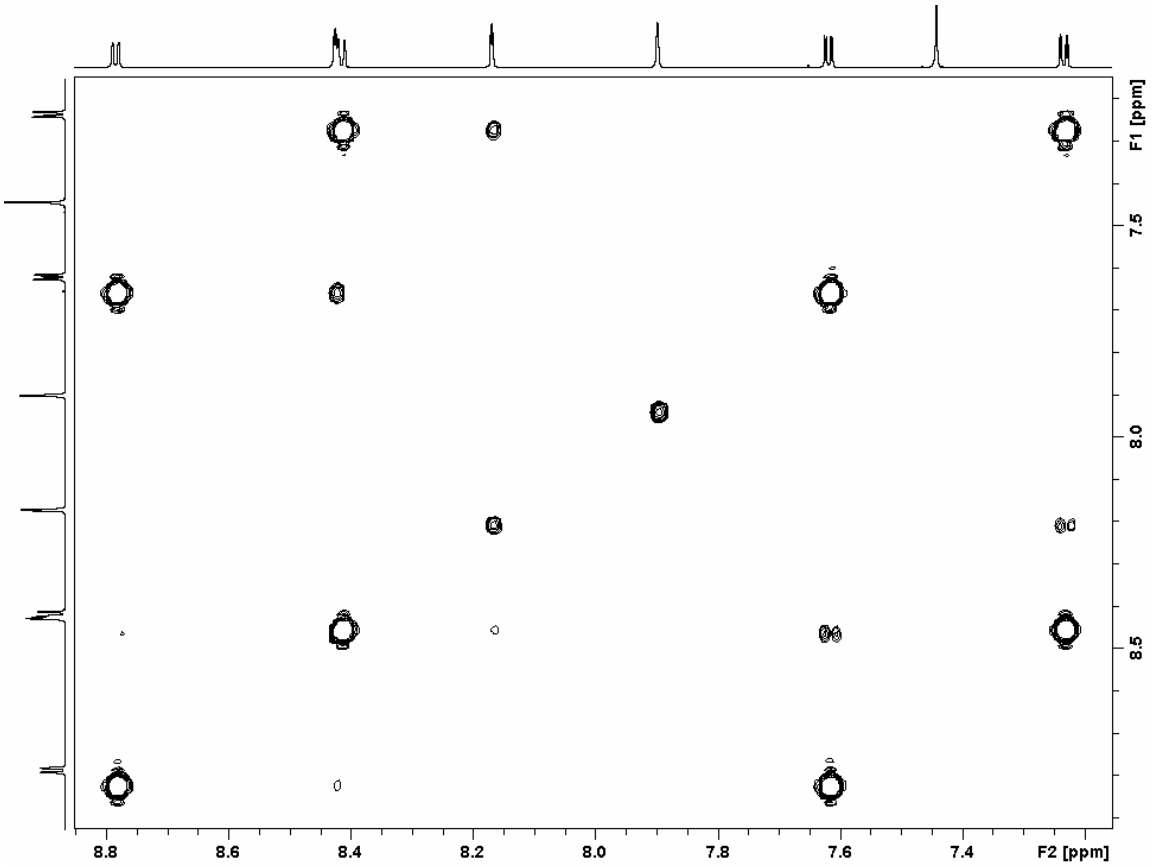

ROESY (500 MHz, $CDCl_3$*/CD_3CN: 6/4):

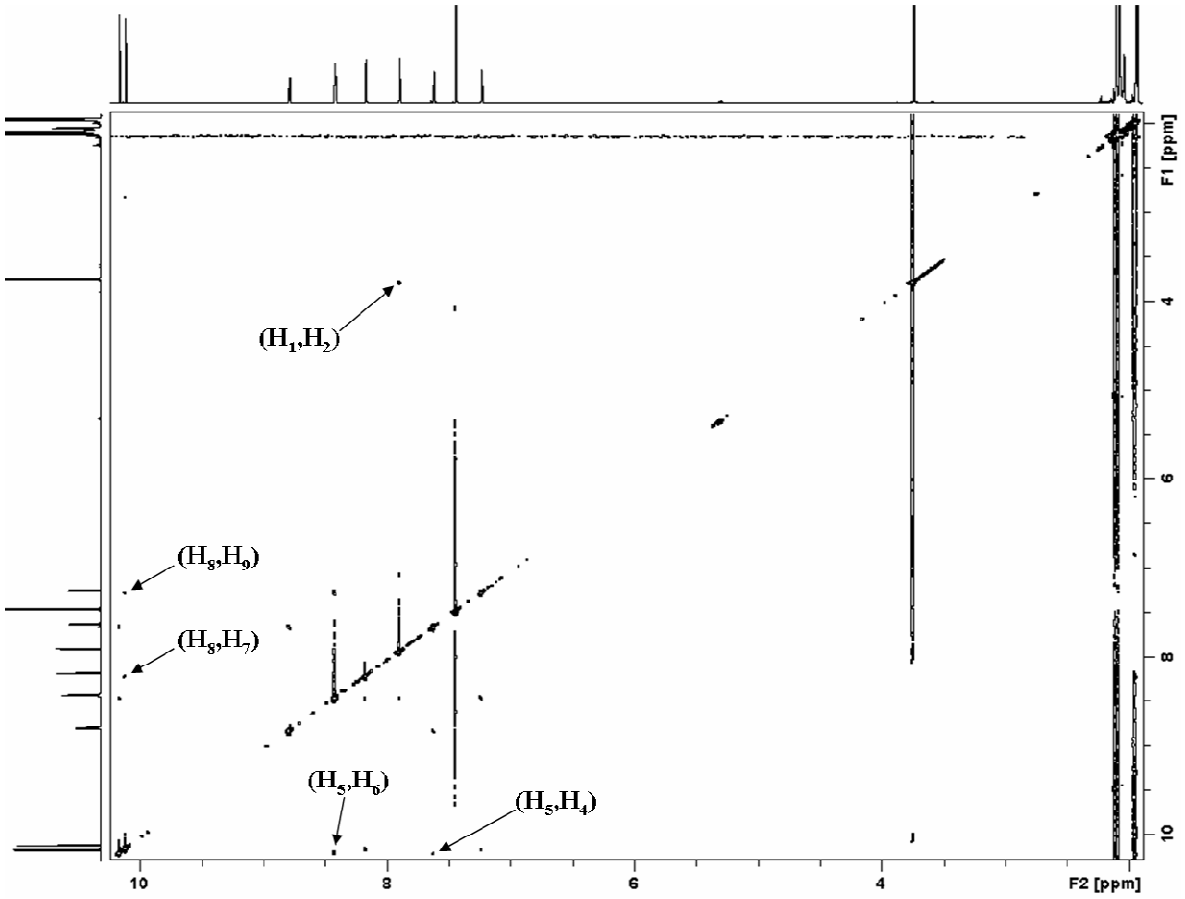

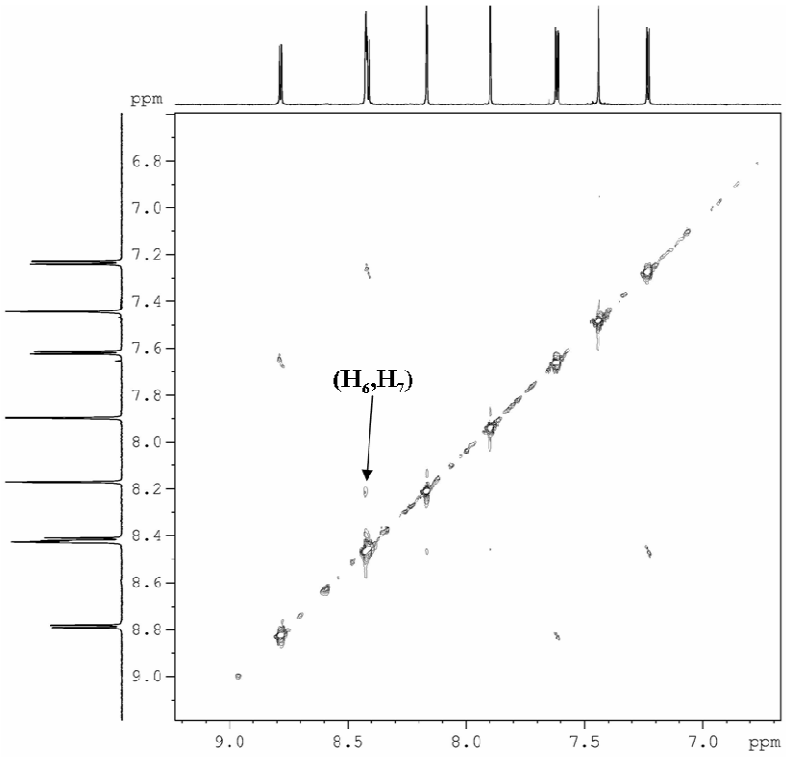

2D NMR analyses of **Zn.1-Me**:

COSY ($CDCl_3$*/CD_3CN: 6/4):

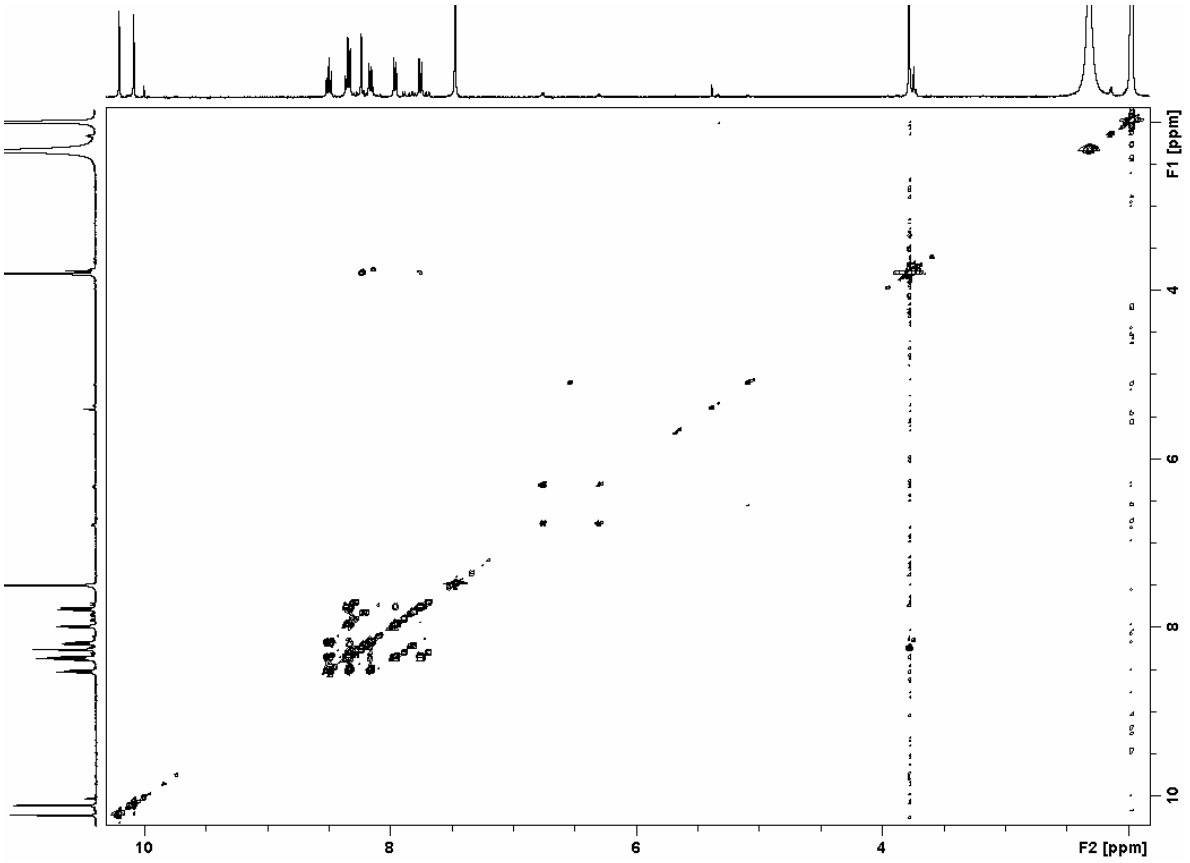

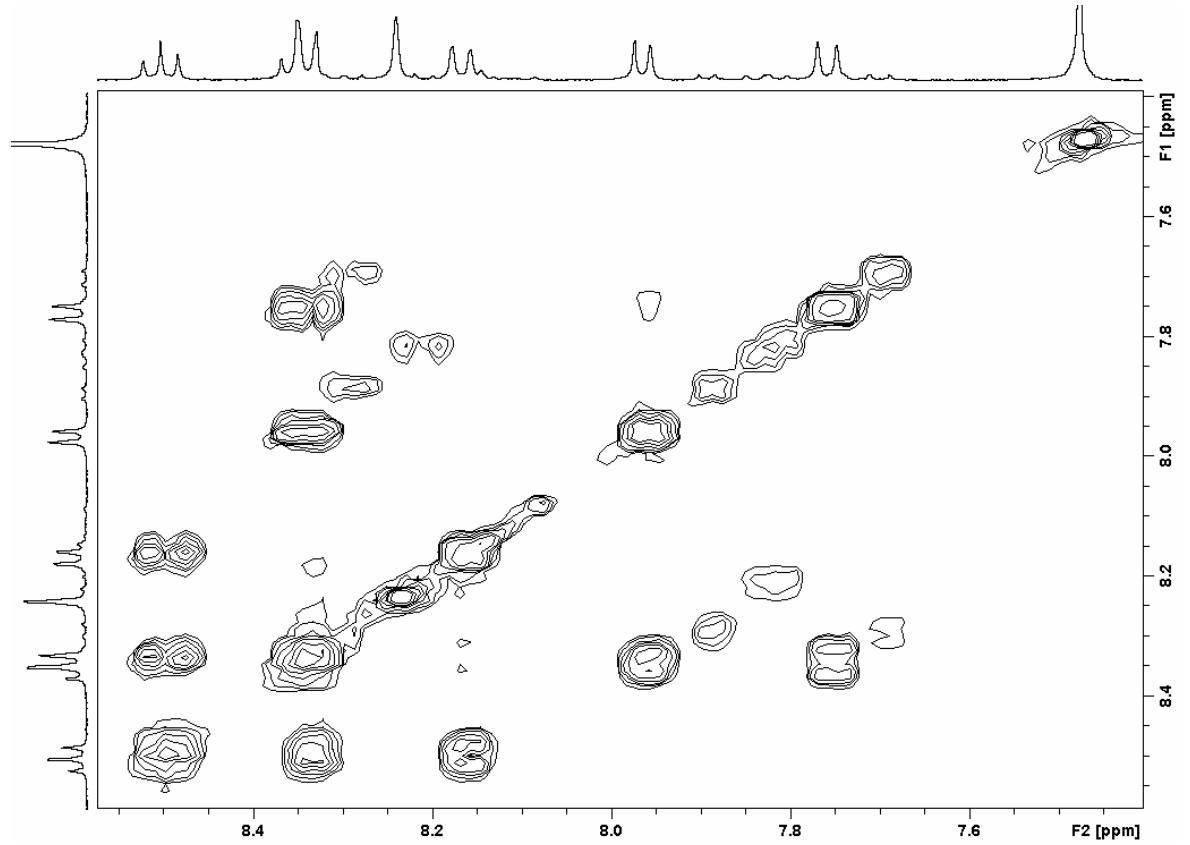

ROESY ($CDCl_3$*/CD_3CN: 6/4):

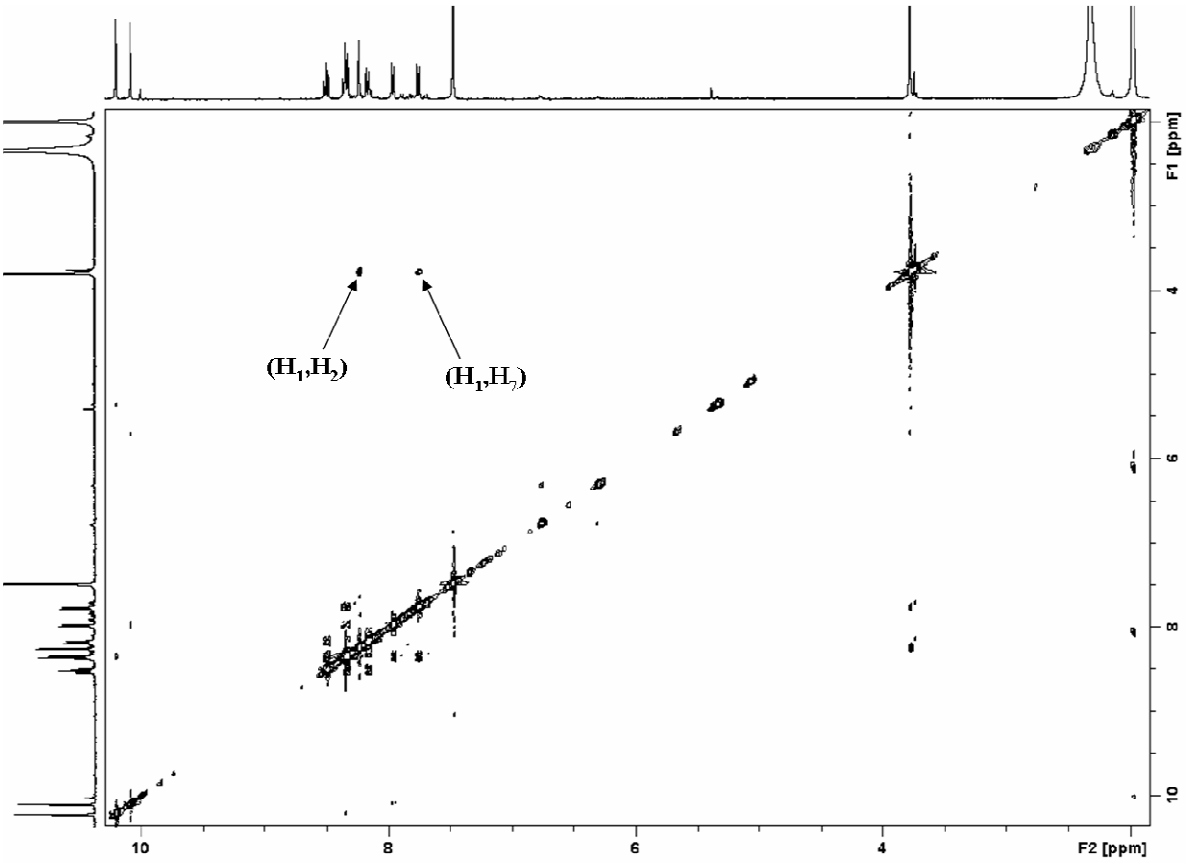

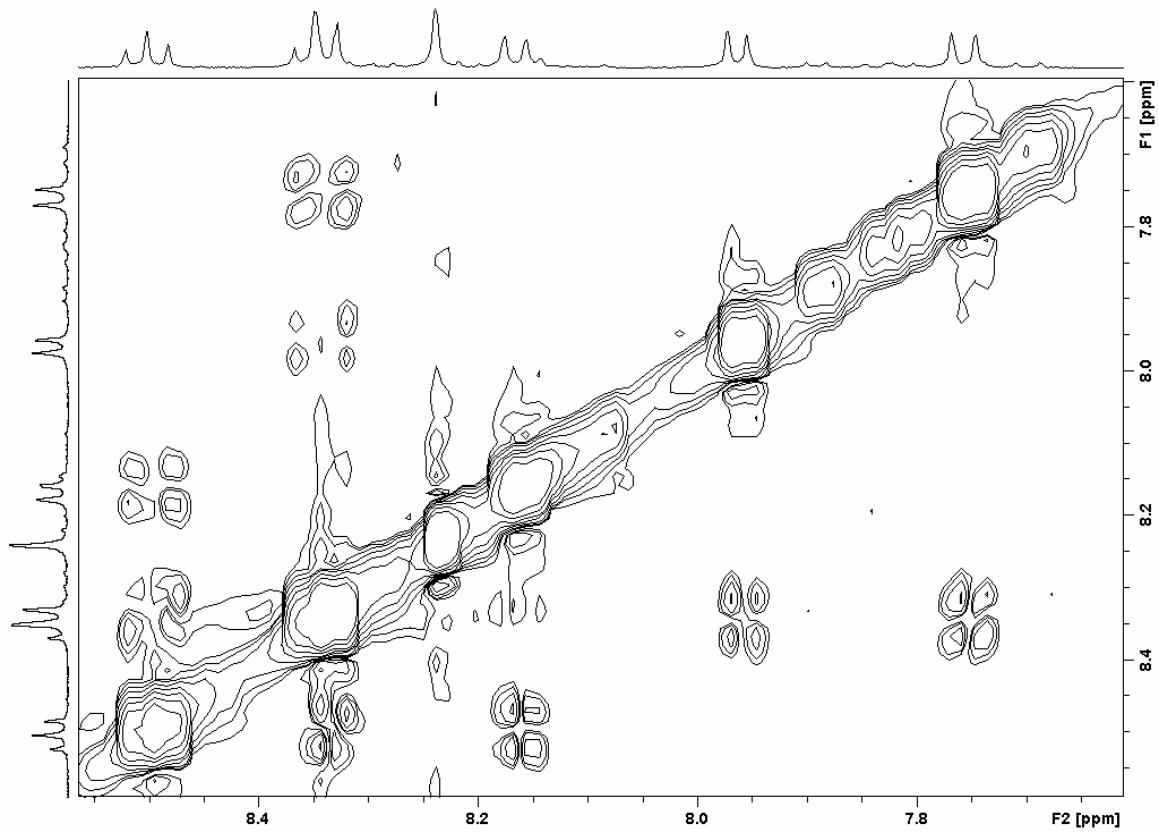

2D NMR analyses of **Zn.2**$_2$:

COSY ($CDCl_3$*/CD_3CN: 6/4):

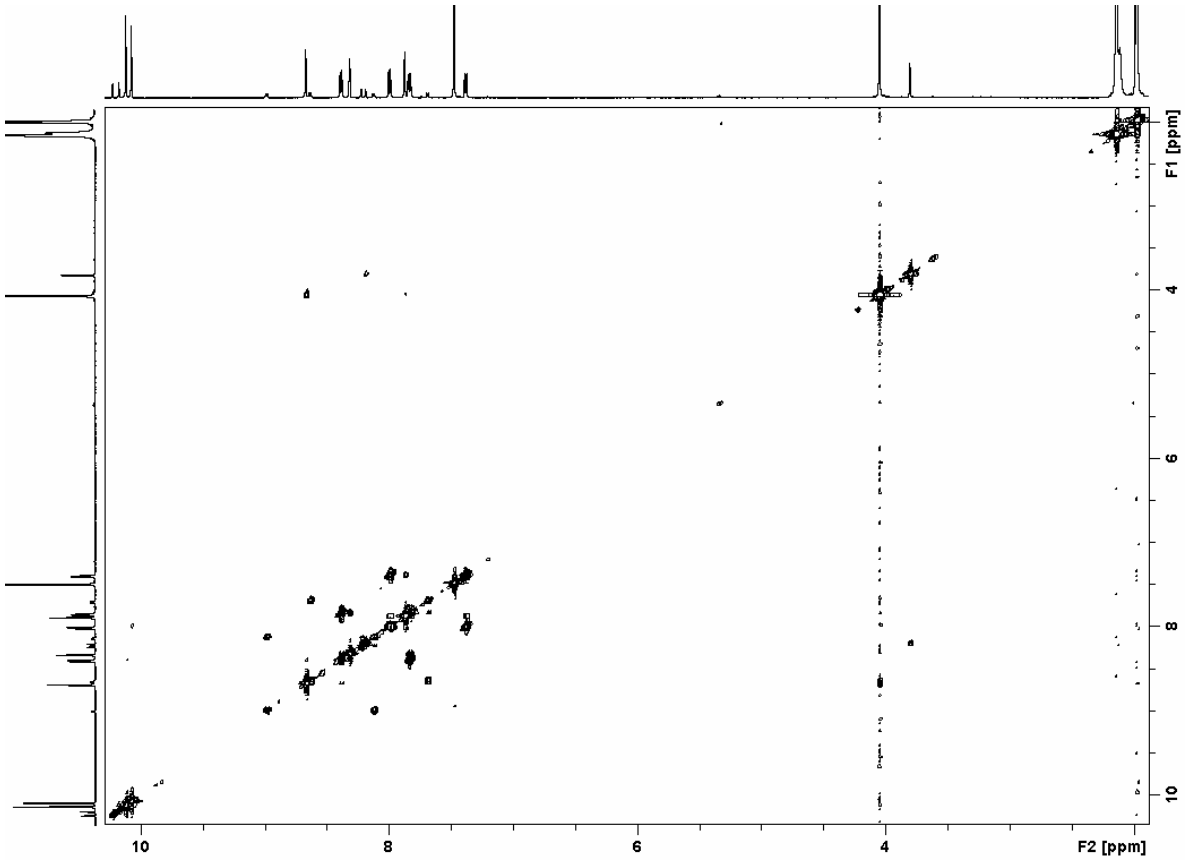

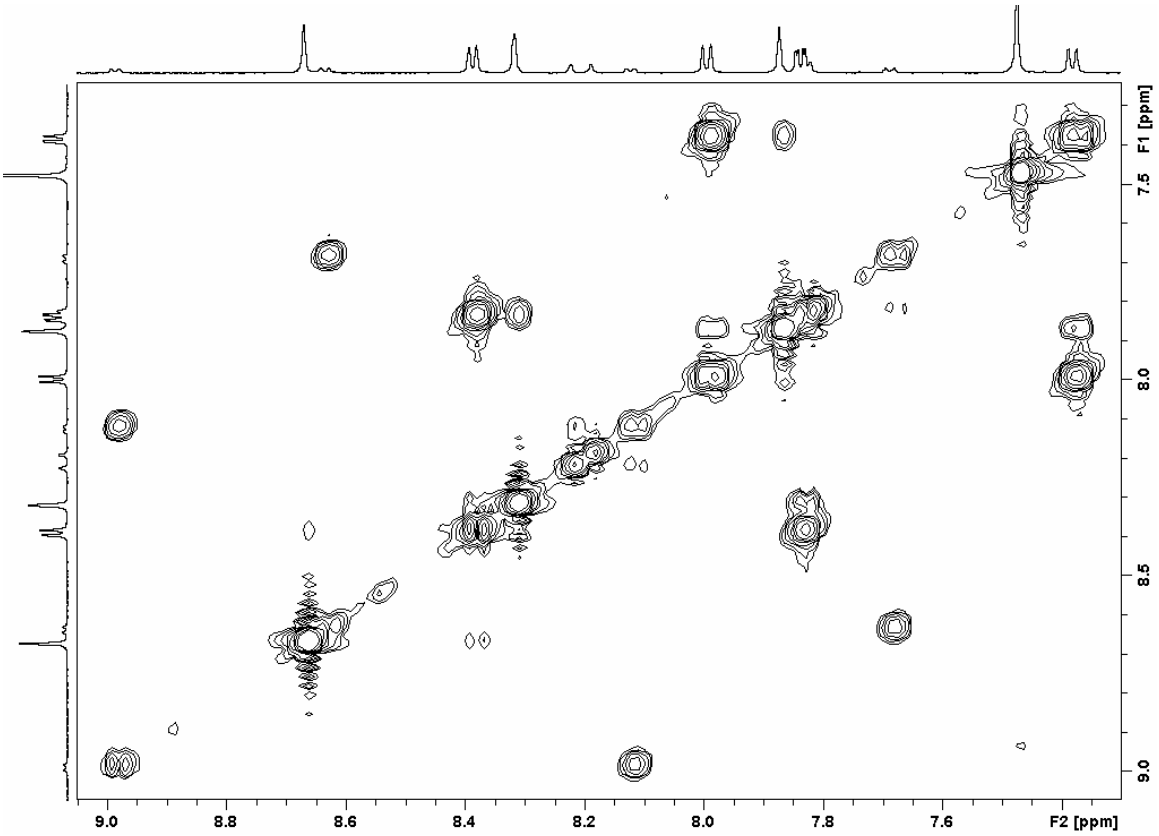

ROESY ($CDCl_3$*/CD_3CN: 6/4):

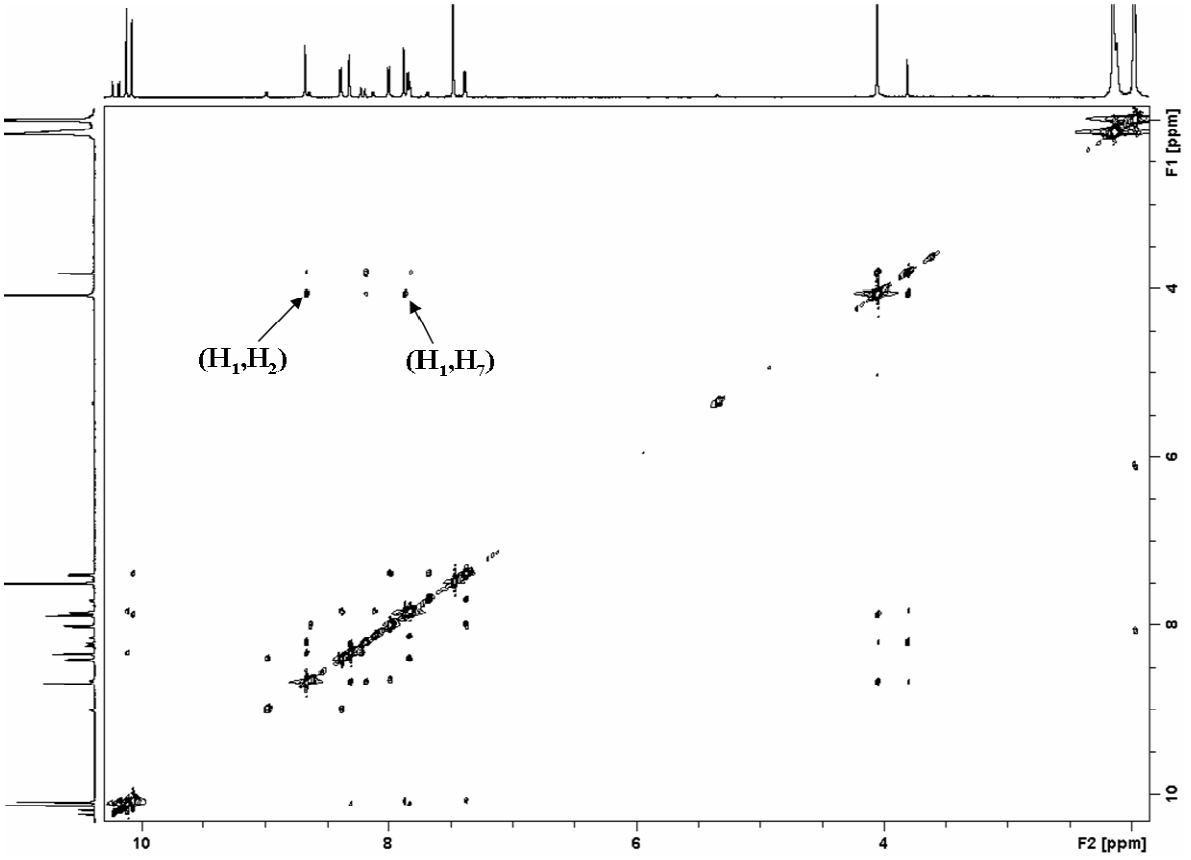

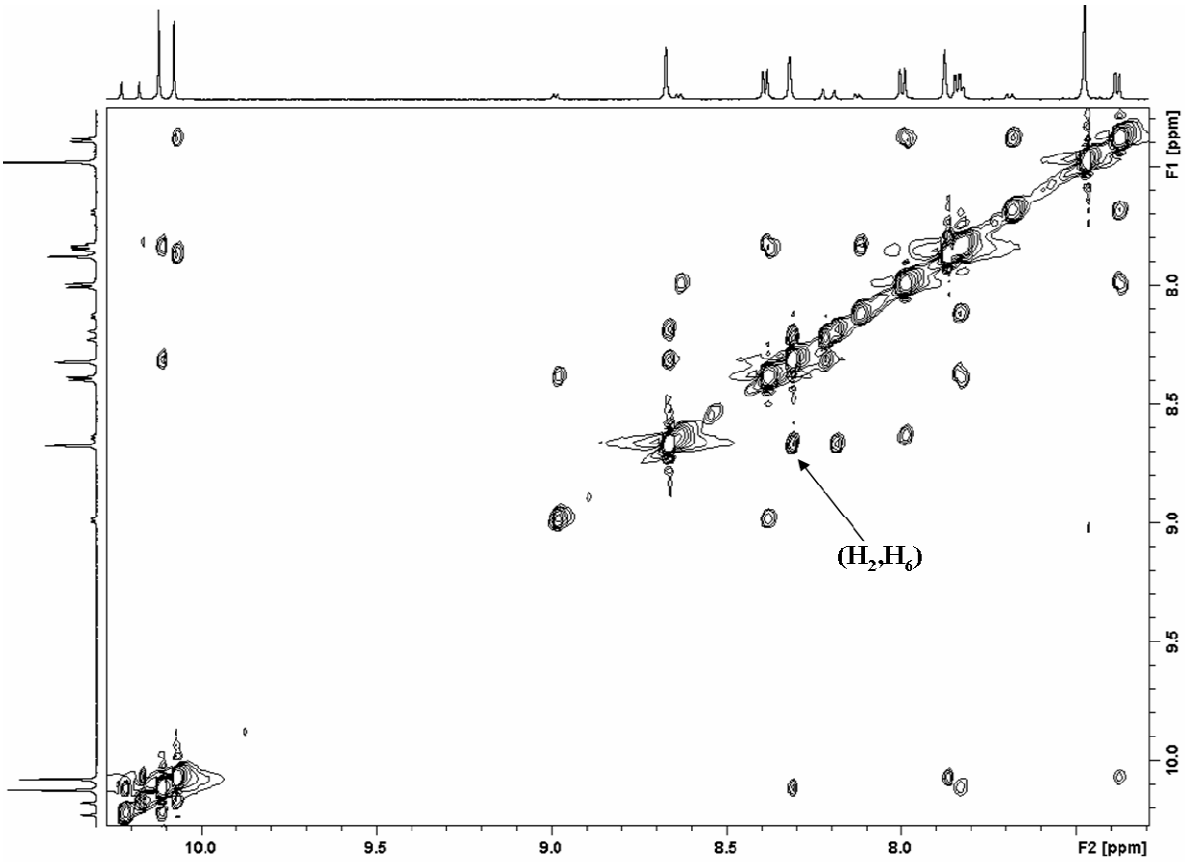

2D NMR analyses of **Zn.2**:

COSY ($CDCl_3$*/CD_3CN: 6/4):

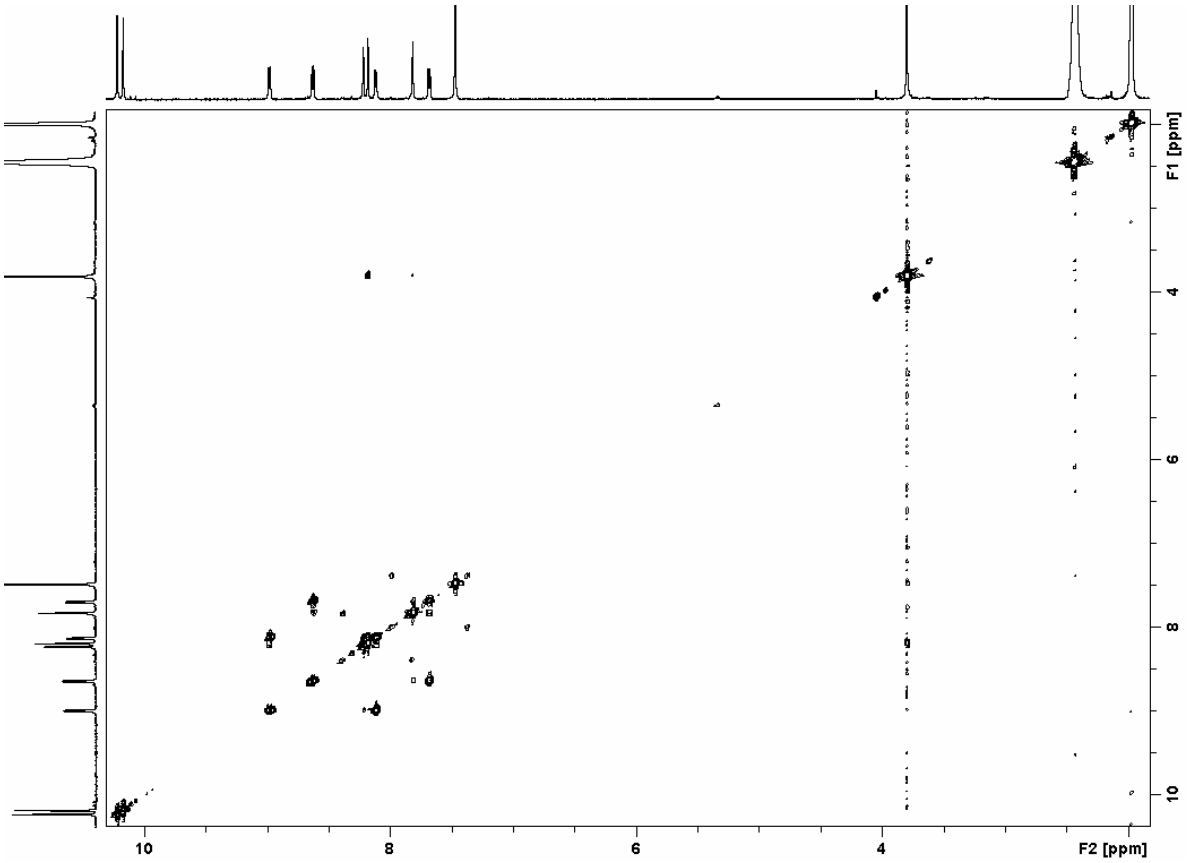

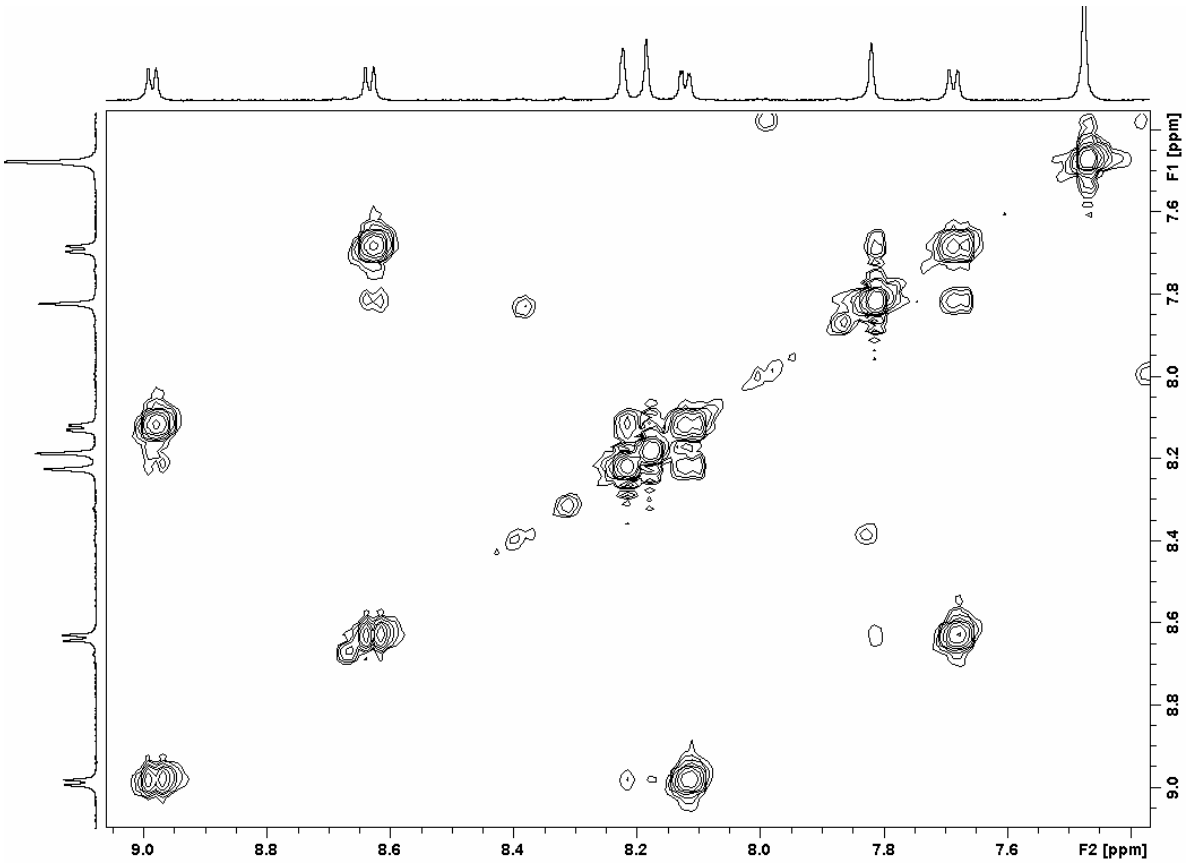

ROESY ($CDCl_3$*/CD_3CN: 6/4):

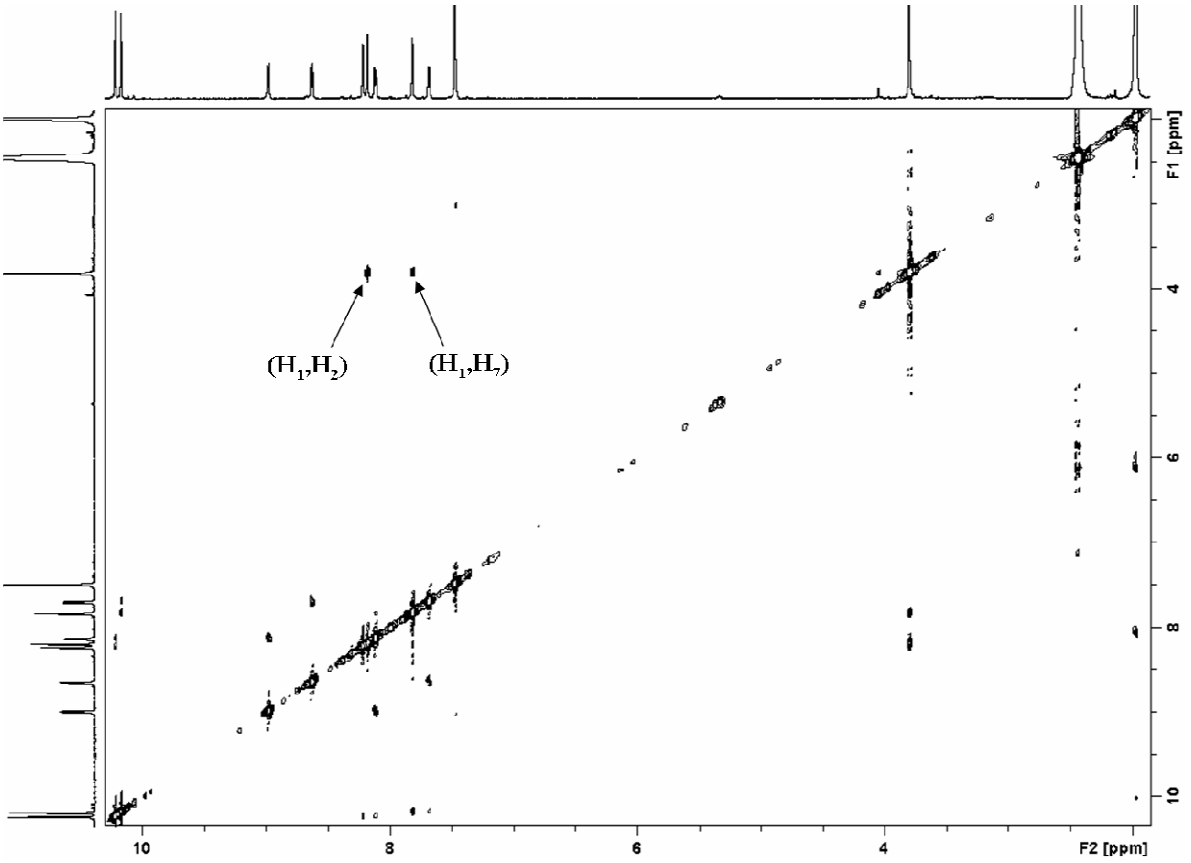

Titration of **1-Me** by $Pb(OTf)_2$ monitored by UV-visible spectroscopy:

The concentration of the ligand was 3.010^{-5}M in $CHCl_3$*/CH_3CN: 6/4. Samples were prepared with a different molar ratio of $Pb(OTf)_2$ in respect to the ligand and the mixtures were left a few hours to equilibrate.

UV-Visible spectra of ligand with different ratios of metal ion (inset: evolution of absorbance along the titration at different wavelengths):

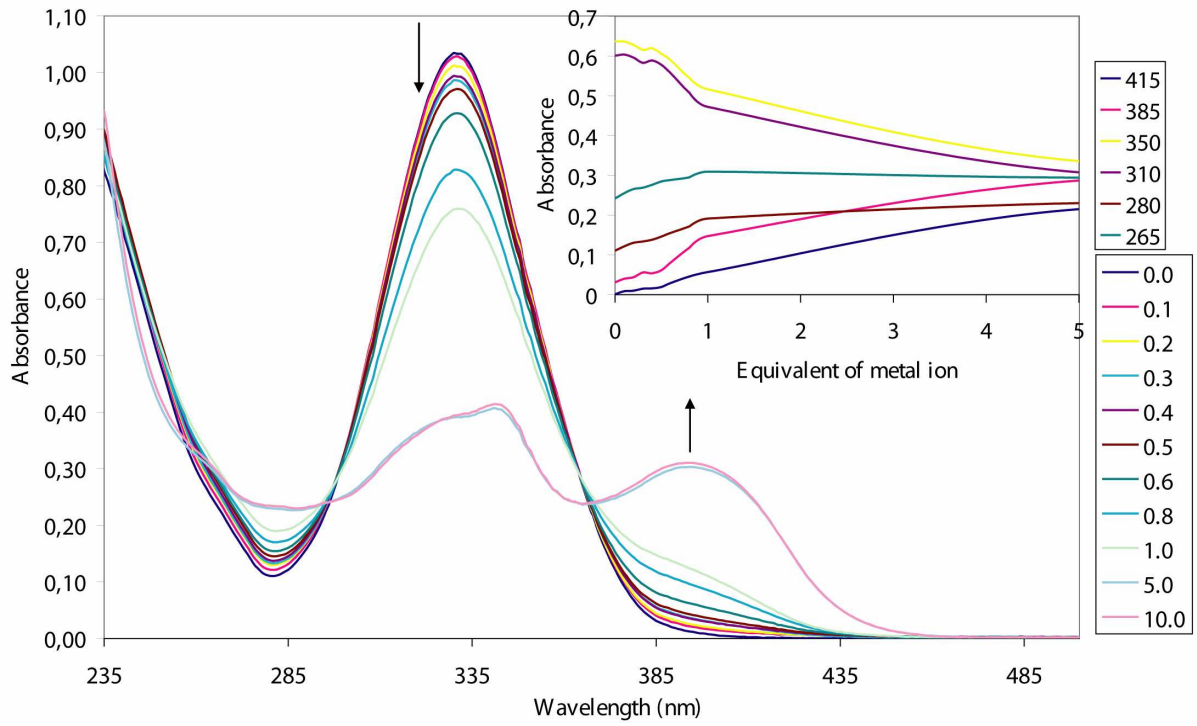

Titration of **2** by $Pb(OTf)_2$ monitored by UV-visible spectroscopy:

The concentration of the ligand was 4.010^{-5}M in $CHCl_3$*/CH_3CN: 6/4. Samples were prepared with a different molar ratio of $Pb(OTf)_2$ in respect to the ligand and the mixtures were left a few hours to equilibrate.

UV-Visible spectra of ligand with different ratios of metal ion (inset: evolution of absorbance along the titration at different wavelengths):

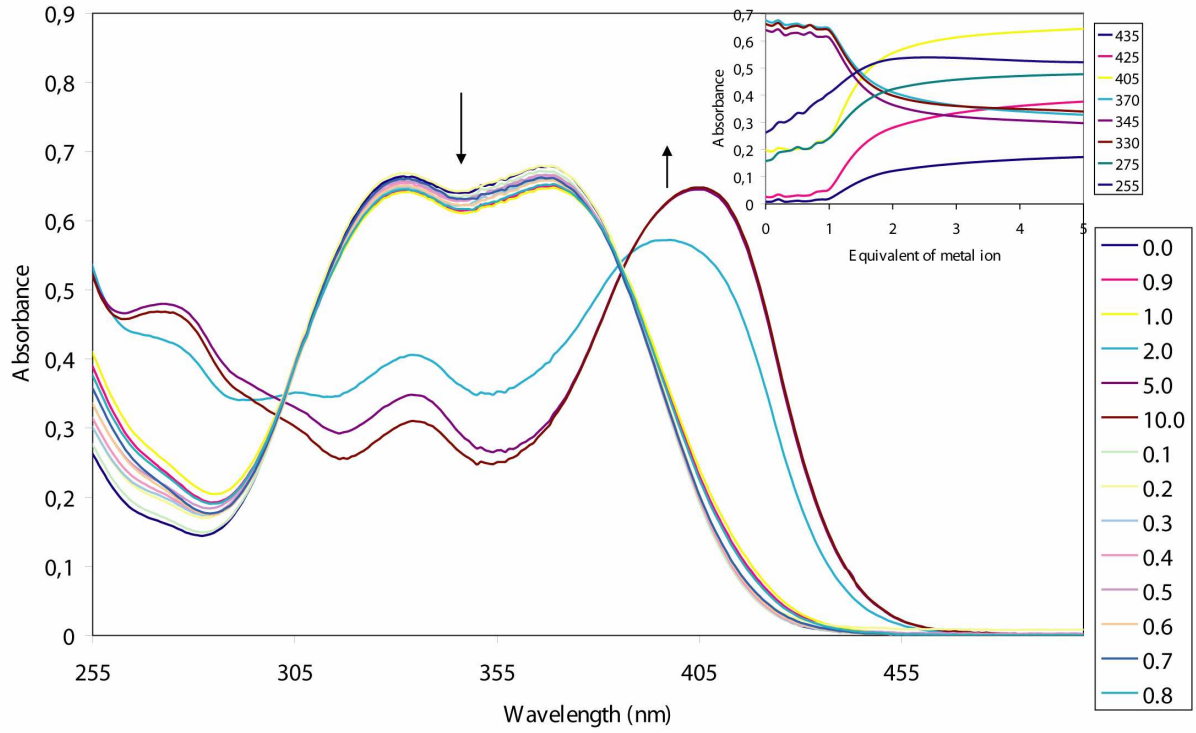

General procedure for the kinetic experiments:

A 5 mM solution of the dialdehyde (3 μmoles) in $CDCl_3/CD_3CN$: 6/4 (0.6 mL) was prepared. The diamine (50 μL of a 60 mM solution in $CDCl_3^*/CD_3CN$: 6/4, 3 μmoles) or monoamine (50 μL of a 120 mM solution in $CDCl_3^*/CD_3CN$: 6/4, 6 μmoles) was added and the reaction was monitored by ^1H NMR.

Here are the data obtained after fitting the concentration-time plot with pseudo-first order equations:

Starting from **1-Me** and *n*-octylamine:

Monitoring by ^1H NMR:

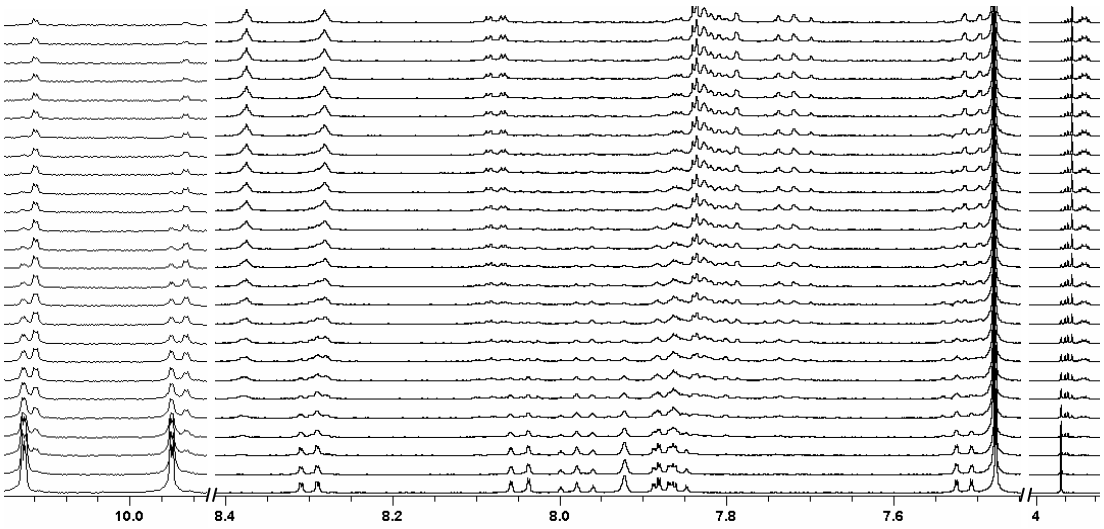

^1H NMR kinetic analysis of the condensation between **1-Me** and *n*-octylamine **NC_8**. Bottom: ligand **1-Me**, then spectrum after addition of 2.0 equivalent of *n*-octylamine, then each spectrum was recorded every 3 minutes.

Disappearance of the dialdehyde:

$$y = P1 + P2 * \exp(-k * t)$$ //

P1 = 0.028 ± 0.009
P2 = 4.47 ± 0.04
k = 0.076 ± 0.002
$t_{1/2}$ = 9.1
r = 0.9974

Appearance of one monoimine:

$$y = P1 + P2 * \exp(-k_1 * t) + P3 * \exp(-k_2 * t)$$

P1 = 0
P2 = 1.97 ± 0.08
P3 = -1.96 ± 0.08

$k_1 = 0.028 \pm 0.001$
$k_2 = 0.115 \pm 0.006$
r = 0.9949

Appearance of the other monoimine:

$$y = P1 + P2 * \exp(-k_1 * t) + P3 * \exp(-k_2 * t)$$

P1 = 0
P2 = 2.9 ± 0.1
P3 = -3.0 ± 0.1
$k_1 = 0.025 \pm 0.001$
$k_2 = 0.090 \pm 0.004$
r = 0.9954

Appearance of the bisimine:

$$y = P1 + P2 * \exp(-k * t)$$

P1 = 4.615
P2 = -4.615
$k = 0.023 \pm 0.001$
$t_{1/2} = 30.1$
r = 0.9867

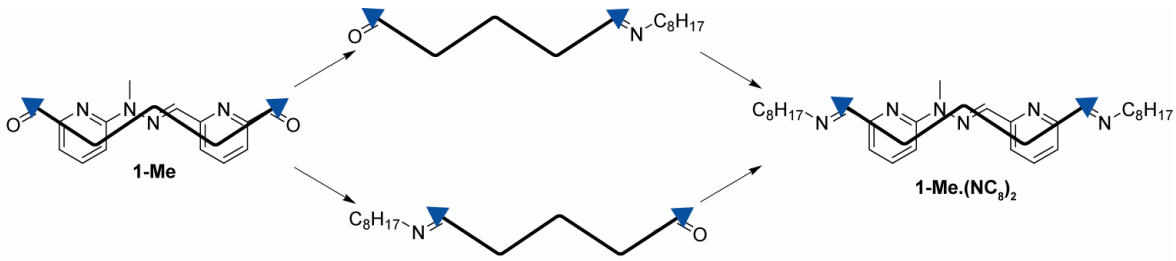

Schematic representation of the pathway from dialdehyde **1-Me** to the diimine product when *n*-octylamine **NC$_8$** is added. Note that the two intermediates are not equivalent due to the presence of the hydrazone unit in the ligand which induces a dissymmetry.

Starting from **2** and *n*-octylamine:

Monitoring by ^{1}H NMR:

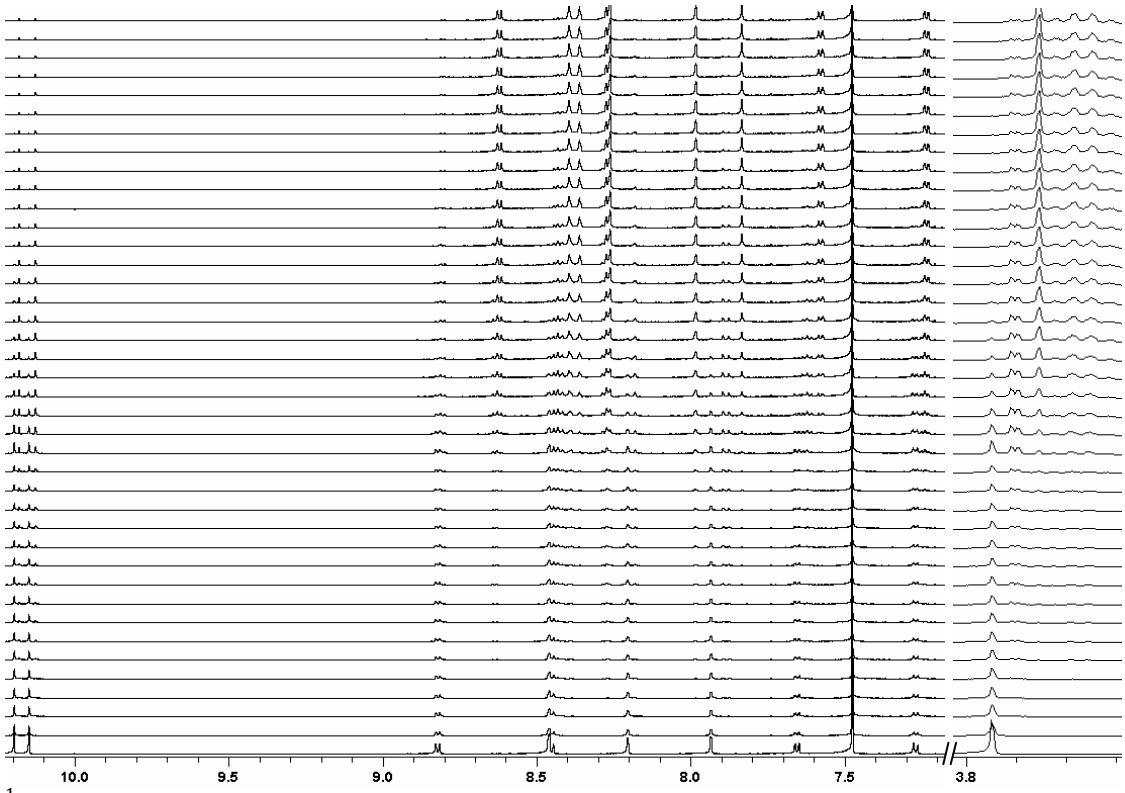

^{1}H NMR kinetic analysis of the condensation between **2** and *n*-octylamine **NC$_8$**. Bottom: ligand **2**, then spectrum after addition of 2.0 equivalent of *n*-octylamine, then each spectrum was recorded every 3 minutes.

Concentration-time curve:

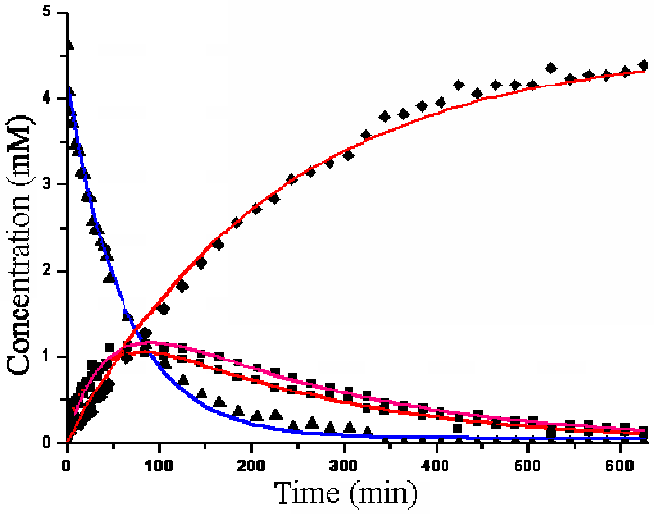

Disappearance of the dialdehyde:

$$y = P1 + P2 * \exp(-k * t)$$

P1 = 0.05 ± 0.03
P2 = 4.08 ± 0.05
k = 0.016 ± 0.001
$t_{1/2}$ = 43.3

r = 0.9948

Appearance of one monoimine:

$$y = P1 + P2 * \exp(-k_1 * t) + P3 * \exp(-k_2 * t)$$

P1 = 0
P2 = -1.7 ± 0.1
P3 = 1.9 ± 0.1
k_1 = 0.024 ± 0.001
k_2 = 0.0046 ± 0.0002
r = 0.9821

Appearance of the other monoimine:

$$y = P1 + P2 * \exp(-k_1 * t) + P3 * \exp(-k_2 * t)$$

P1 = 0
P2 = -2.0 ± 0.1
P3 = 2.1 ± 0.1
k_1 = 0.022 ± 0.002
k_2 = 0.0043 ± 0.0002
r = 0.9742

Appearance of the diimine:

$$y = P1 + P2 * \exp(-k * t)$$

P1 = 4.615
P2 = -4.615
k = 0.0044 ± 0.0001
$t_{1/2}$ = 157.5
r = 0.9957

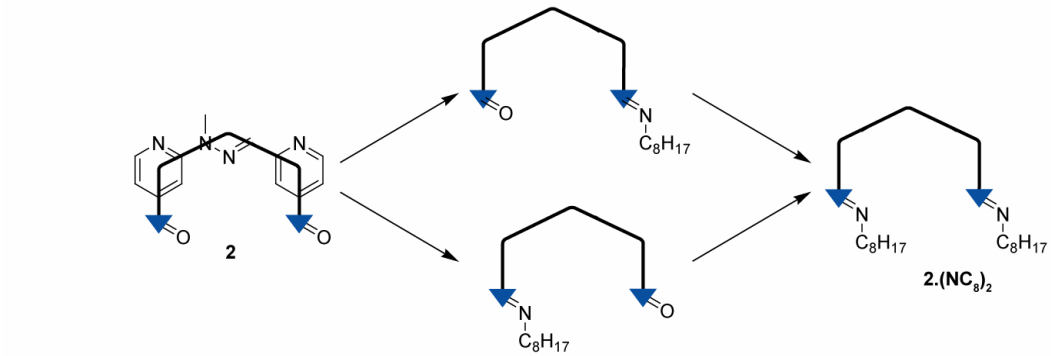

Schematic representation of the pathway from dialdehyde **2** to the diimine product when *n*-octylamine **NC$_8$** is added. Note that the two intermediates are not equivalent due to the presence of the hydrazone unit in the ligand which induces a dissymmetry.

Starting from **2** and 1,5-diaminopentane:

Monitoring by ^{1}H NMR:

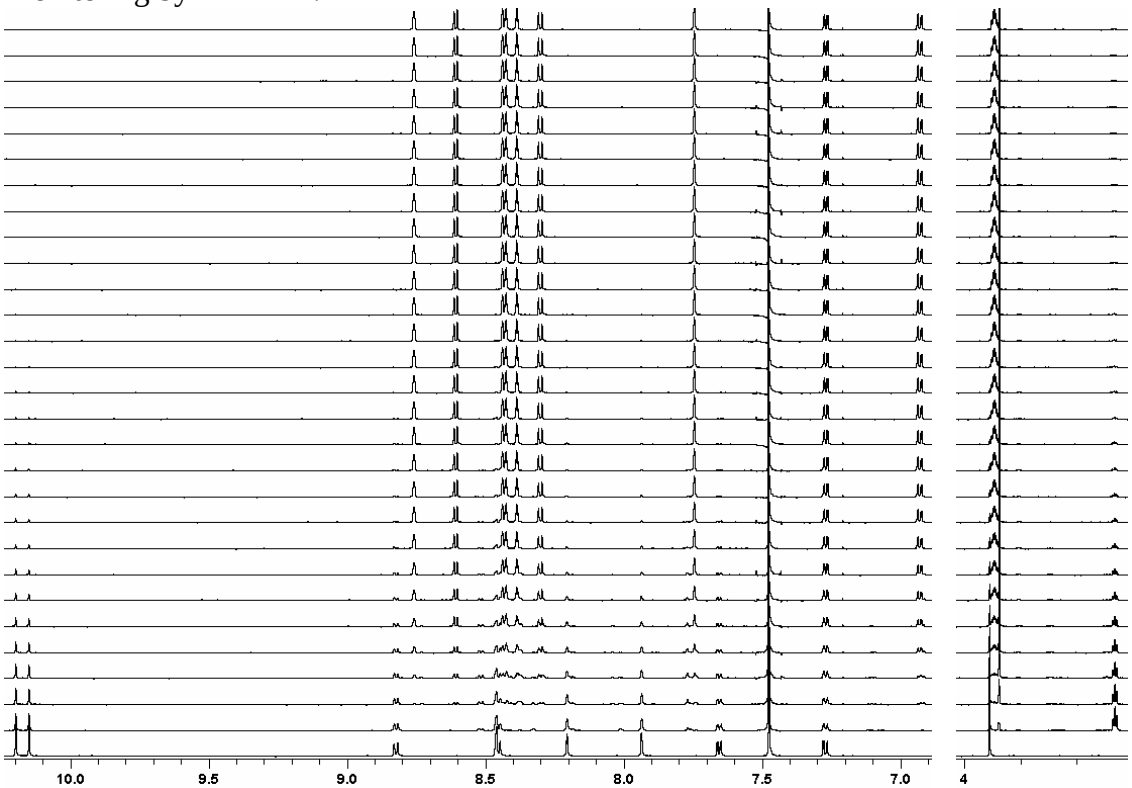

^{1}H NMR kinetic analysis of the condensation between **2** and 1,5-diaminopentane. Bottom: ligand **2**, then spectrum after addition of 2.0 equivalent of 1,5-diaminopentane, then each spectrum was recorded every 3 minutes.

Distribution curves:

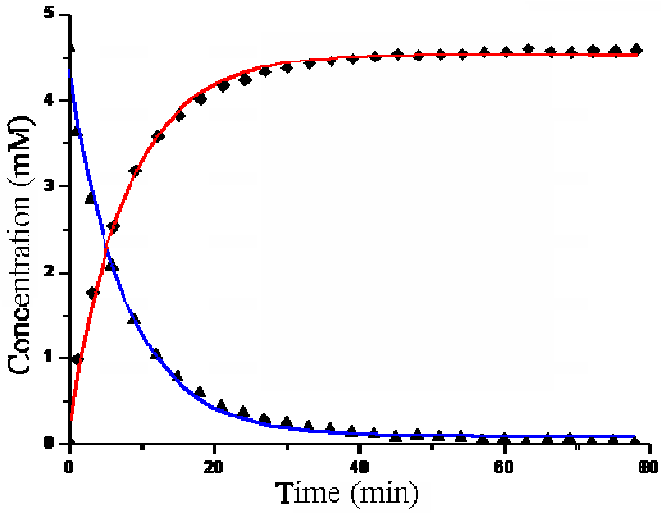

Disappearance of the dialdehyde:

$$y = P1 + P2 * \exp(-k * t)$$

P1 = 0.08 ± 0.02
P2 = 4.26 ± 0.06
k = 0.126 ± 0.004

$t_{1/2}$ = 5.5
r = 0.9951

Appearance of the diimine:

$$y = P1 + P2 * \exp(-k * t)$$

P1 = 4.53 ± 0.02
P2 = -4.26 ± 0.06
k = 0.126 ± 0.004
$t_{1/2}$ = 5.5
r = 0.9951

Kinetic of transimination:

A 5 mM solution of acyclic diimine was prepared from the dialdehyde **2** (3 μmoles) and the *n*-octylamine (6 μmoles) in $CDCl_3/CD_3CN$: 6/4 (0.6 mL) was prepared. The 1,5-diaminopentane (50 μL of a 60 mM solution in $CDCl_3^*/CD_3CN$: 6/4, 3 μmoles) was added and the progress of the reaction was monitored by ^1H NMR.

Monitoring by ^1H NMR:

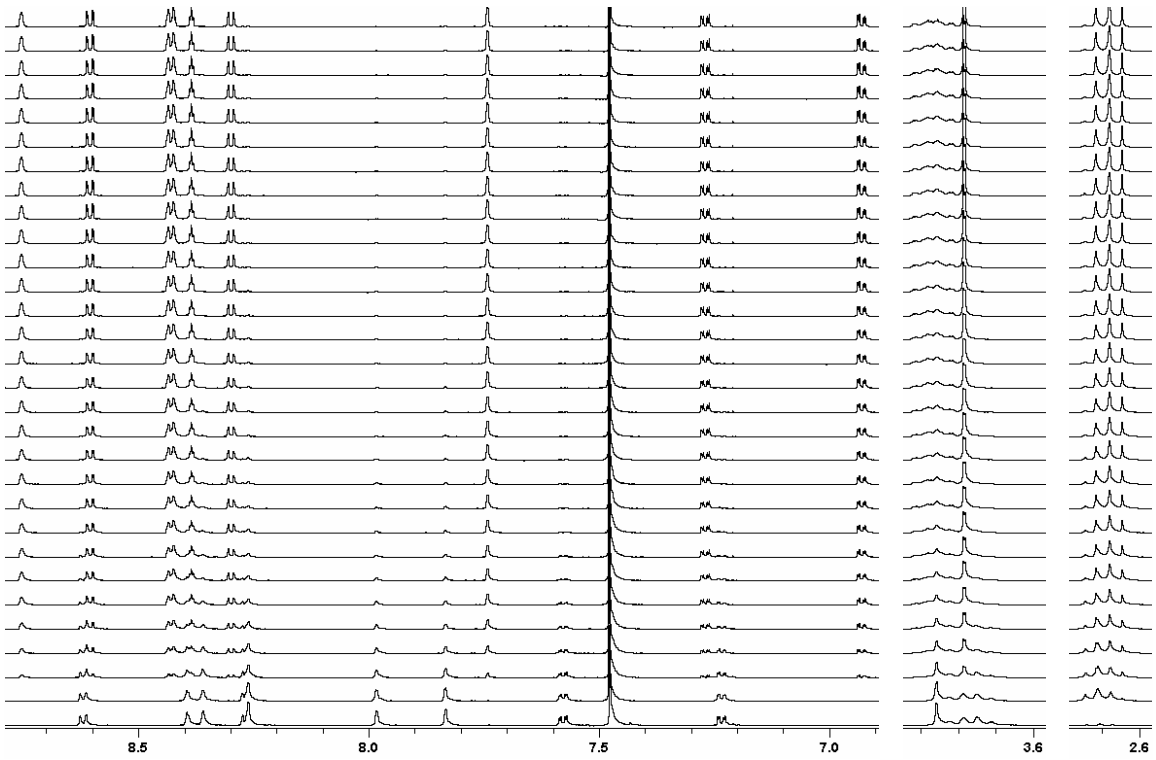

Distribution curves:

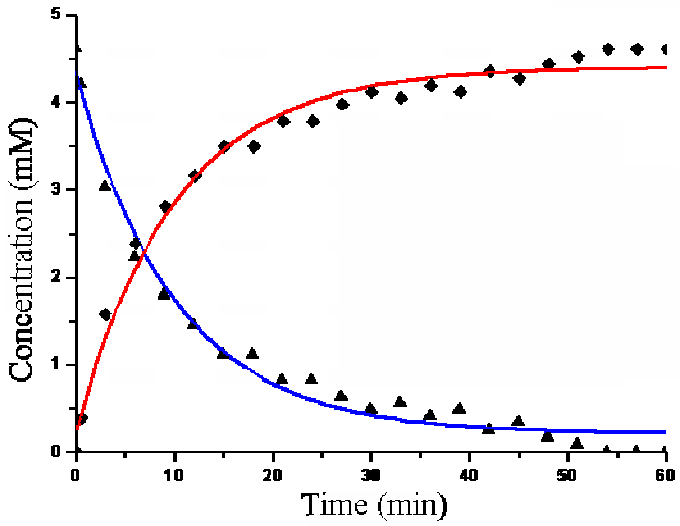

Disappearance of the acyclic bisimine:

$$y = P1 + P2 * \exp(-k * t)$$

P1 = 0.21 ± 0.06
P2 = 4.1 ± 0.1
k = 0.099 ± 0.008
$t_{1/2}$ = 7.0
r = 0.9827

Appearance of the macrocyclic bisimine:

$$y = P1 + P2 * \exp(-k * t)$$

P1 = 4.40 ± 0.06
P2 = -4.1 ± 0.1
k = 0.099 ± 0.008
$t_{1/2}$ = 7.0
r = 0.9827

Solid state MALDI-TOF analysis of $\mathbf{2_2.(N_2C_2)_2}$:

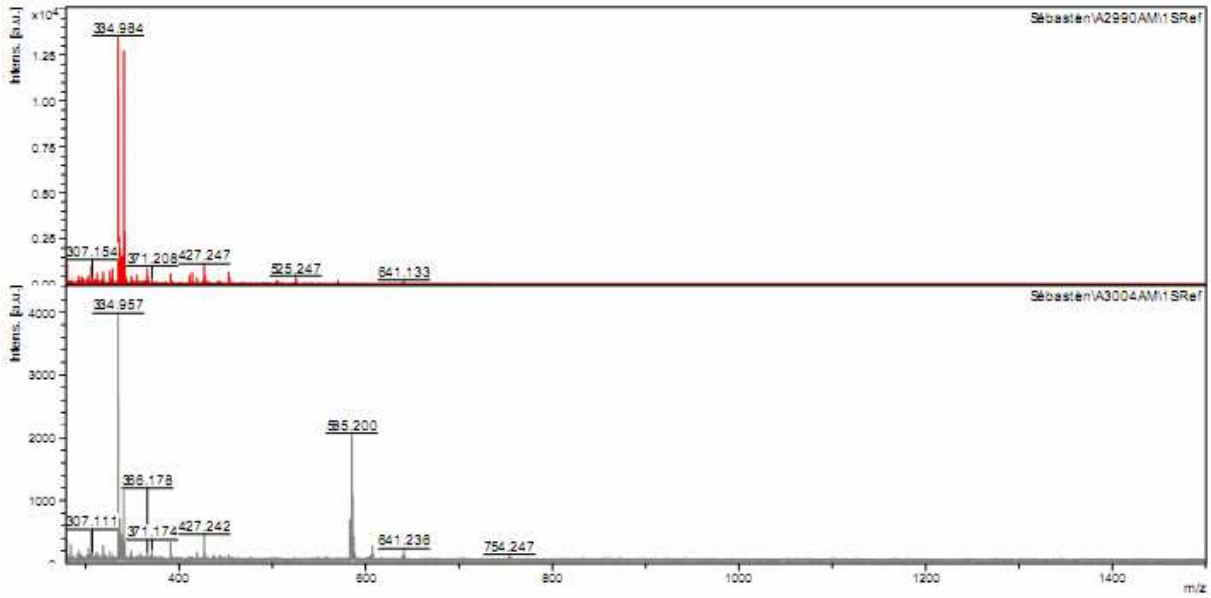

The upper spectrum is without the sample (the peaks therefore belong to the matrix, THAP), the lower was made with the sample.

Solid state MALDI-TOF analysis of $\mathbf{2_2.(N_2C_3)_2}$:

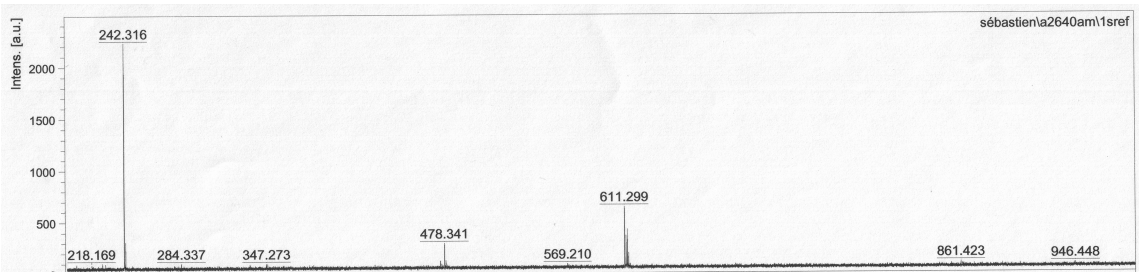

Solid state MALDI-TOF analysis of $\mathbf{2_2.(N_2C_4)_2}$:

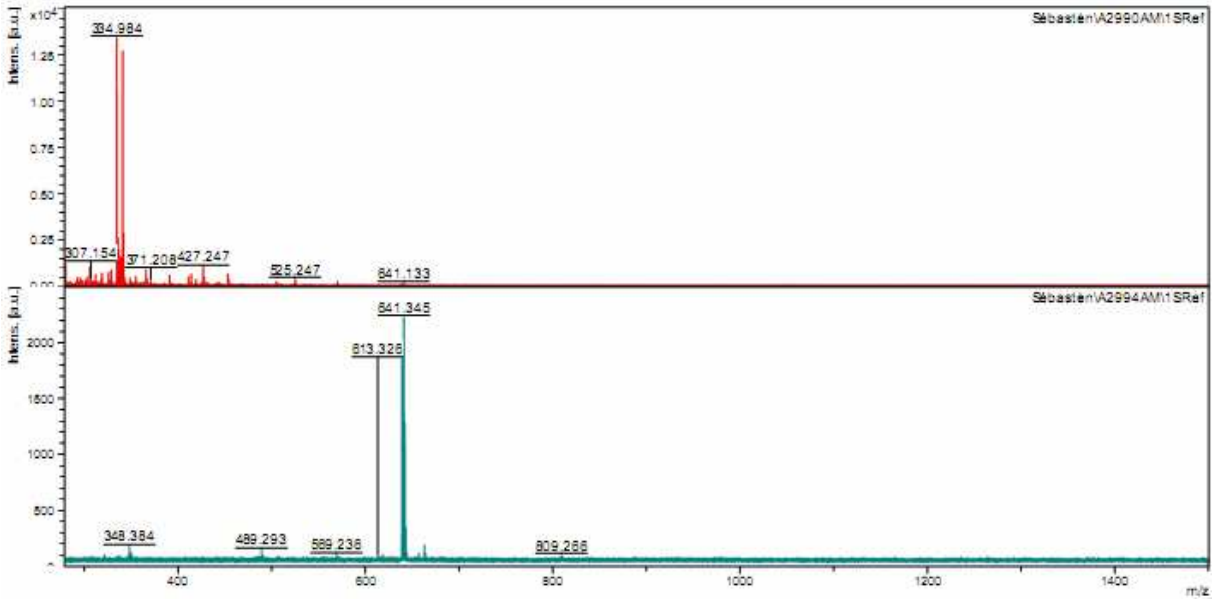

The upper spectrum is without the sample (the peaks therefore belong to the matrix, THAP), the lower was made with the sample.

MALDI-TOF analysis of **$2_2.(N_2C_4)_2$** (from a $CHCl_3$ solution):

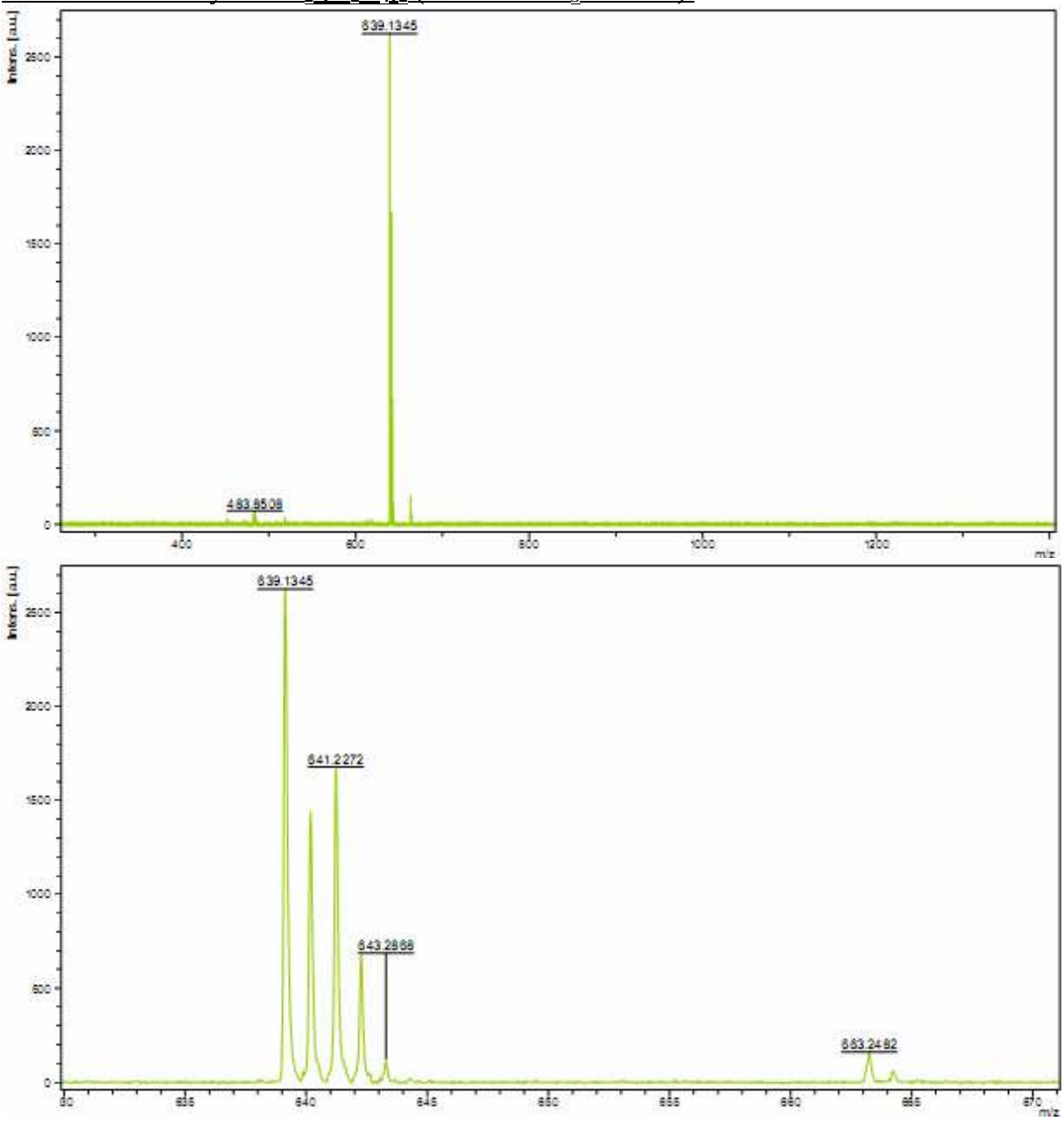

Concentration-dependent NMR spectra of **$2_2.(N_2C_4)_2$** in $CDCl_3$* at various concentrations (from bottom to top: 5, 25 and 50 mM):

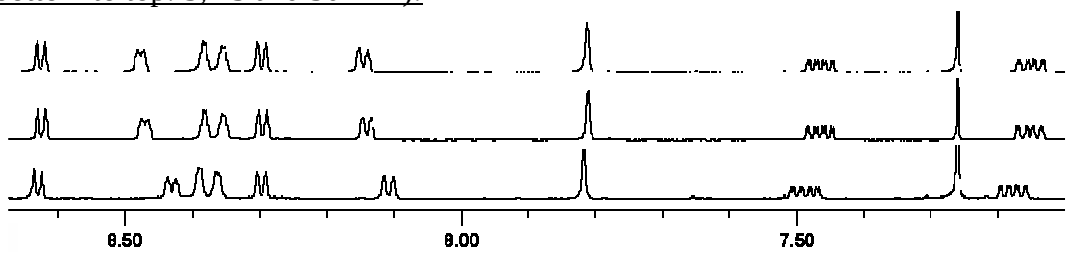

2D NMR analyses of **$2.N_2C_5$**:

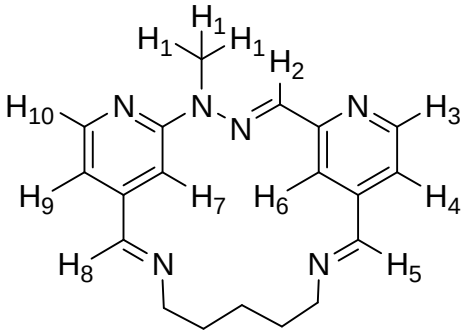

COSY ($CDCl_3$*/CD_3CN: 6/4):

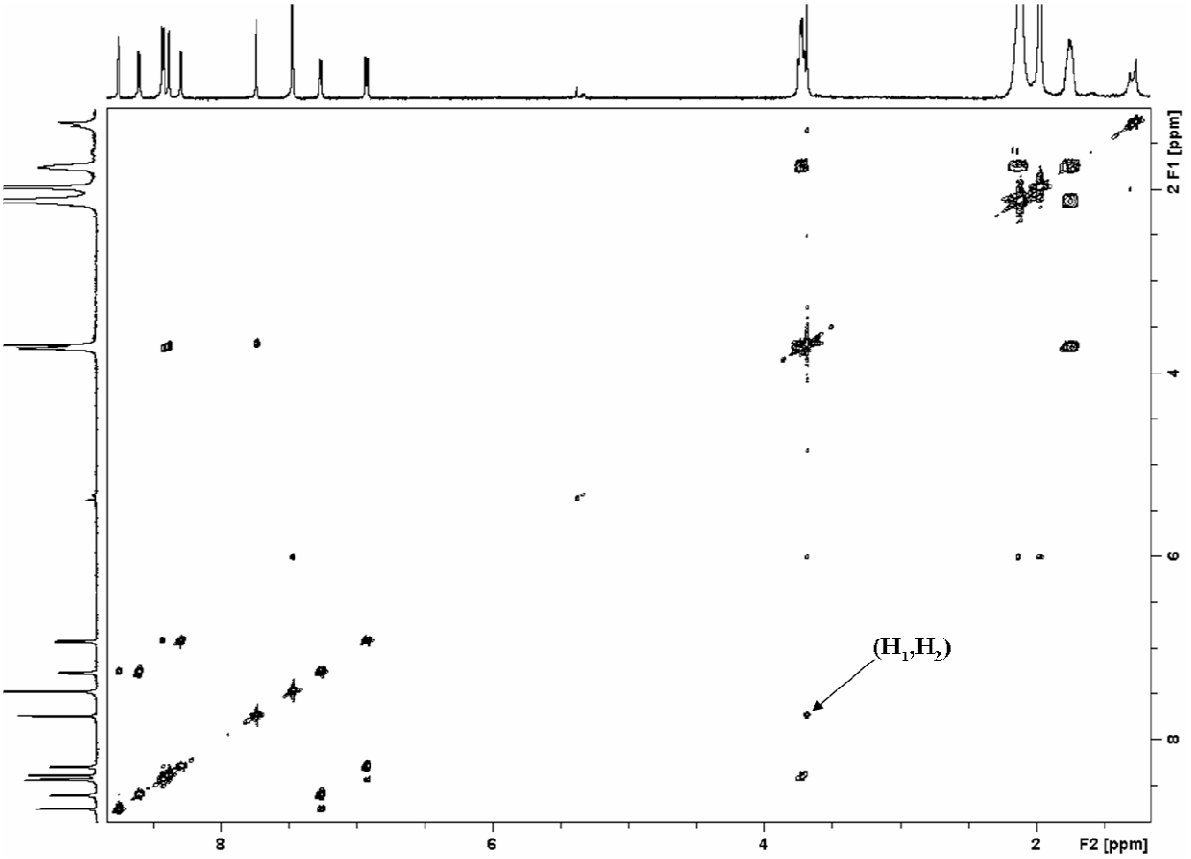

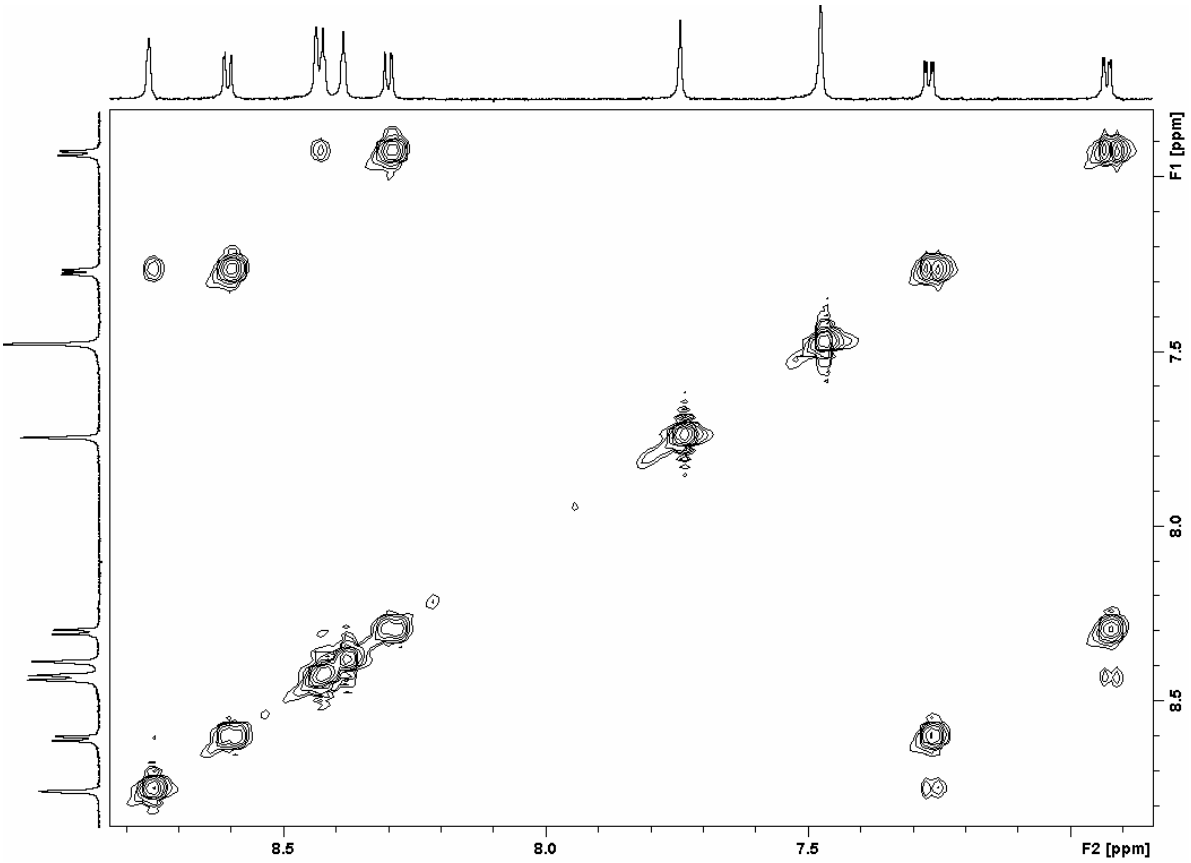

ROESY ($CDCl_3$*/CD_3CN: 6/4):

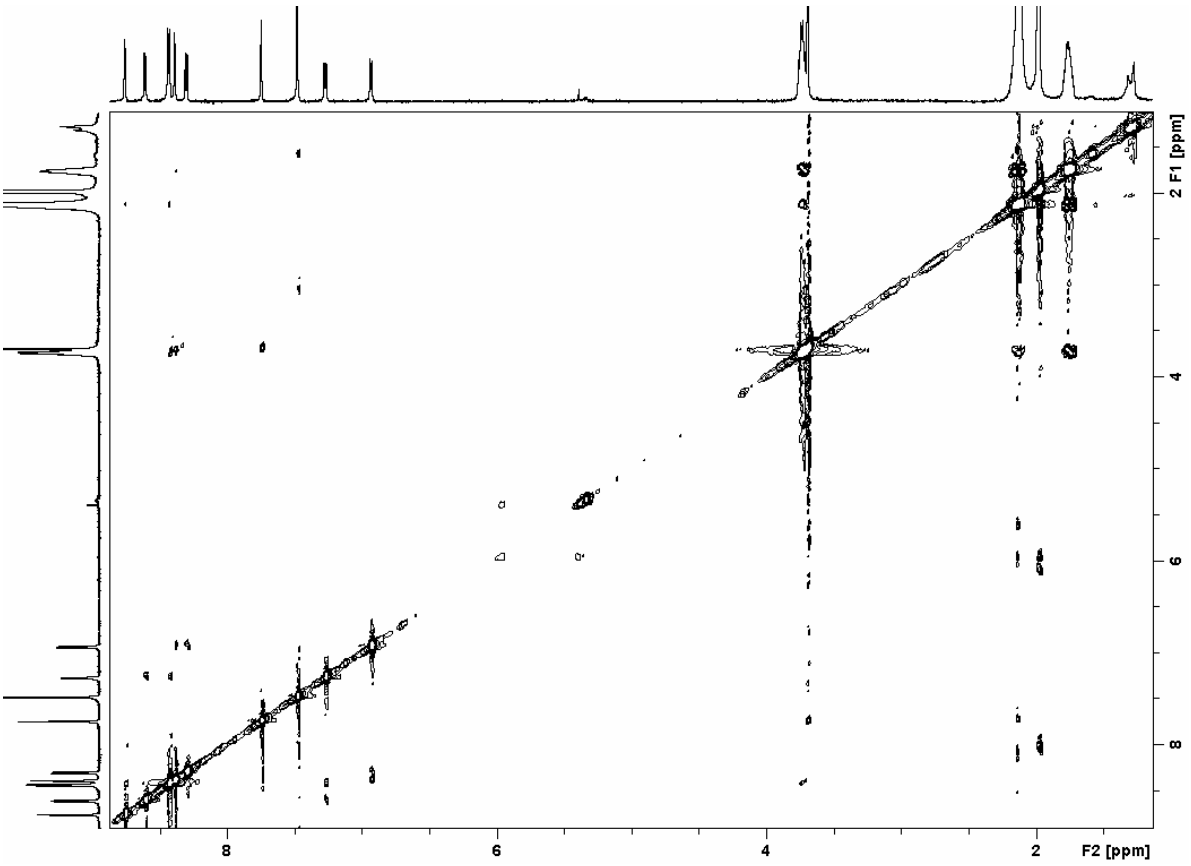

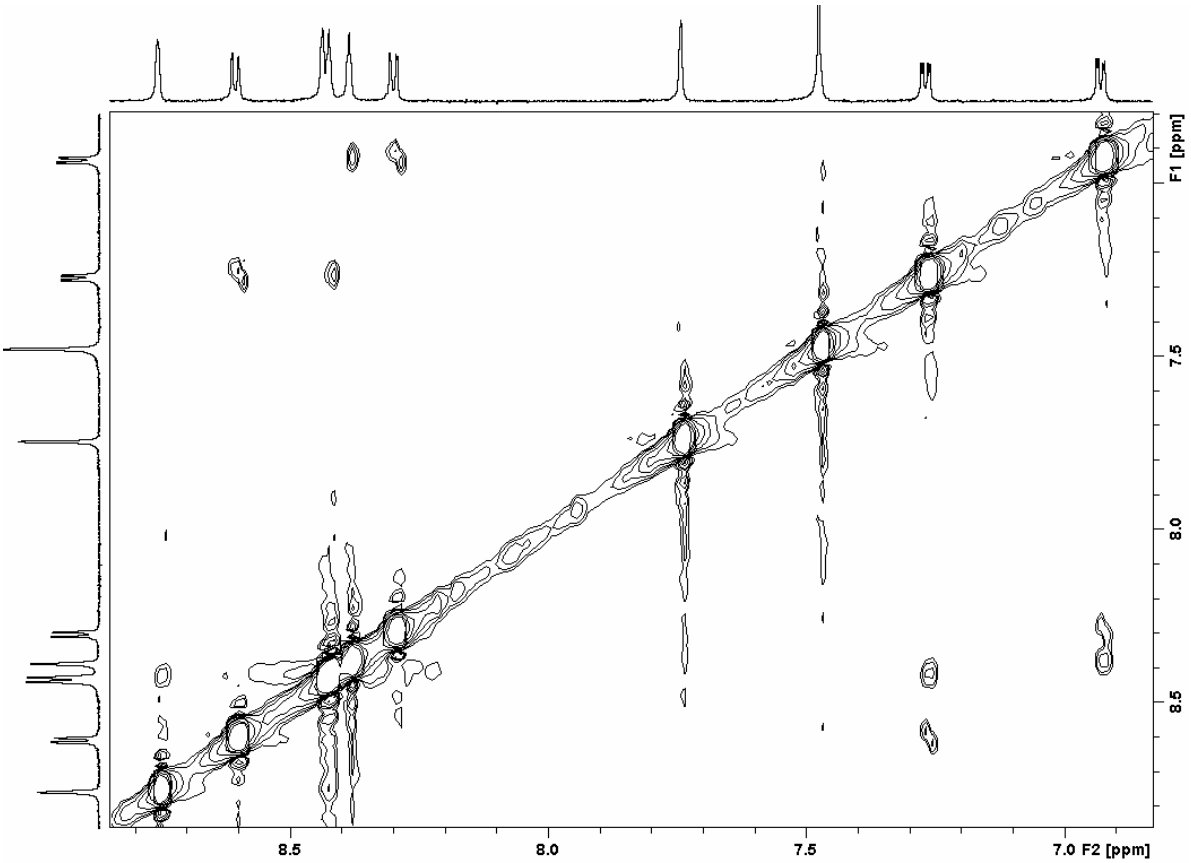

MALDI-TOF analysis of **2.$N_2$$\underline{C}_5$**:

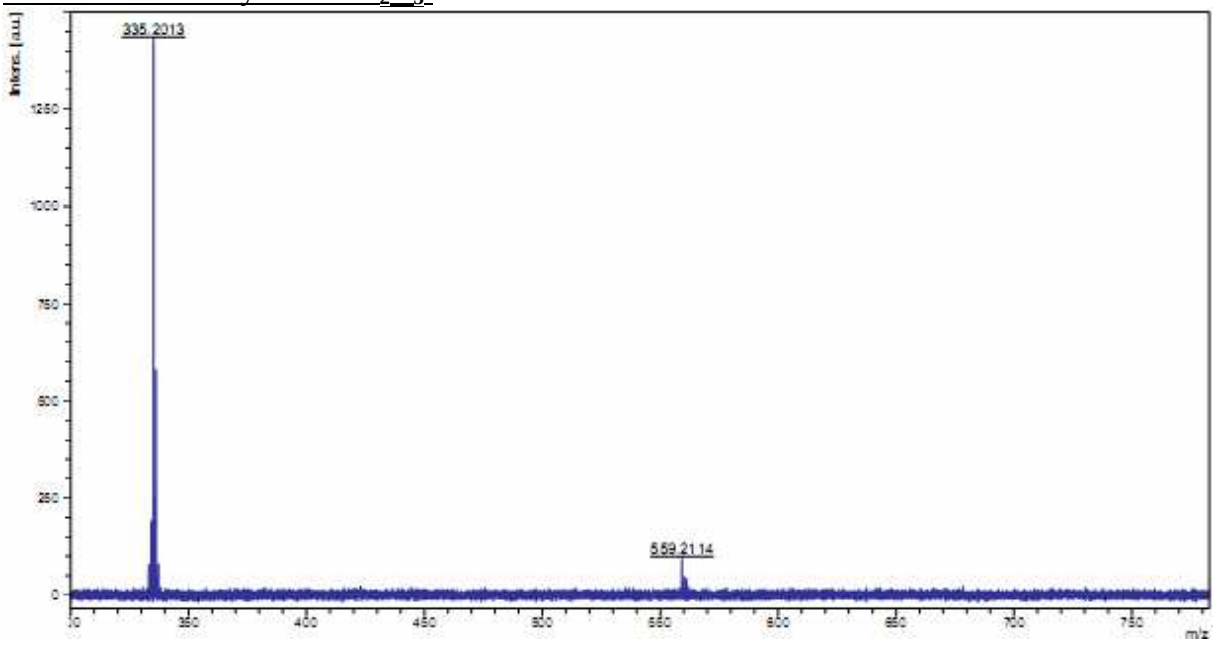

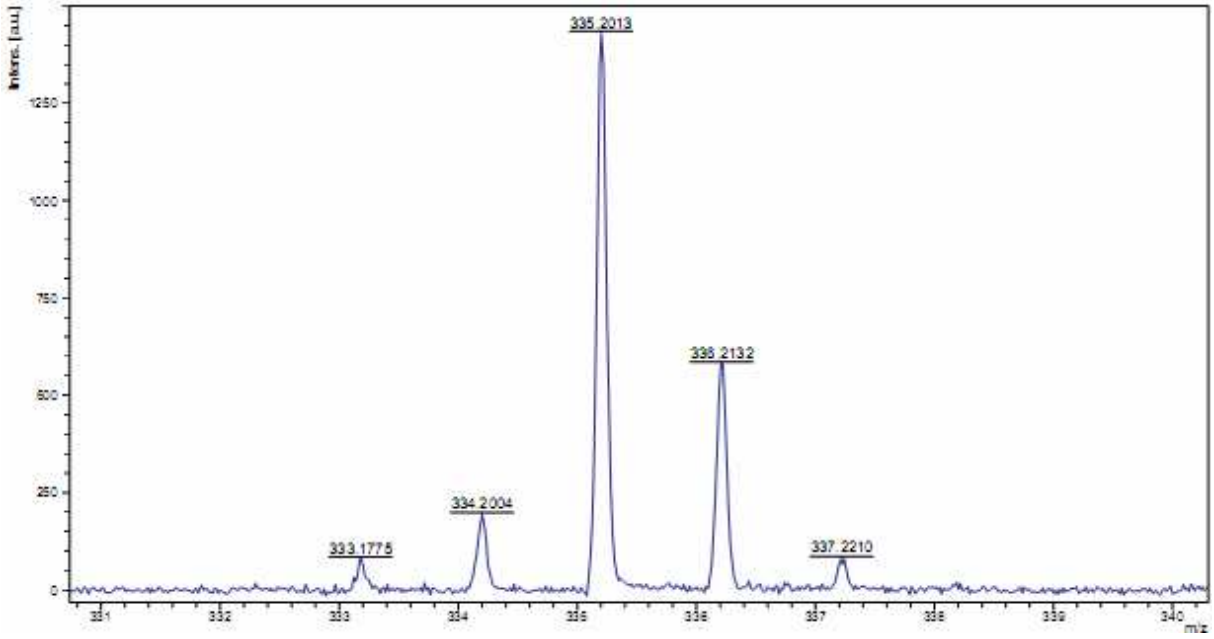

MALDI-TOF analysis of $\mathbf{2_2.(N_2O)_2}$:

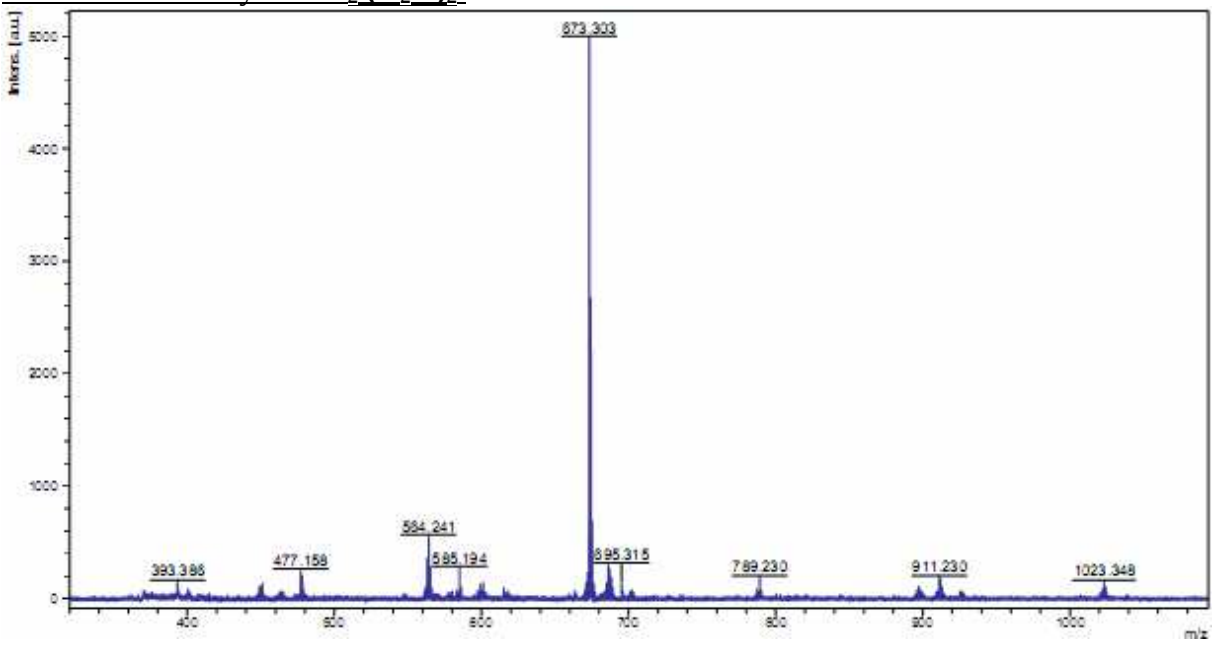

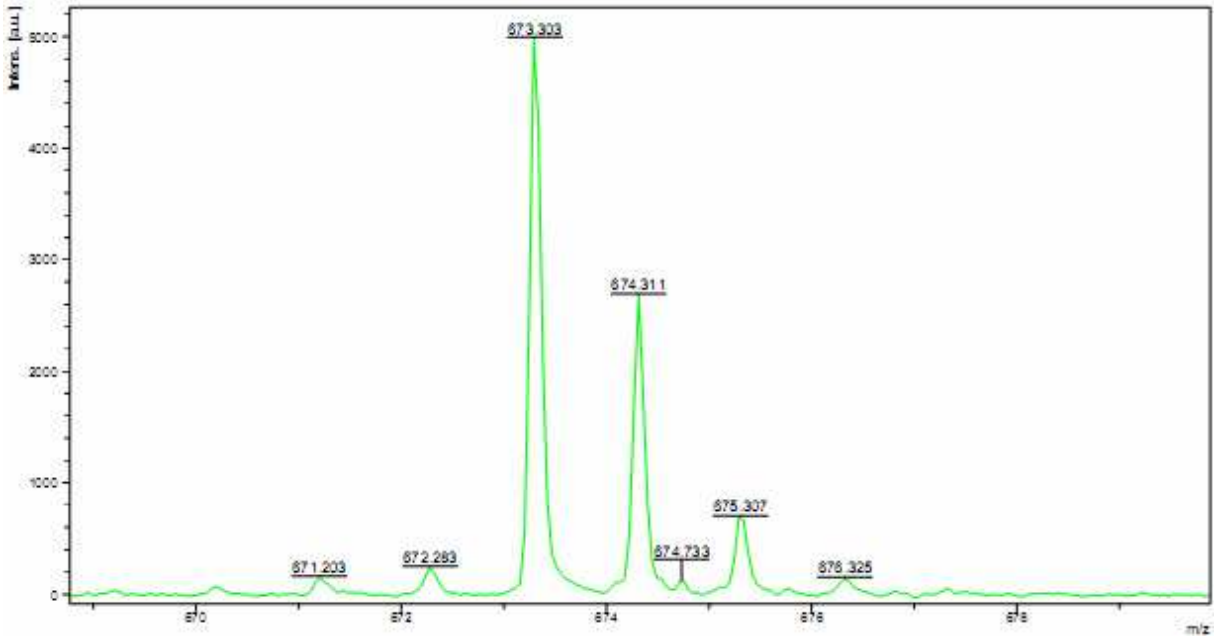

MALDI-TOF analysis of **Zn.1-Me.N_2C_4**:

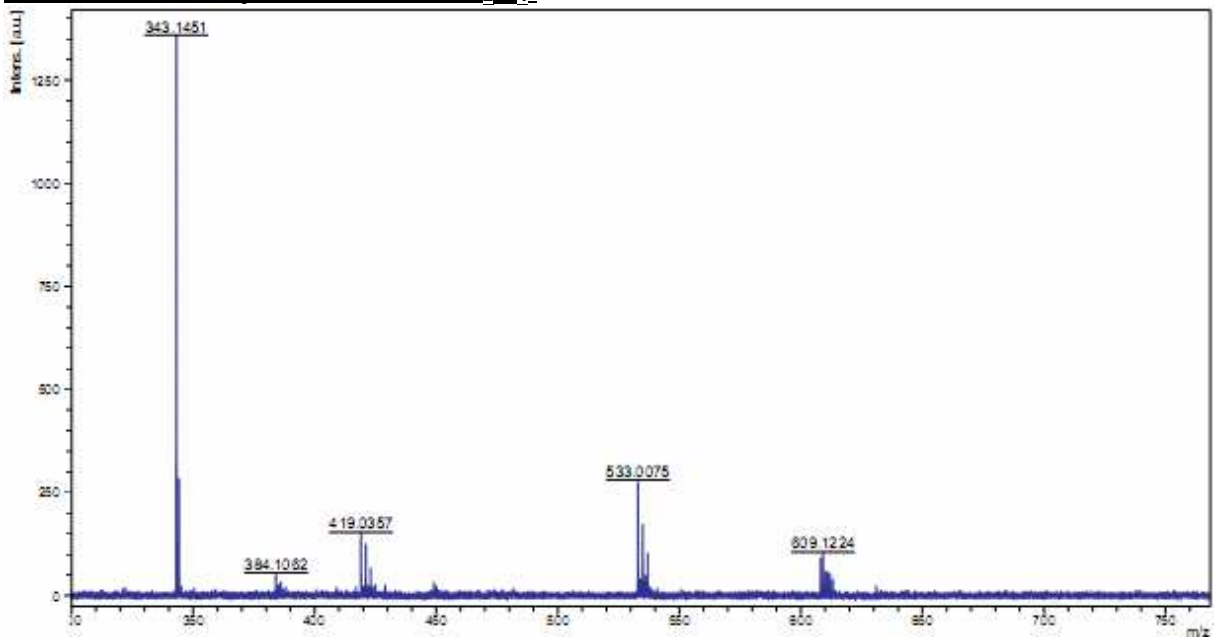

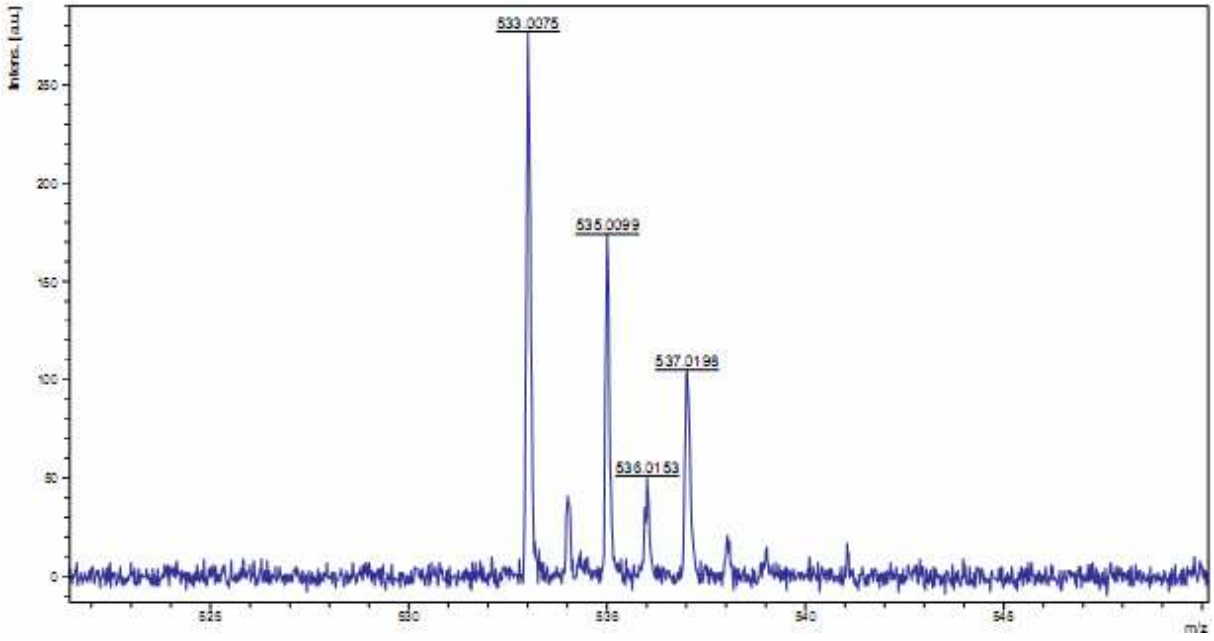

MALDI-TOF analysis of **Zn.1-Oct.N_2C_4**:

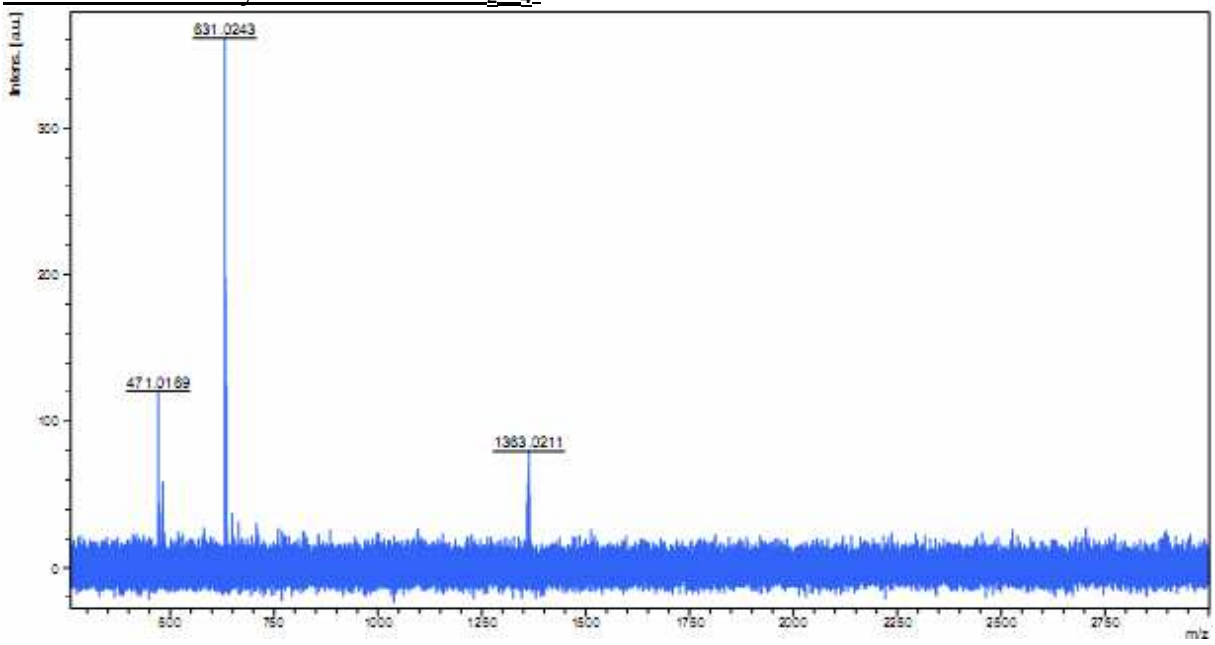

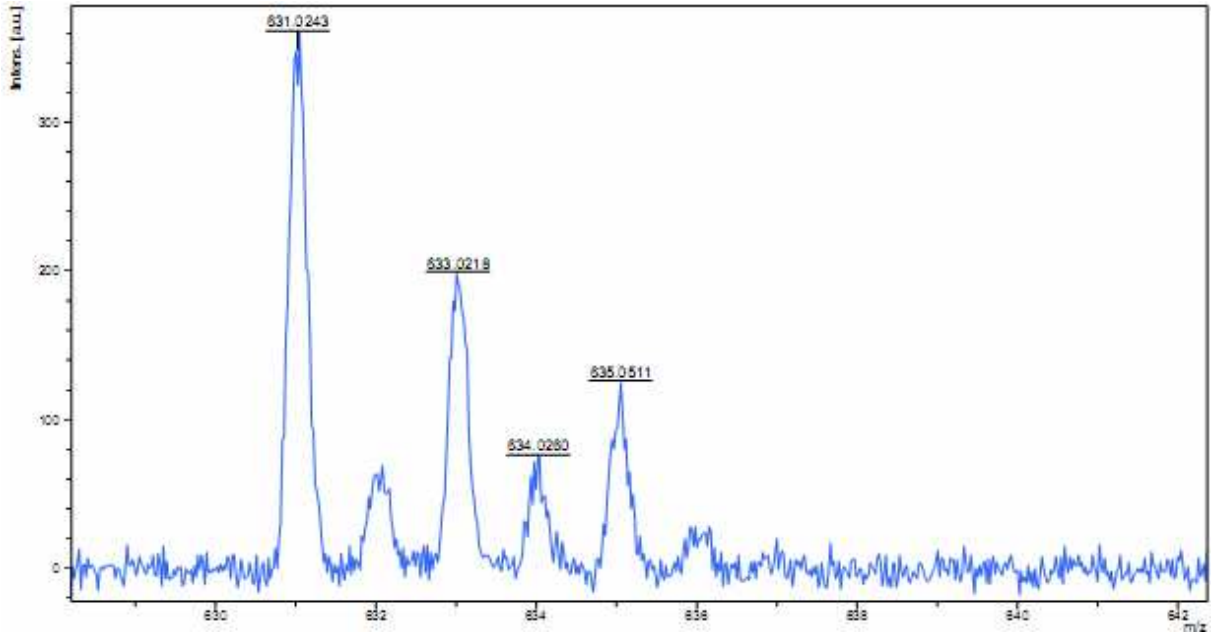

HR-ESI-MS analysis of **Zn.1-Me.N_2C_5**:

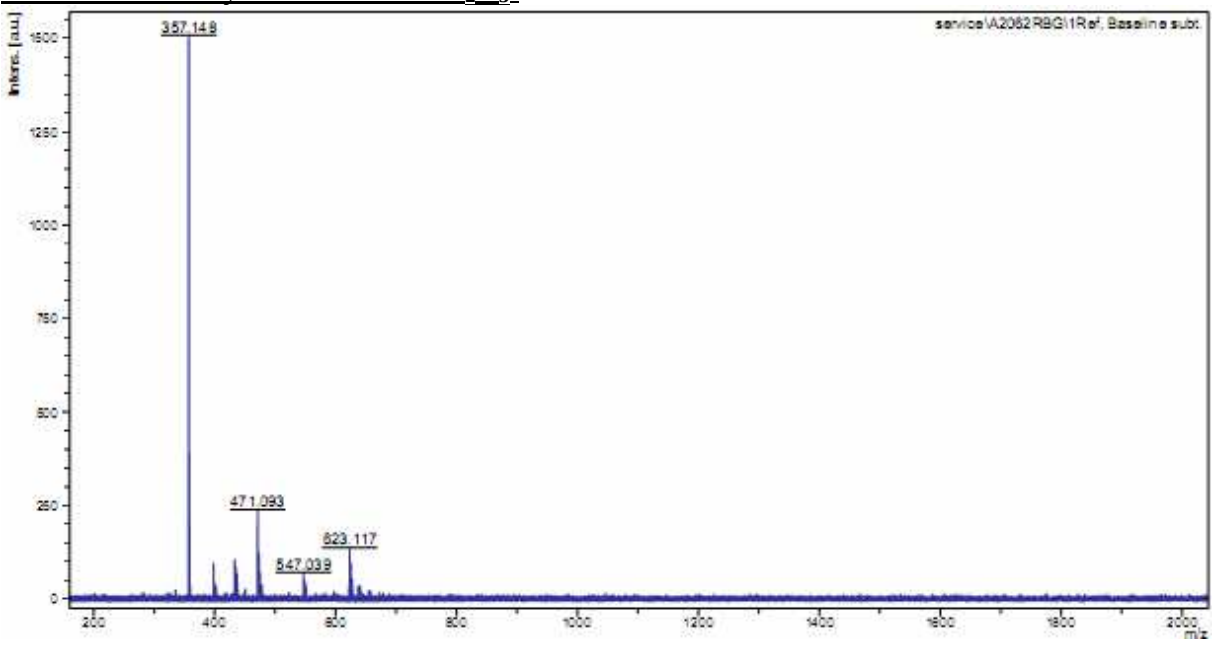

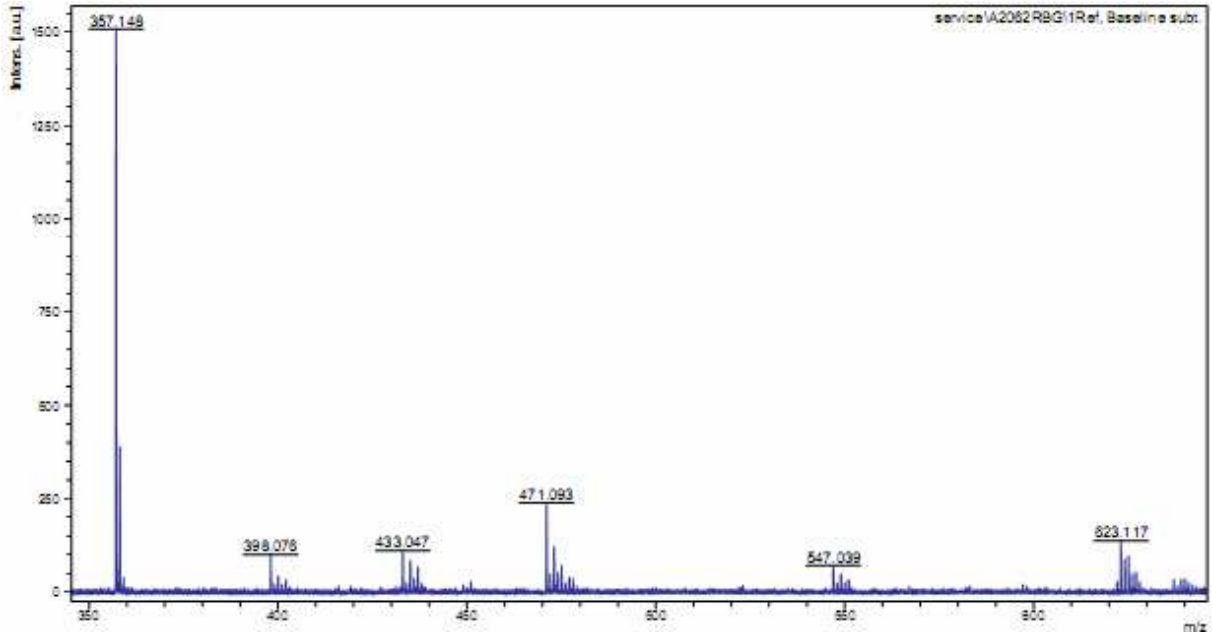

MALDI-TOF analysis of **Zn.1-Oct.N_2C_5**:

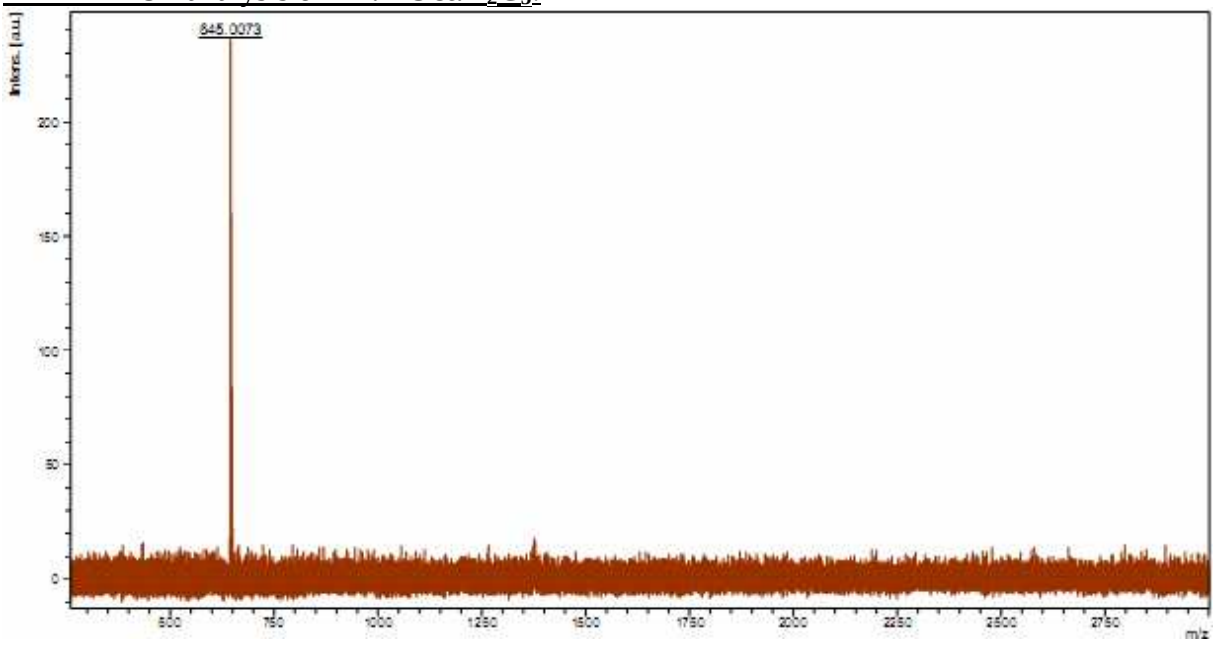

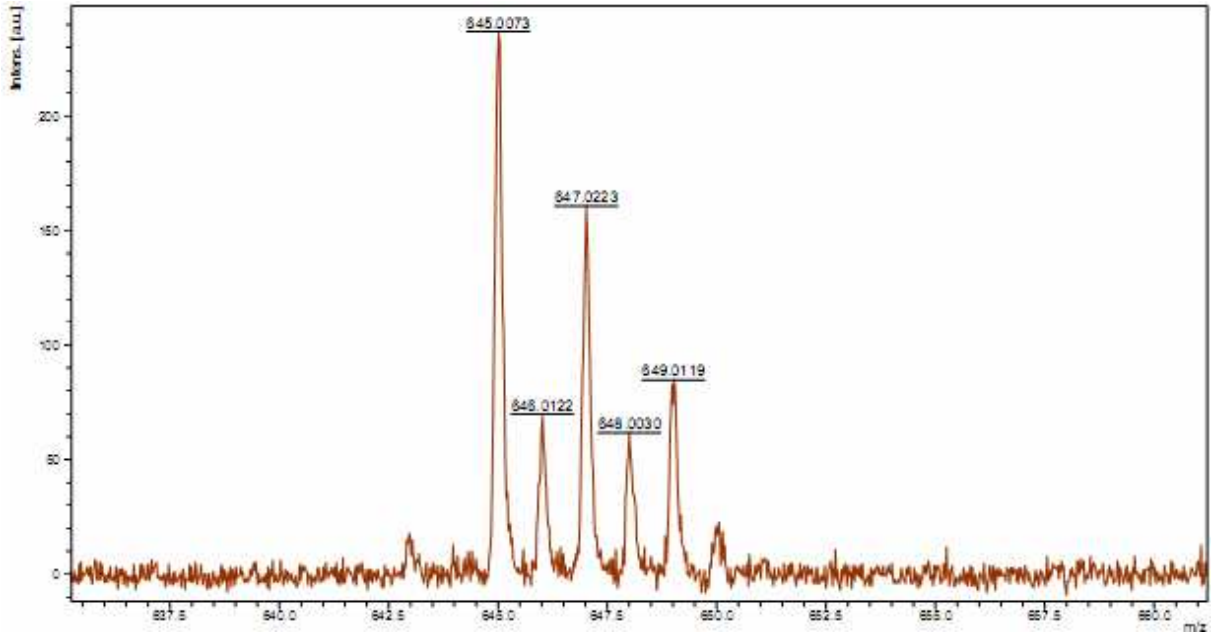

MALDI-TOF analysis of **Zn.1-Me.N_2O**:

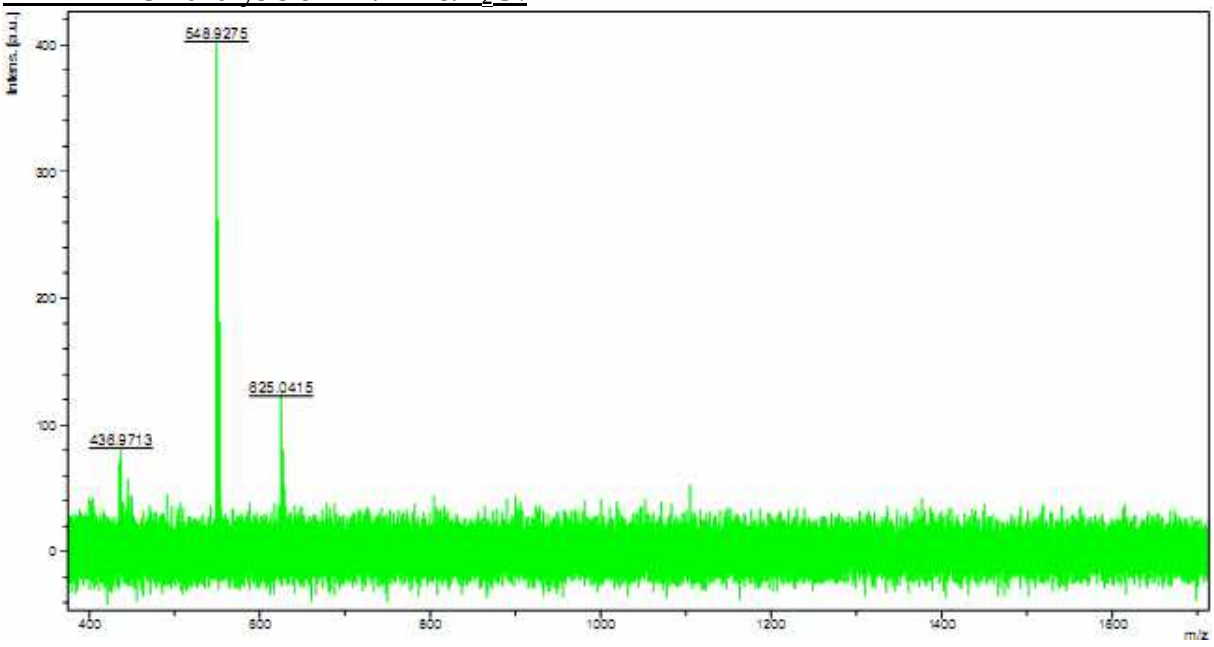

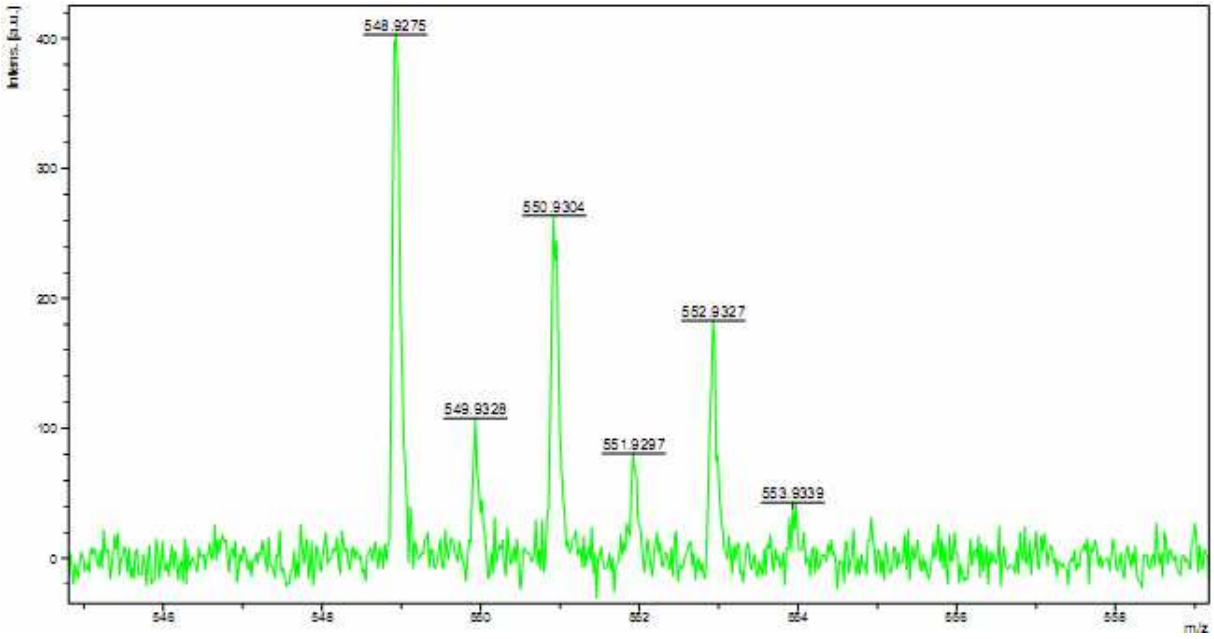

MALDI-TOF analysis of **Pb.1-Me.N_2O_2**:

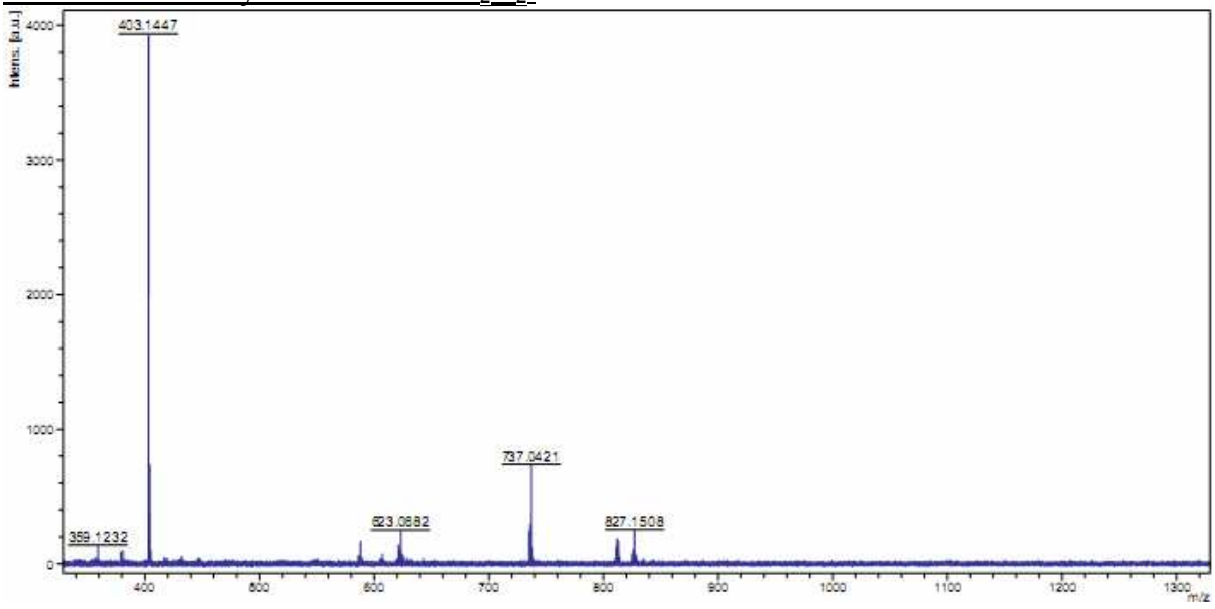

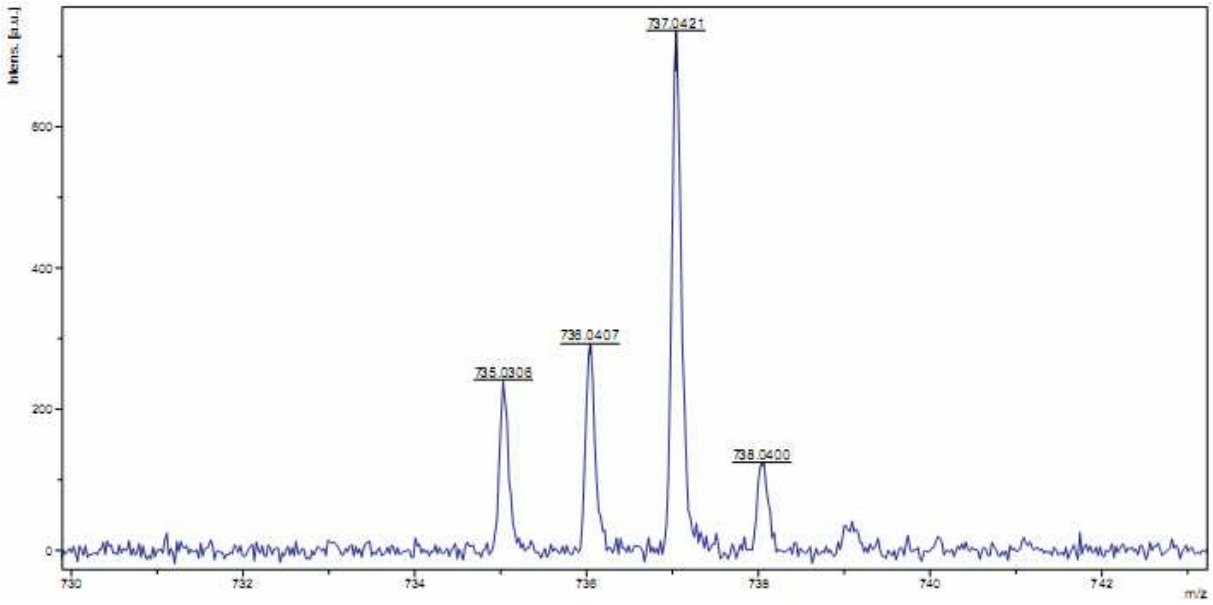

MALDI-TOF analysis of **Pb.1-Me.N_2O_3**:

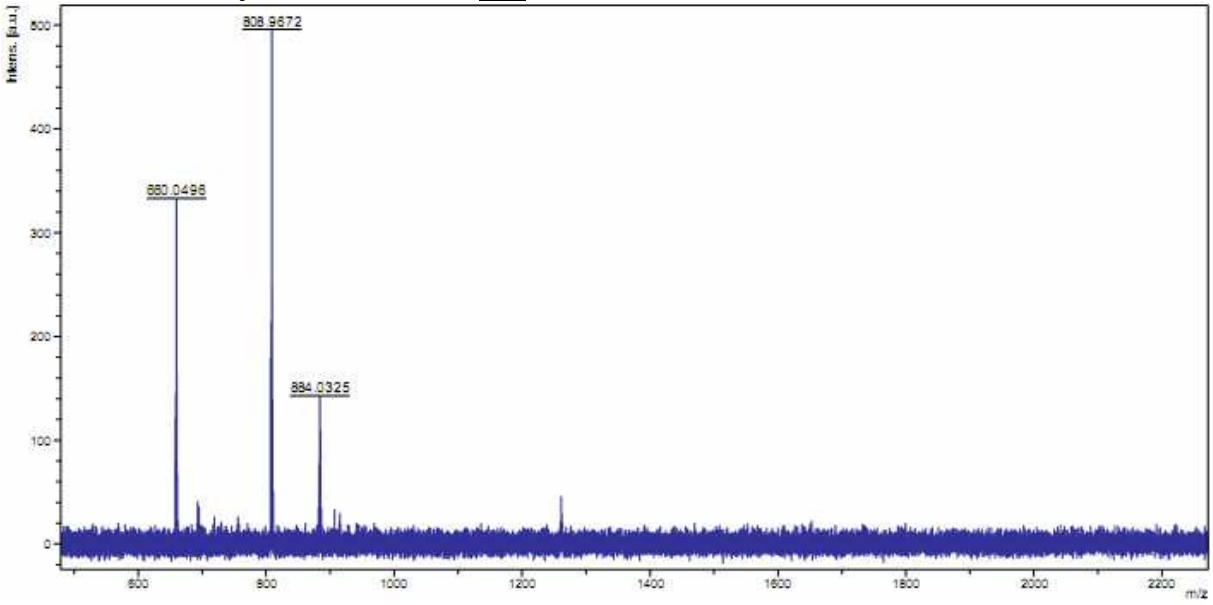

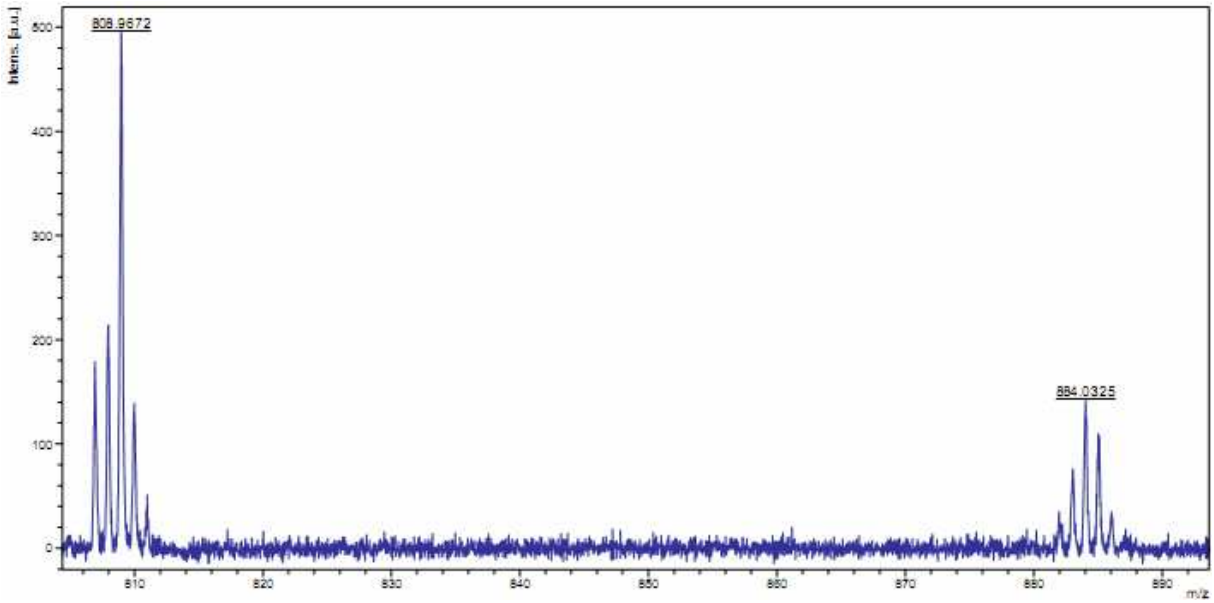

MALDI-TOF analysis of **Pb.1-Oct.N_2O_3**:

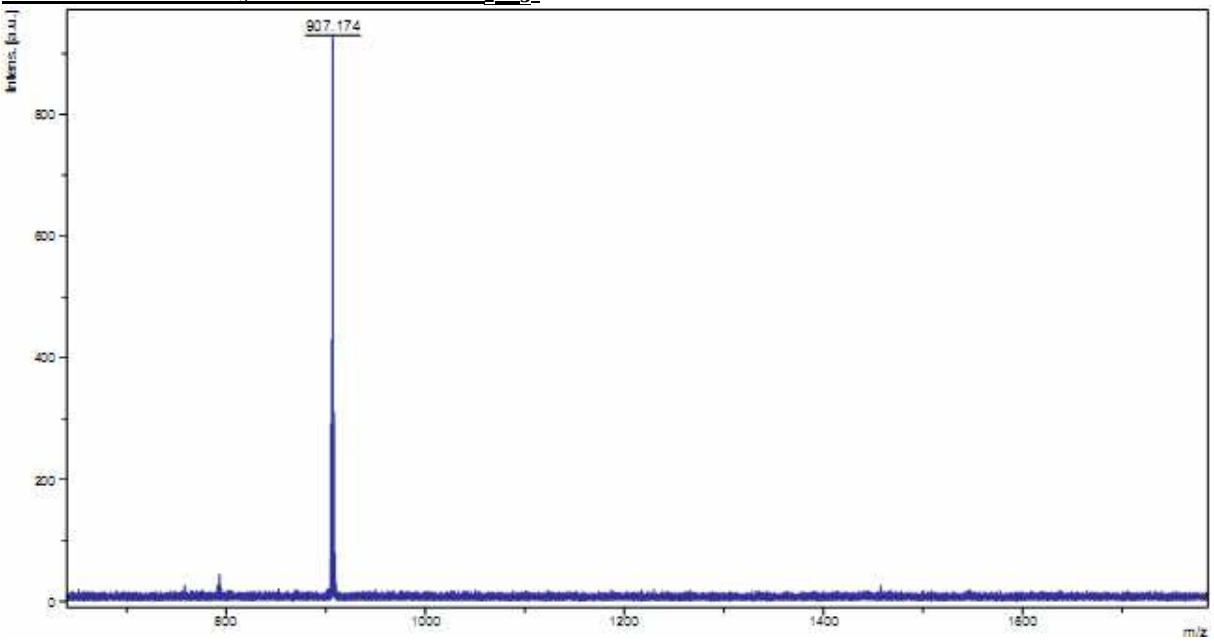

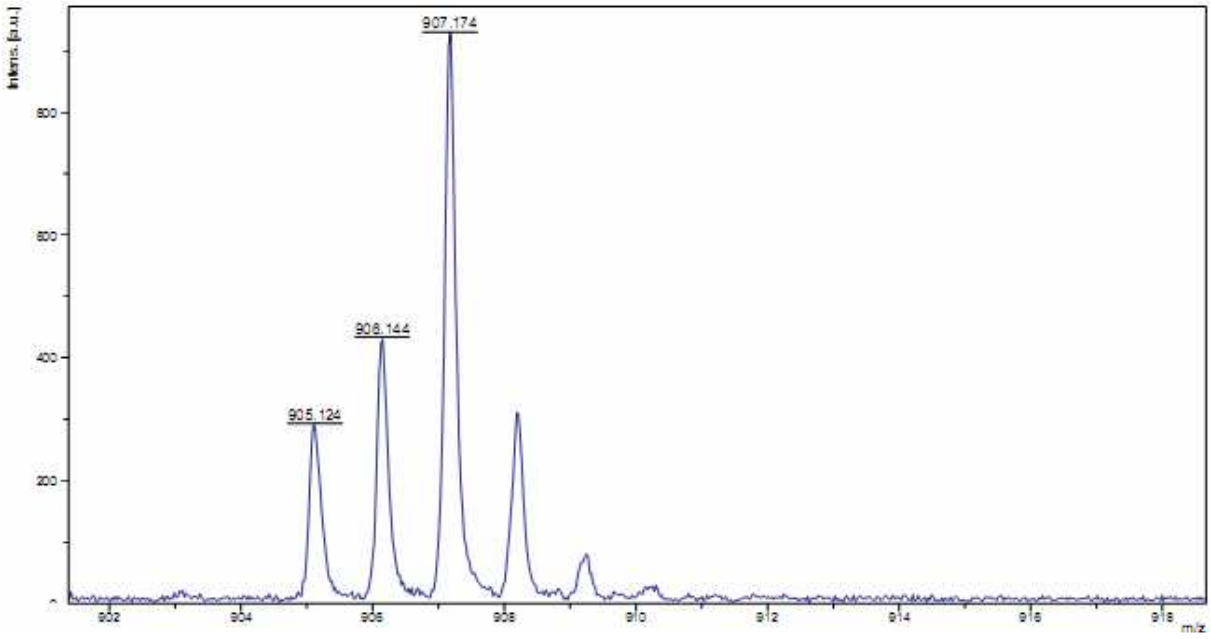

Concentration-dependent NMR spectra of the self-assembly between **1-Oct** and $\mathbf{N_2C_5}$ in $CDCl_3$*/CD_3CN: 8/2 at various concentrations (from bottom to top: 5, 25 and 50 mM):

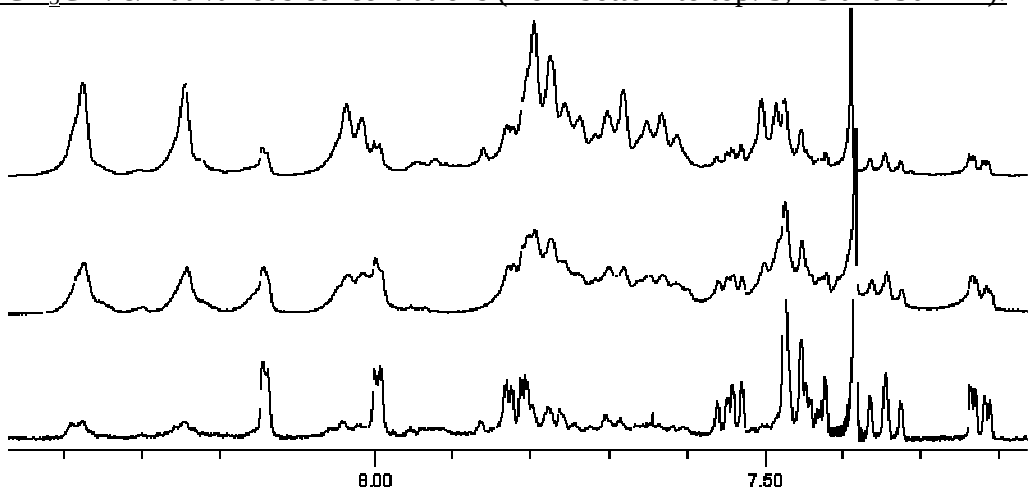

Concentration-dependent NMR spectra of the self-assembly between **1-Oct** and $\mathbf{N_2C_5}$ in $CDCl_3$ at various concentrations (from bottom to top: 5, 50 and 100 mM):

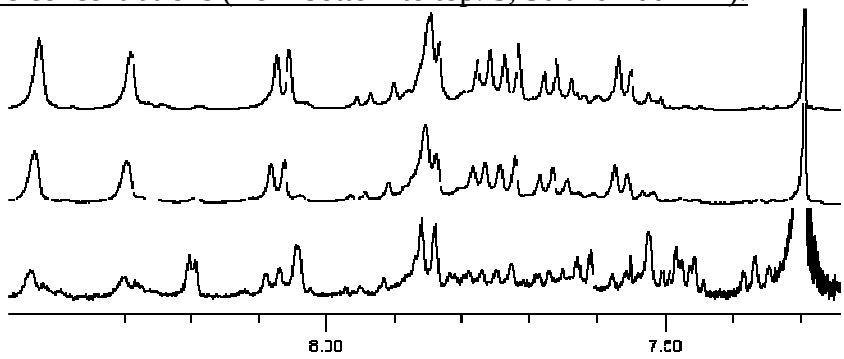

Concentration-dependent NMR spectra of the self-assembly between **1-Oct** and $\mathbf{N_2C_4}$ in $CDCl_3$*/CD_3CN: 8/2 at various concentrations (from bottom to top: 5, 25 and 50 mM):

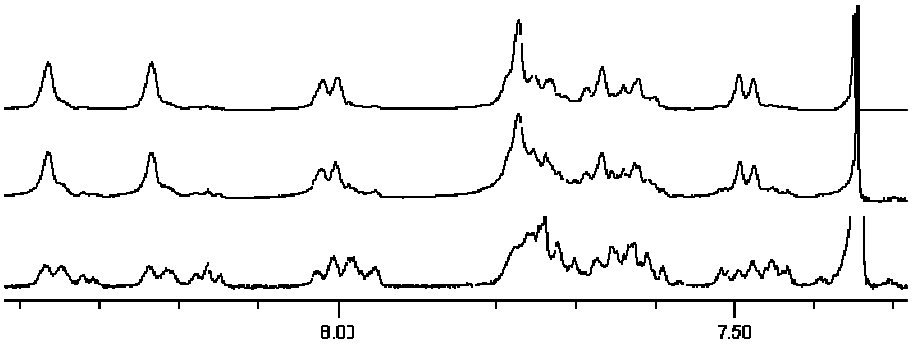

Concentration-dependent NMR spectra of the self-assembly between **1-Oct** and $\mathbf{N_2O_3}$ in $CDCl_3$* at various concentrations (from bottom to top: 5, 50, 77 and 100 mM):

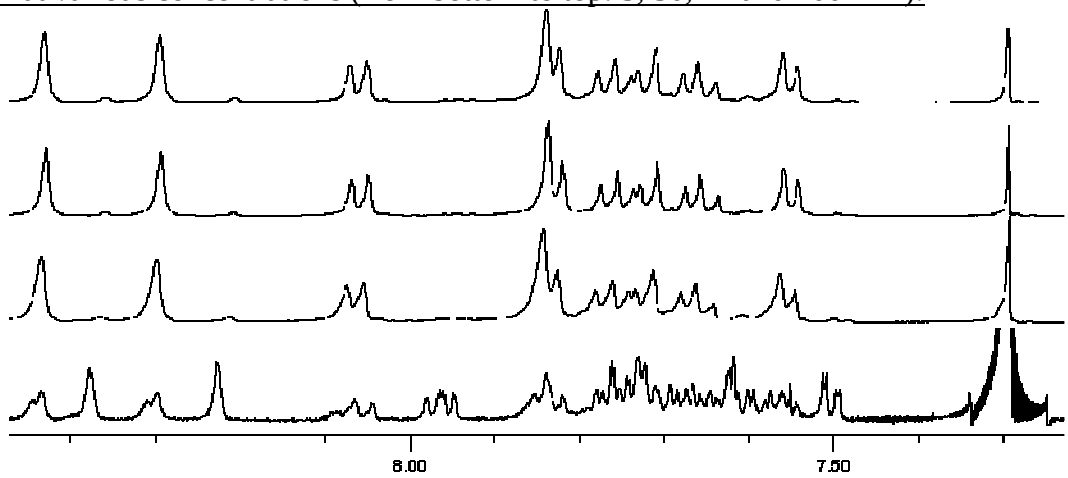

Concentration-dependent NMR spectra of the self-assembly between **1-Oct** and $\mathbf{N_2O_3}$ in $CDCl_3$*/CD_3CN: 6/4 at various concentrations (from bottom to top: 5, 25, and 50 mM):

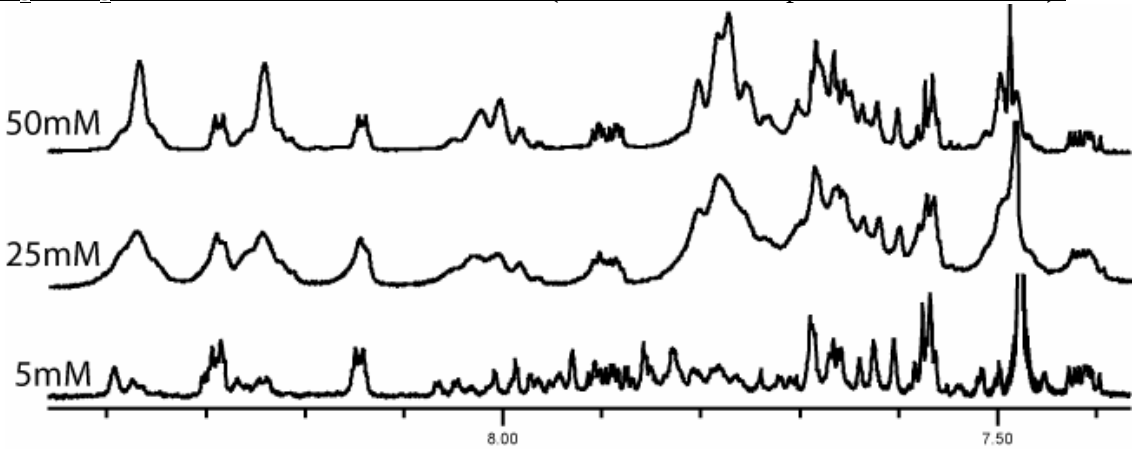

Concentration-dependent NMR spectra of the self-assembly between **1-Me** and $\mathbf{N_2C_5}$ in $CDCl_3$* at various concentrations (from bottom to top: 5, 25 and 50 mM):

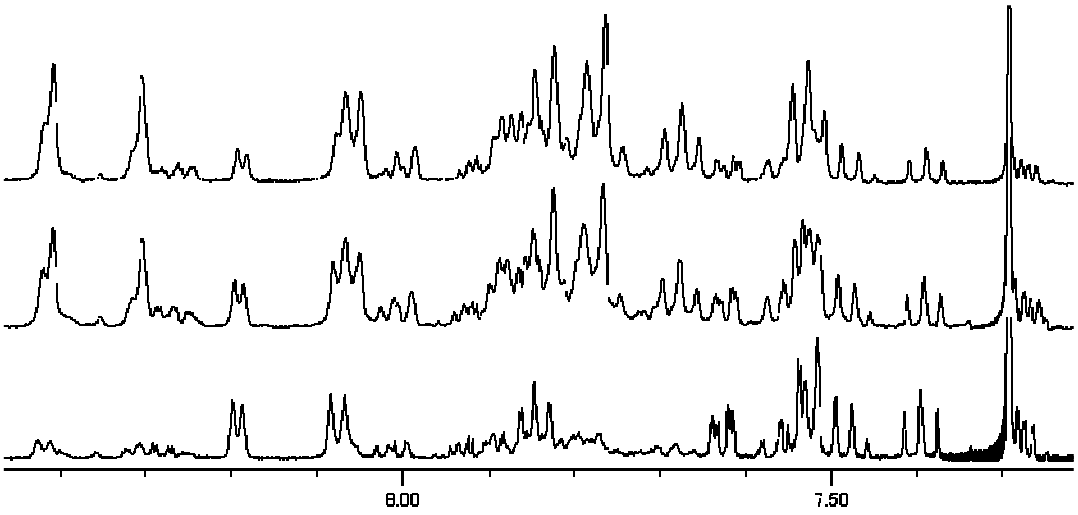

Concentration-dependent NMR spectra of the self-assembly between **1-Me** and $\mathbf{N_2O_2}$ in $CDCl_3$* at various concentrations (from bottom to top: 5, 25 and 50 mM):

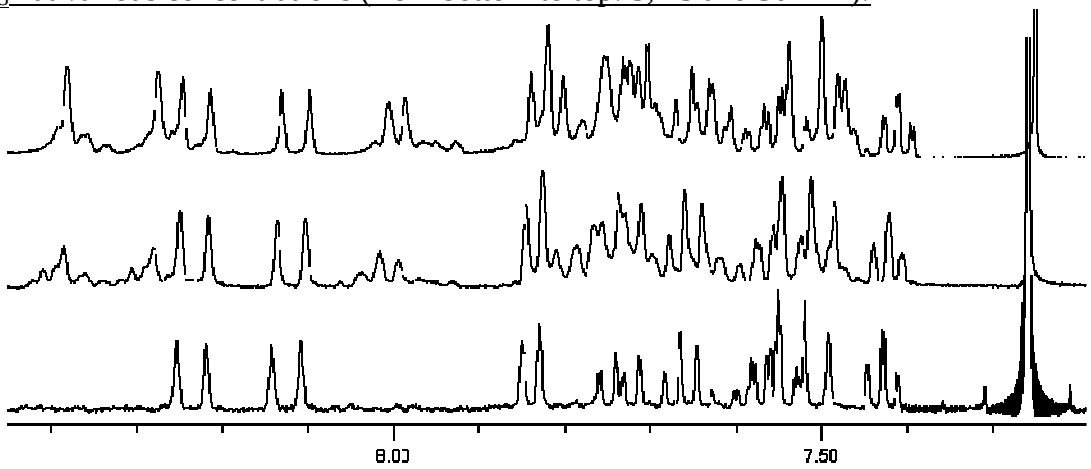

DSC analysis of **P4**:

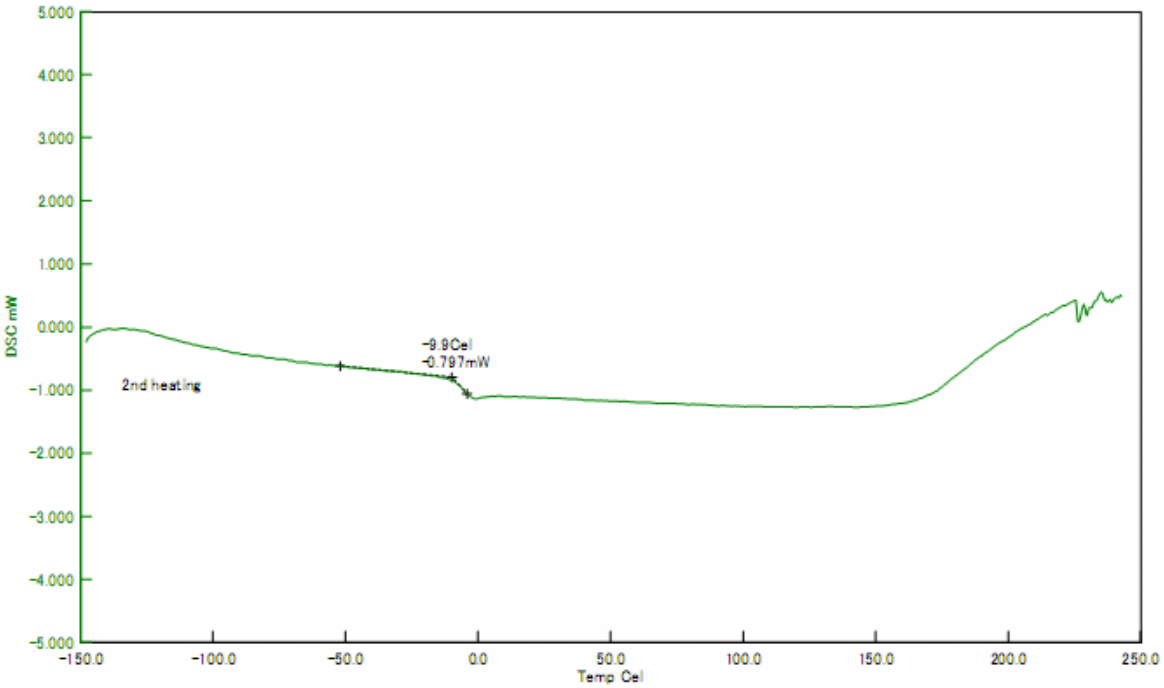

DSC analysis of **P2**:

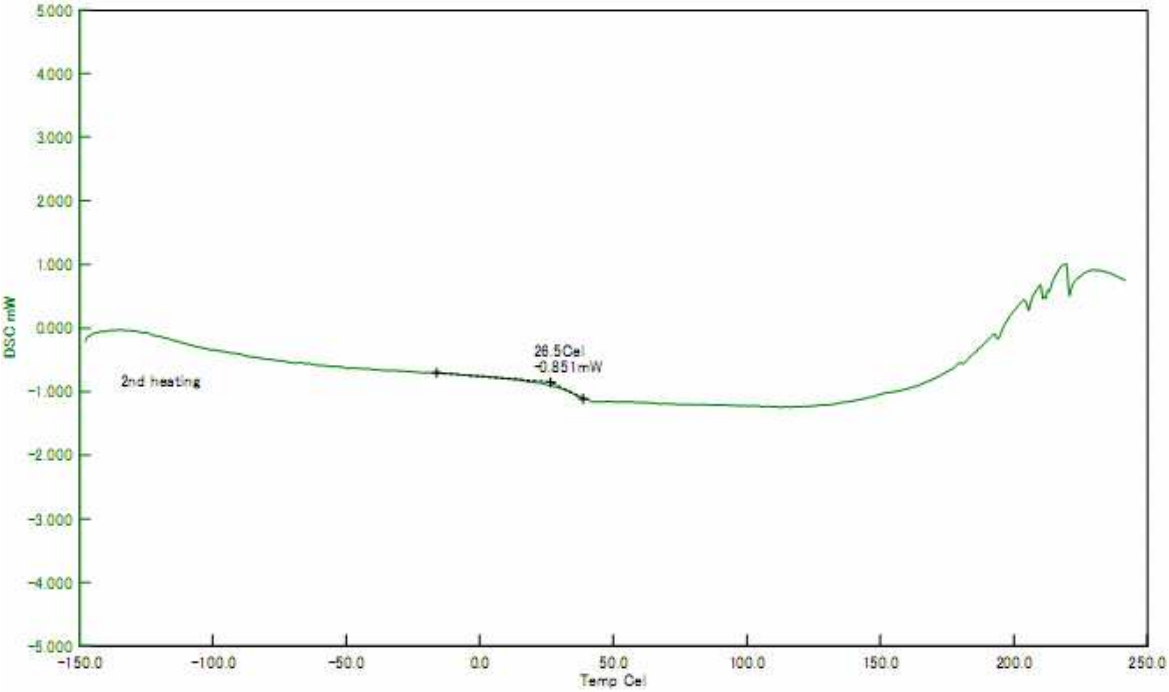

DSC analysis of **P4'**:

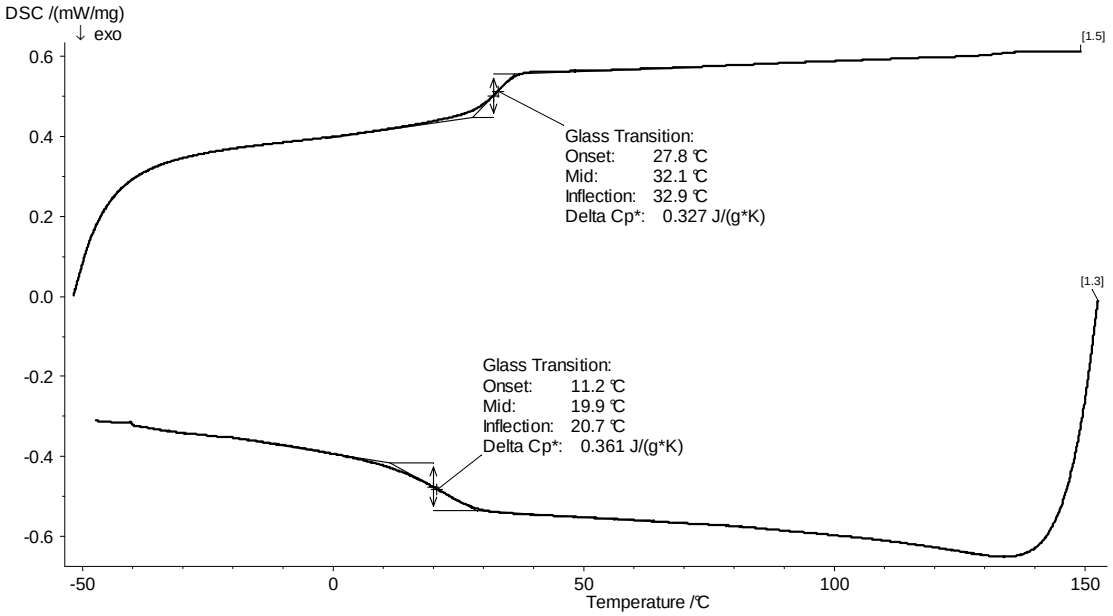

MALDI-TOF analysis of the self-assembly between **1-Oct** and $\mathbf{N_2C_4}$ showing the macrocyclic species present at low concentration:

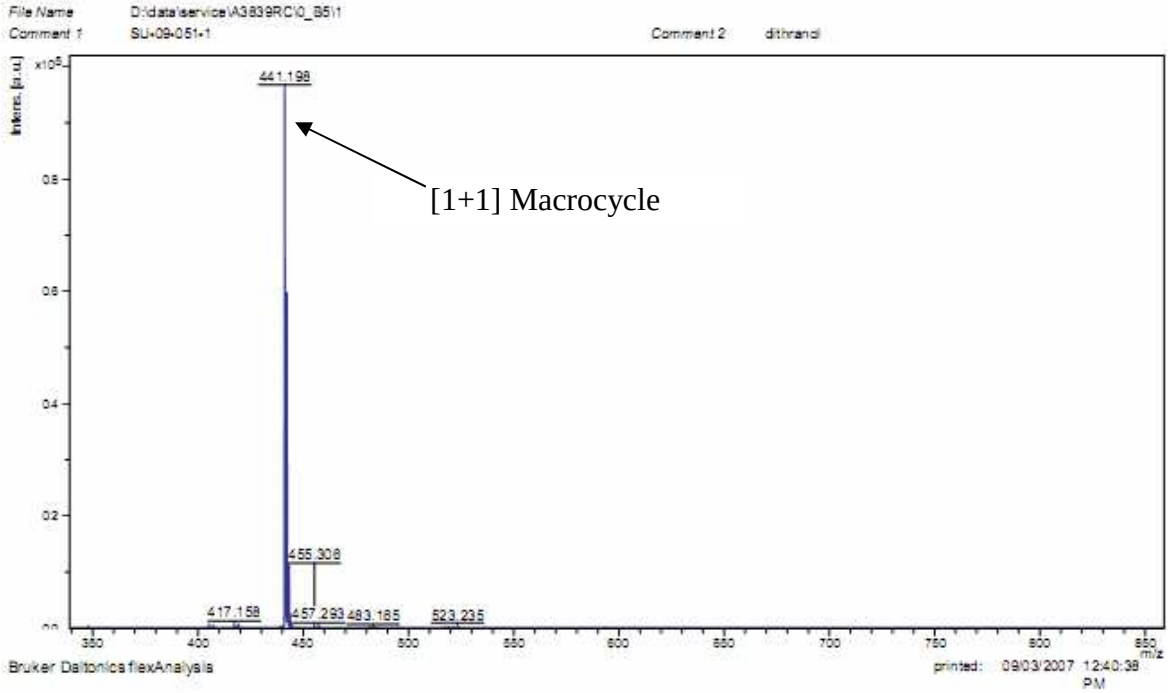

Calculated for $[C_{25}H_{34}N_6+Na]^+$ (m/z): 441.2743 (100.0%), 442.2776 (27.0%), 443.2810 (3.5%)

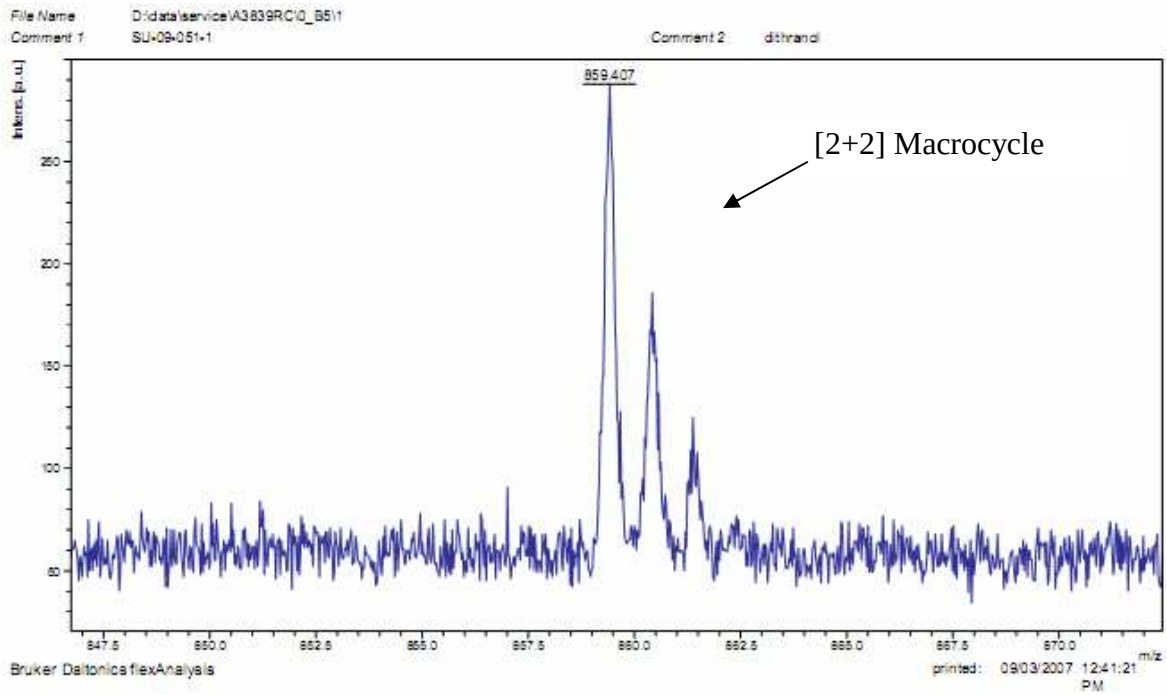

Calculated for $[C_{50}H_{68}N_{12}+Na]^+$ (m/z): 859.5588 (100.0%), 860.5621 (54.1%), 861.5655 (14.3%)

MALDI-TOF analysis of the self-assembly between **1-Oct** and $\mathbf{N_2C_5}$ showing the macrocyclic species present at low concentration:

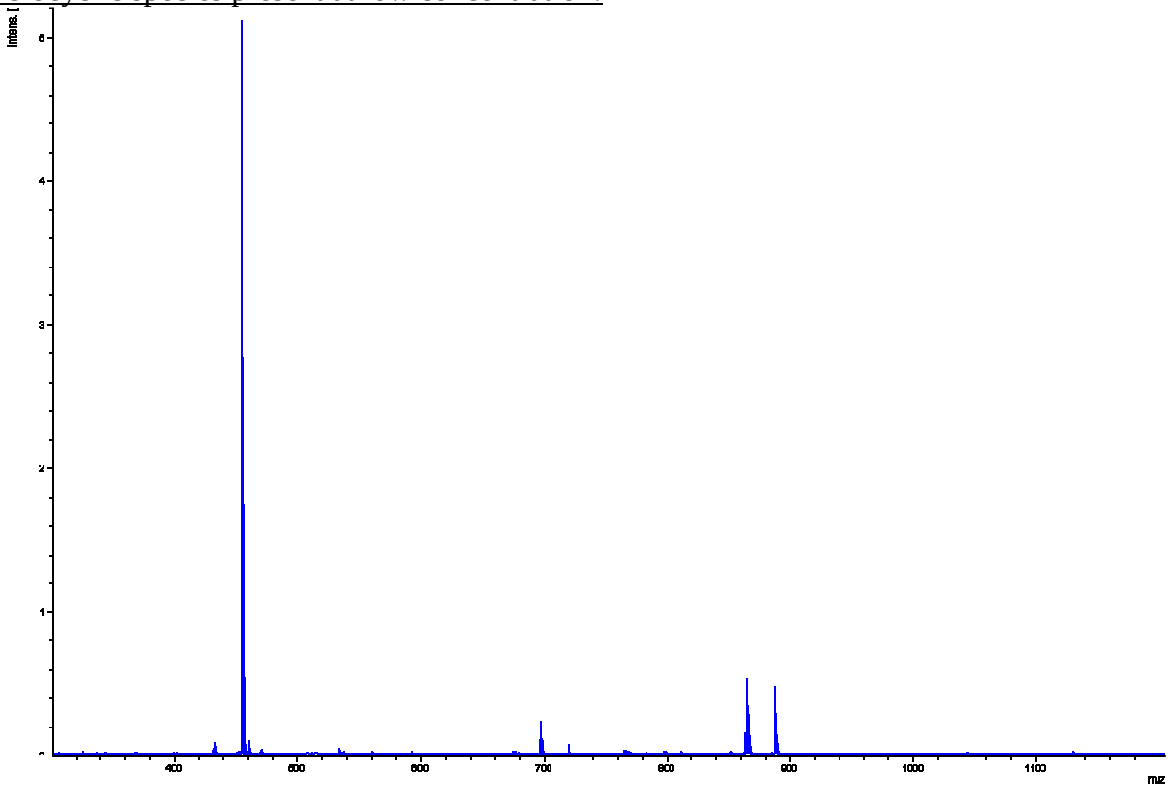

Calculated for $[C_{26}H_{36}N_6+H]^+$ (m/z): 433.3080 (100.0%), 434.3113 (28.1%), 435.3147 (3.8%) ; $[C_{26}H_{36}N_6+Na]^+$ (m/z): 455.2899 (100.0%), 456.2933 (28.1%), 457.2966 (3.8%).

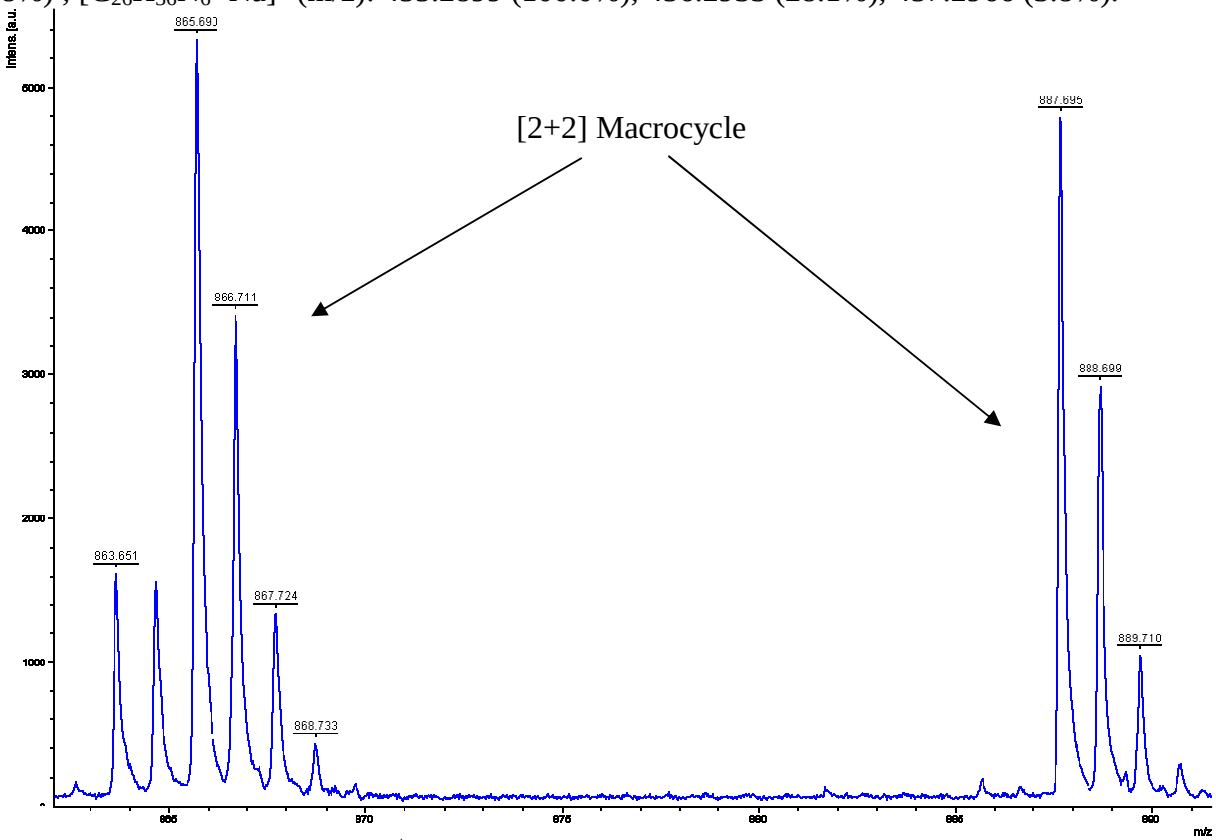

Calculated for $[C_{52}H_{72}N_{12}+H]^+$ (m/z): 865.6081 (100.0%), 866.6115 (56.2%), 867.6148 (15.5%) ; $[C_{52}H_{72}N_{12}+Na]^+$ (m/z): 887.5901 (100.0%), 888.5934 (56.2%), 889.5968 (15.5%).

MALDI-TOF analysis of the self-assembly between **1-Oct** and $\mathbf{N_2O_3}$ showing the macrocyclic species present at low concentration:

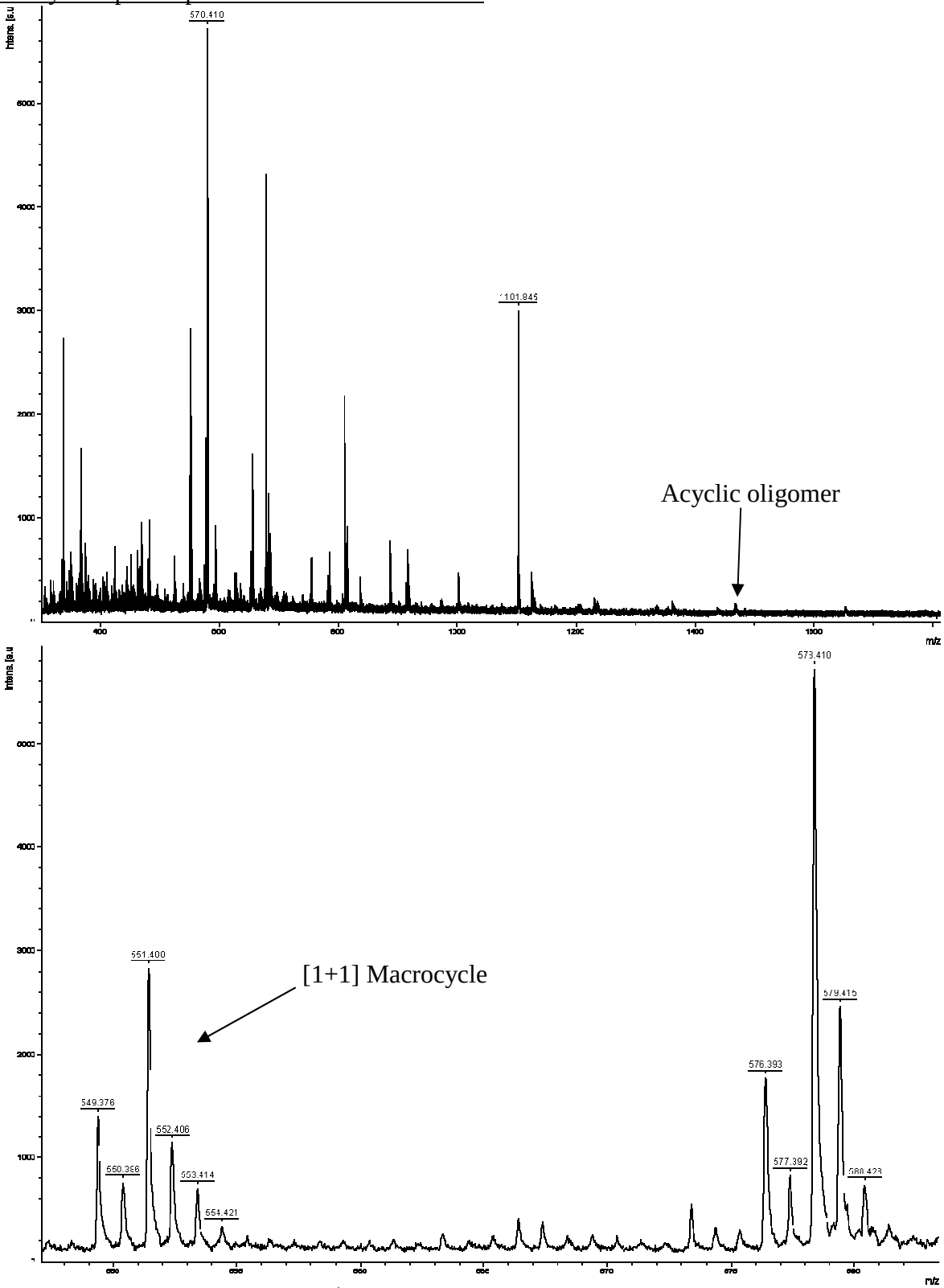

Calculated for $[C_{31}H_{47}N_6O_3+H]^+$ (m/z): 551.3710 (100.0%), 552.3743 (33.5%), 553.3777 (5.4%).

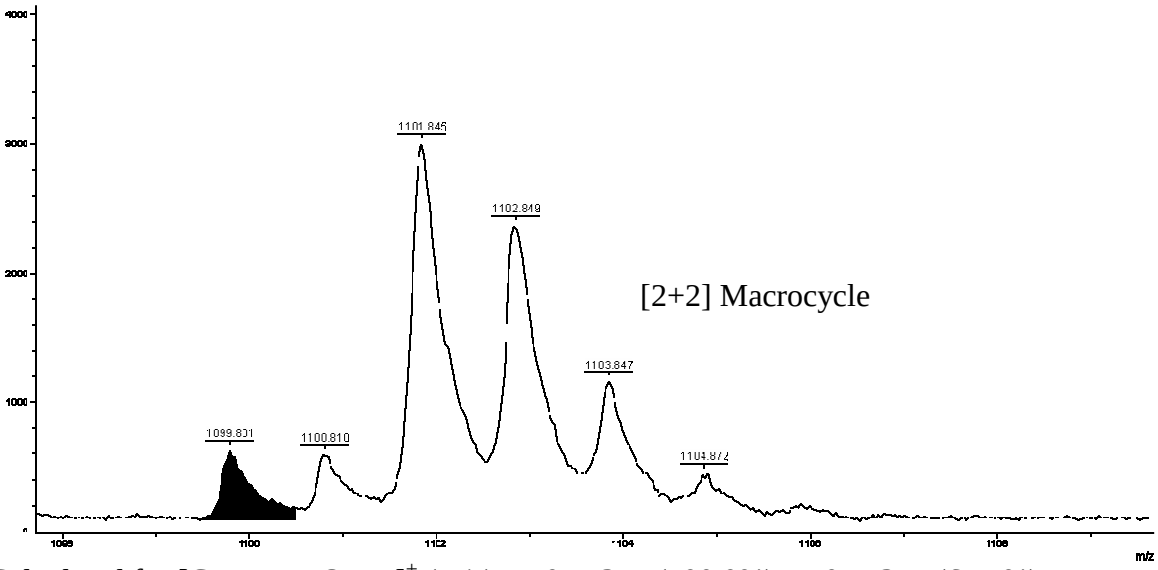

Calculated for $[C_{62}H_{93}N_{12}O_6+H]^+$ (m/z): 1101.7341 (100.0%), 1102.7375 (67.1%).

MALDI-TOF (dithranol) analysis of the self-assembly between **1**-**Me** and **N_2C_5** showing the macrocyclic species present at low concentration:

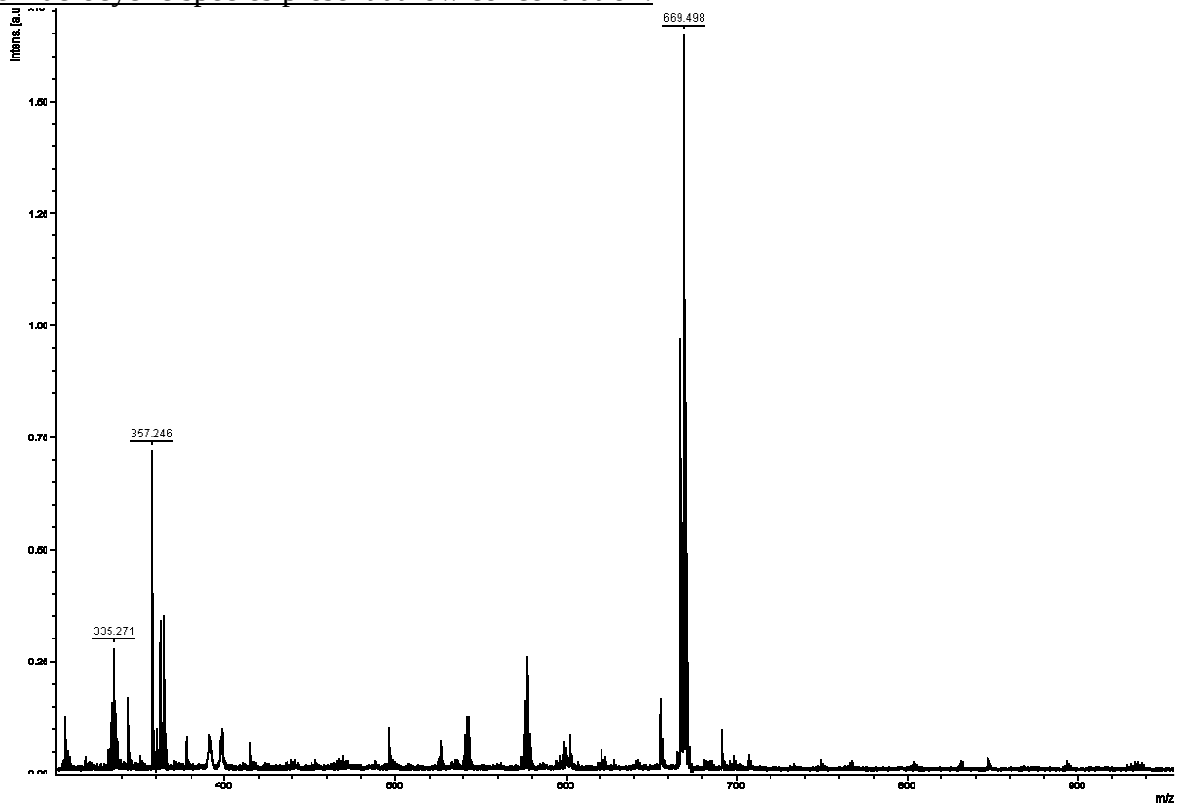

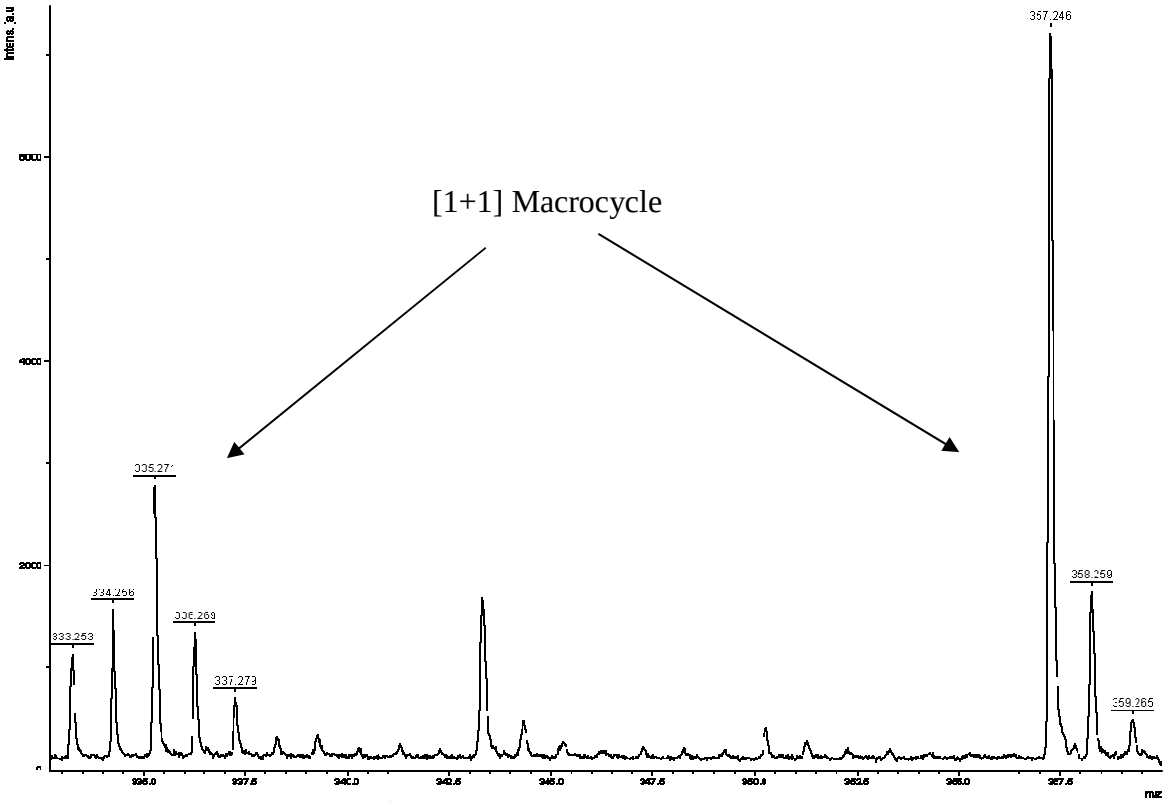

Calculated for $[C_{19}H_{23}N_6+H]^+$ (m/z): 335.1984 (100.0%), 336.2018 (20.5%), 336.1955 (2.2%) ; $[C_{19}H_{23}N_6+Na]^+$ (m/z): 357.1804 (100.0%), 358.1837 (20.5%), 358.1774 (2.2%).

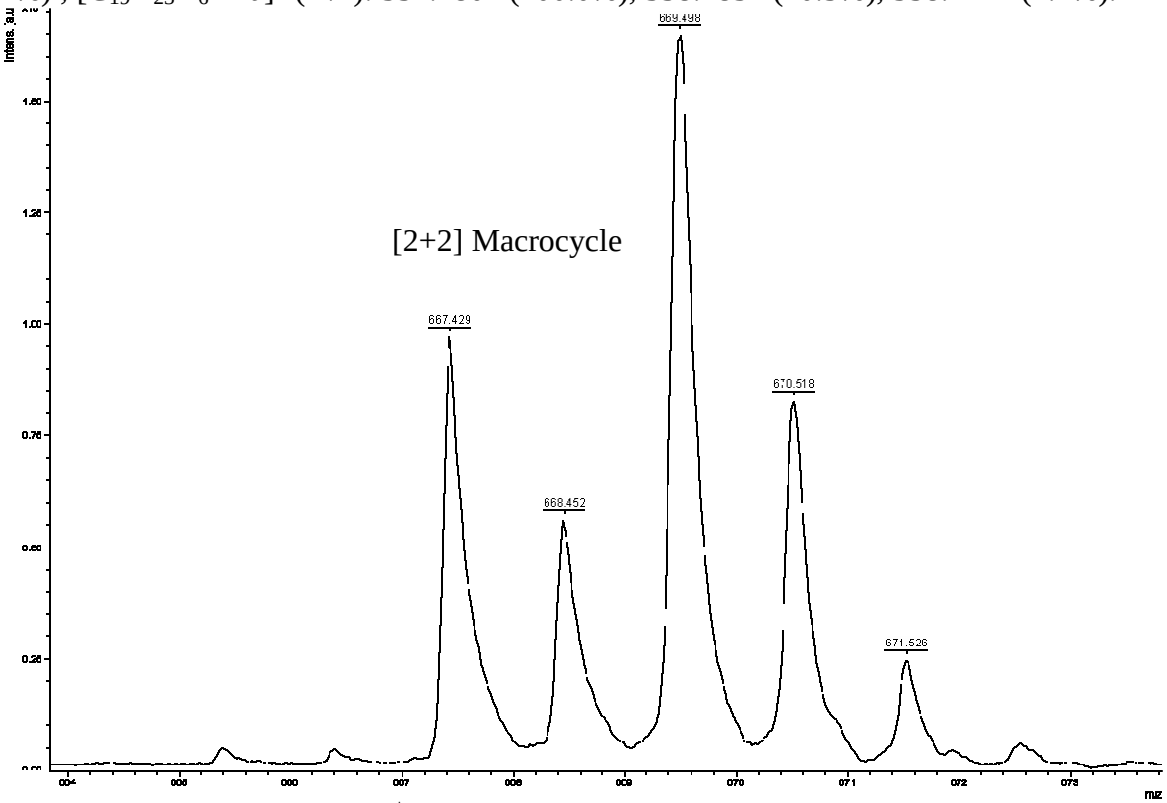

Calculated for $[C_{38}H_{45}N_{12}+H]^+$ (m/z): 669.3890 (100.0%), 670.3924 (41.1%), 671.3957 (8.2%).

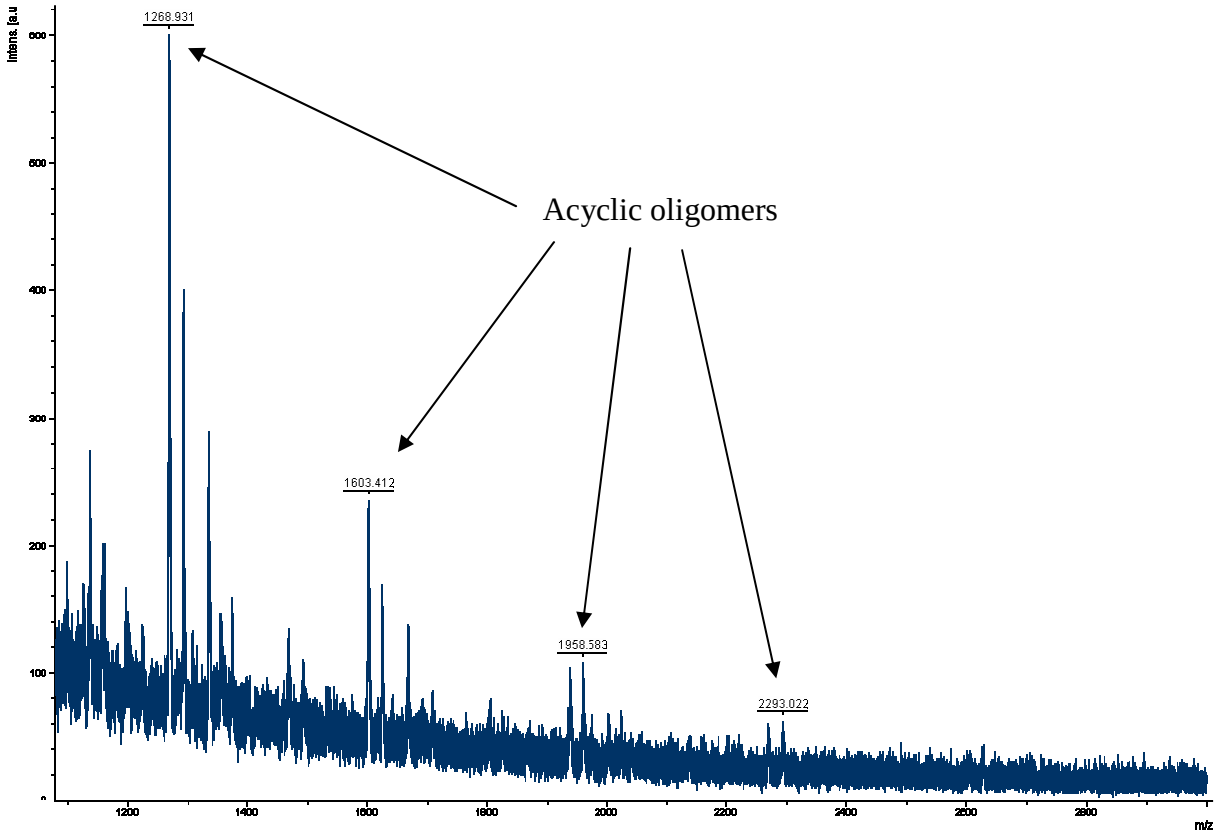

MALDI-TOF analysis of the self-assembly between **1-Me** and **N_2O_2** showing the macrocyclic species present at low concentration:

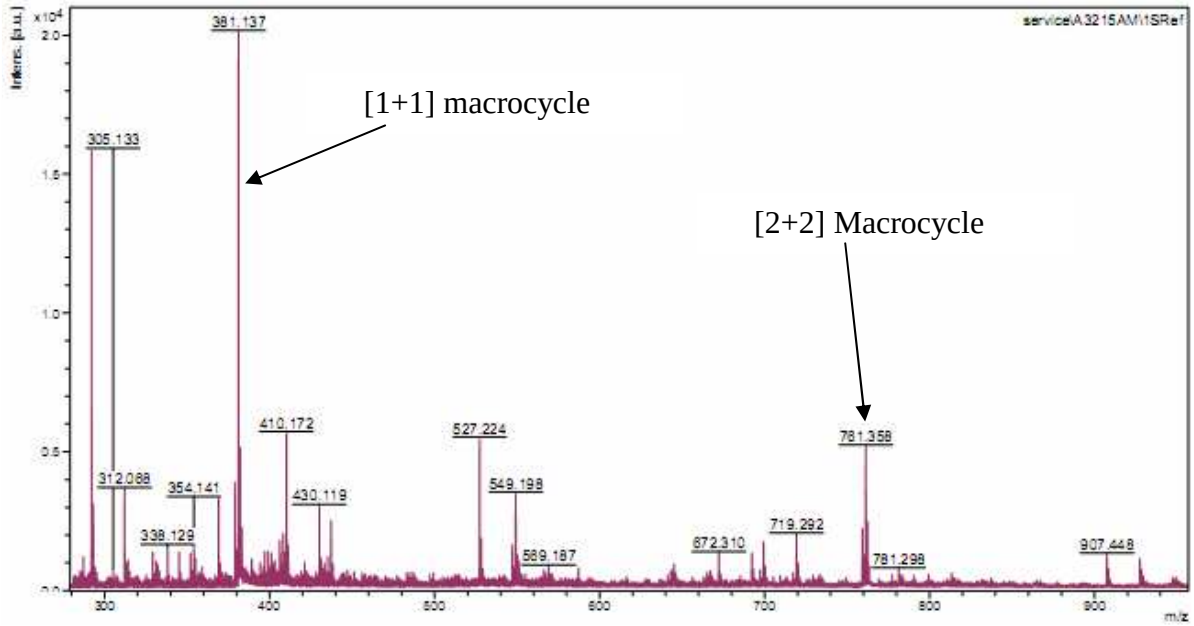

Calculated for $[C_{20}H_{25}N_6O_2+H]^+$ (m/z): 381.2039 (100.0%), 382.2073 (21.6%), 383.2106 (2.2%) ; $[C_{40}H_{49}N_{12}O_4+H]^+$ (m/z): 761.4000 (100.0%), 762.4033 (43.3%), 763.4067 (9.1%).

MALDI-TOF analysis of the self-assembly between **1-Me** and **N_2O_3** showing the macrocyclic species present at low concentration:

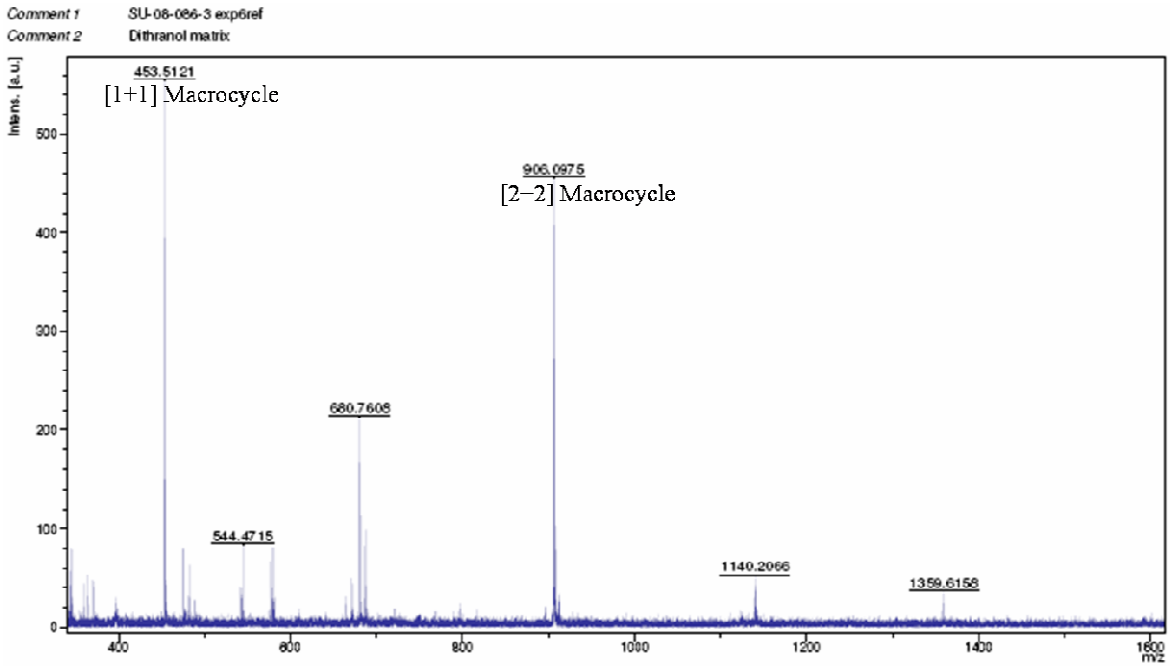

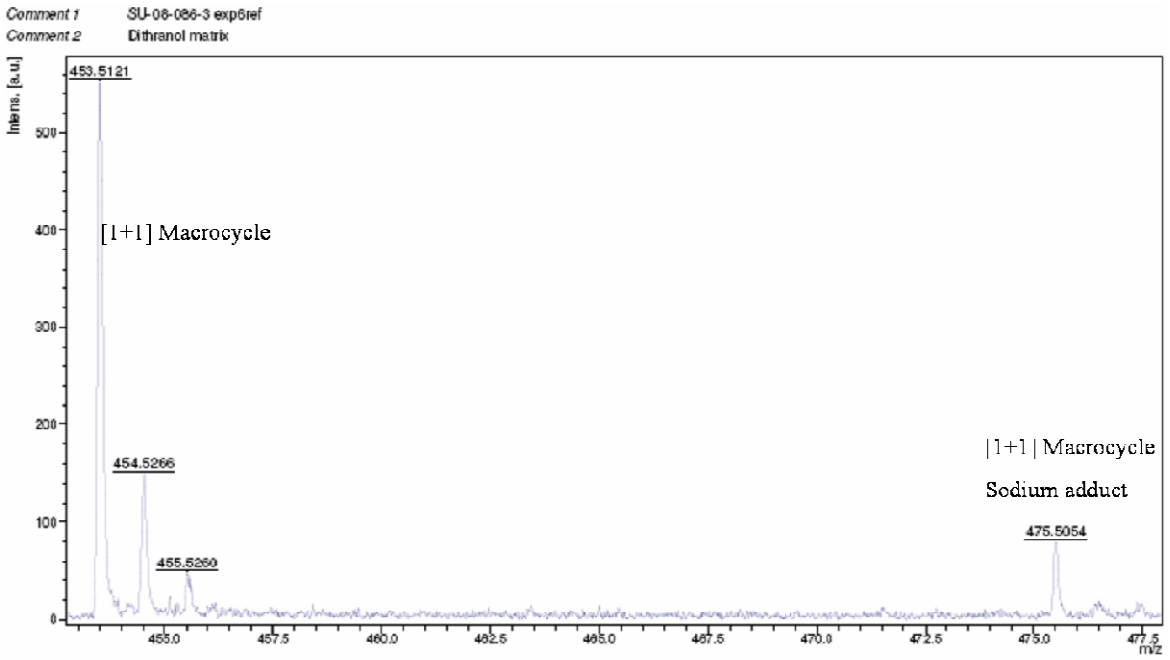

Calculated for $[C_{24}H_{32}N_6O_3+H]^+$ (m/z): 453.2614 (100.0%), 454.2648 (26.0%), 455.2681 (3.2%)

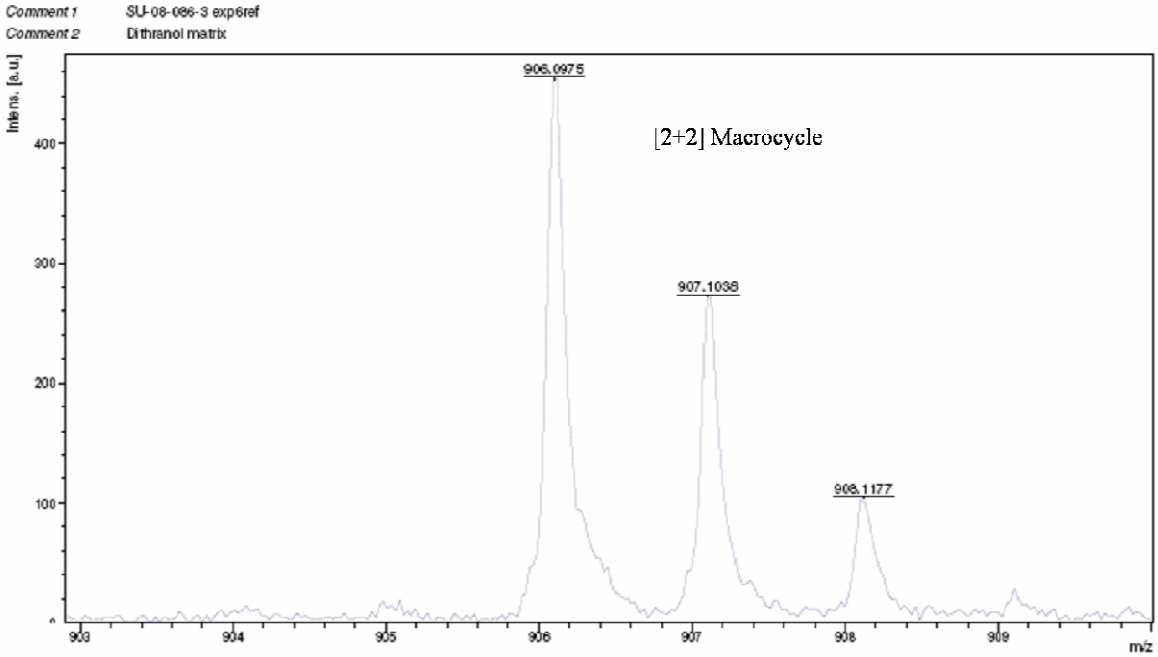

Calculated for $[C_{48}H_{64}N_{12}O_6+H]^+$ (m/z): 905.5150 (100.0%), 906.5184 (51.9%), 907.5217 (13.2%), 906.5120 (4.4%), 907.5154 (2.3%), 908.5251 (2.2%), 907.5192 (1.2%)

DOSY NMR of the self-assembly between **1-Me** and $\mathbf{N_2O_3}$ at 50 mM in $CDCl_3$* (fresh sample):

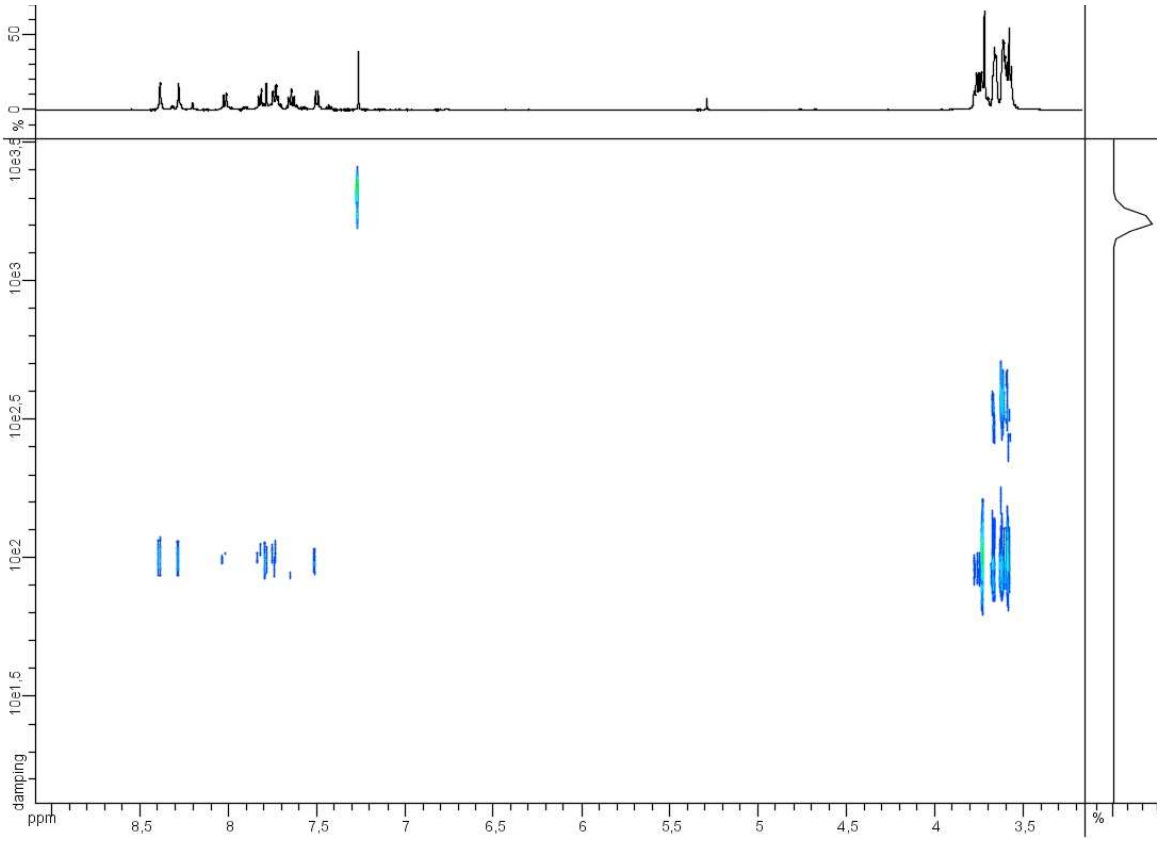

Small Angle Neutrons Scattering curves of **P2**:

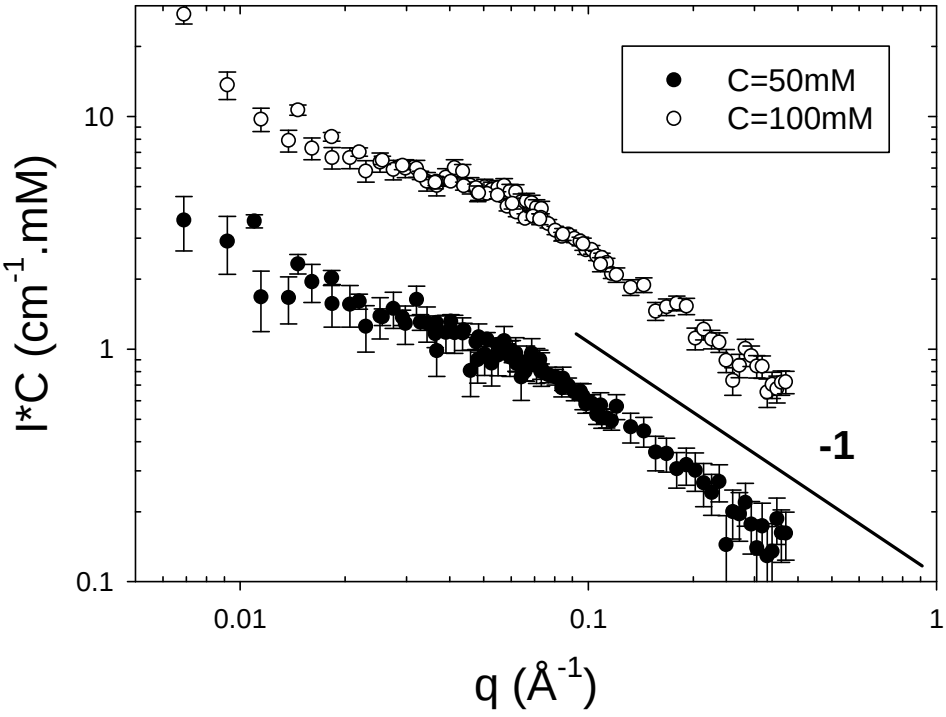

Small Angle Neutrons Scattering curves of **P4'**:

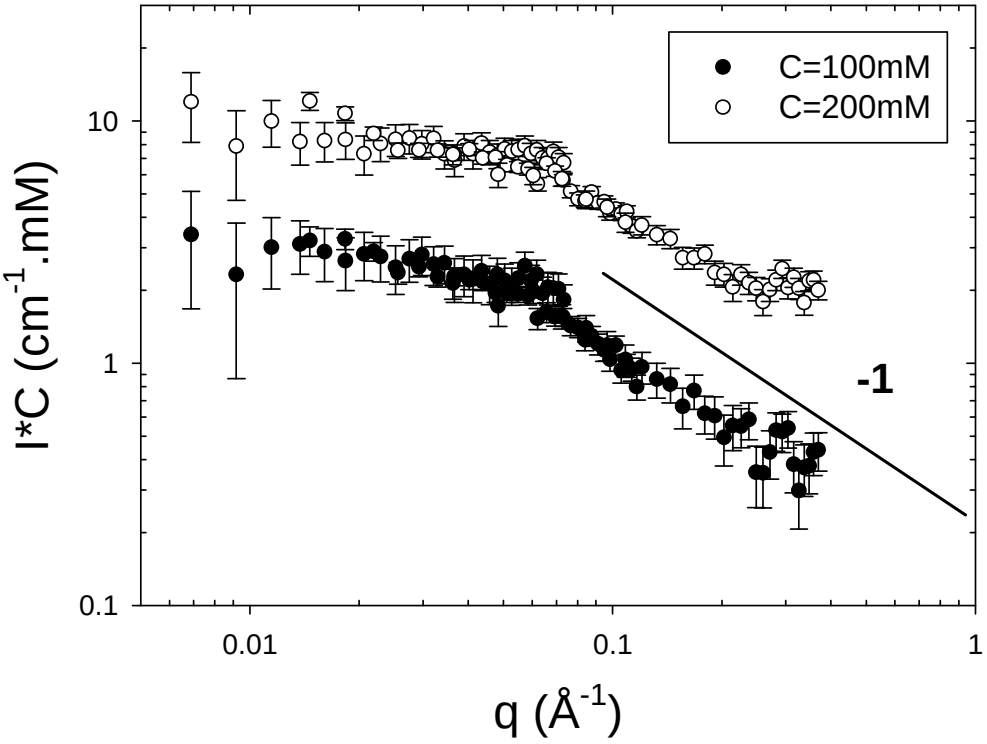

Small Angle Neutrons Scattering curves of **P4** (T=52.3°C):

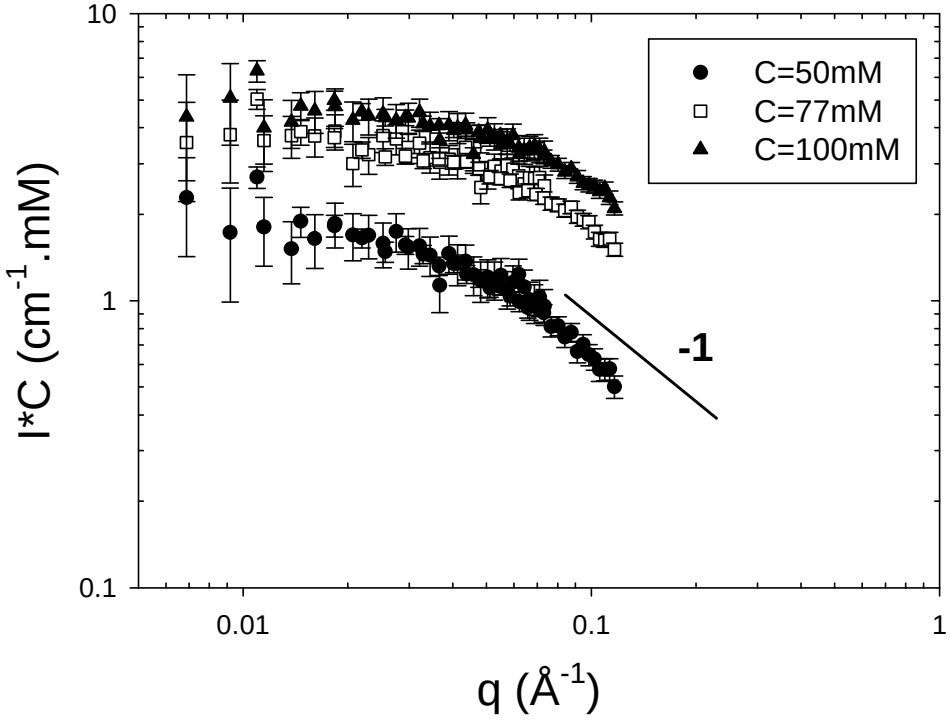

Small Angle Neutrons Scattering curves of dehydrated **P4**:

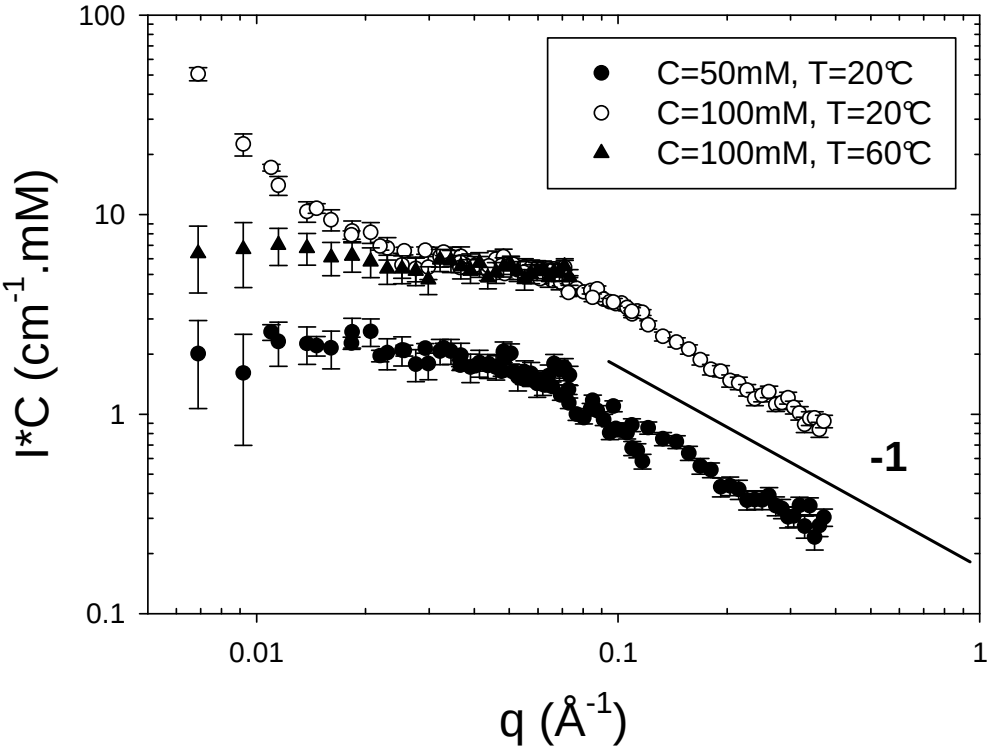

Dehydration was performed by leaving the chloroform solution containing the polymer onto anhydrous sodium sulfate. The aggregation behaviour observed may be due to a too long storage before analysis (see text).

DOSY NMR of the self-assembly between **1-Me** and **N_2O** at 5 mM in $CDCl_3$*:

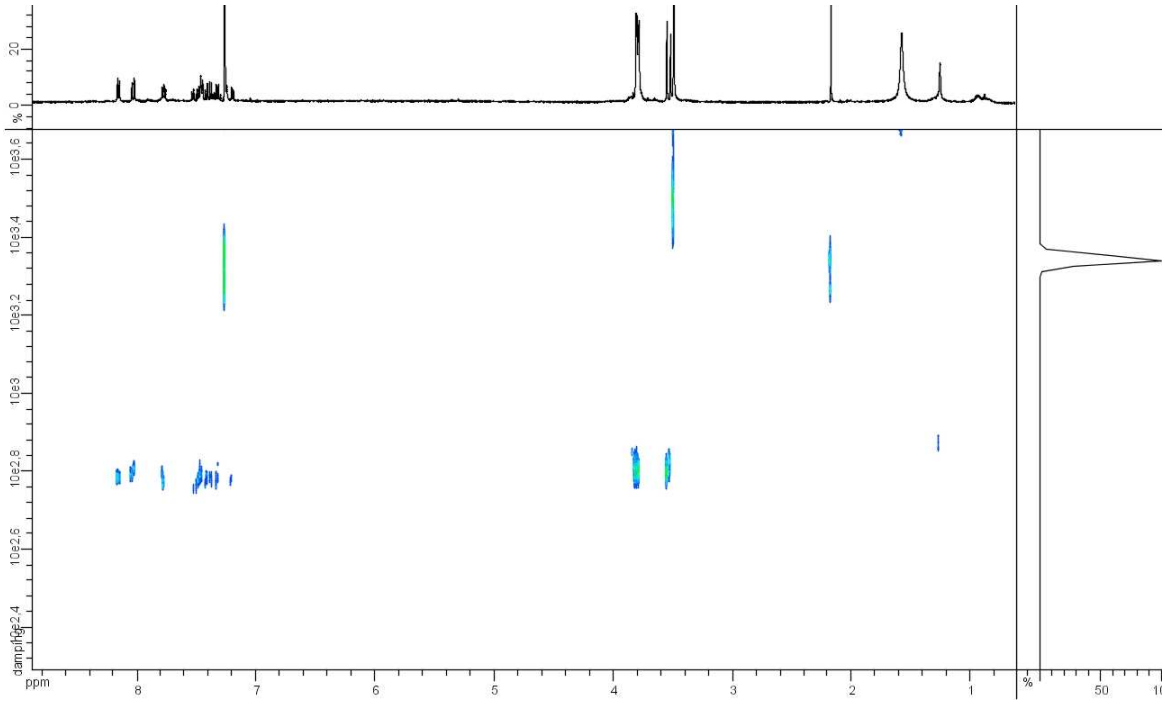

DOSY NMR of the self-assembly between **1-Me** and **N_2O** at 50 mM in $CDCl_3$*:

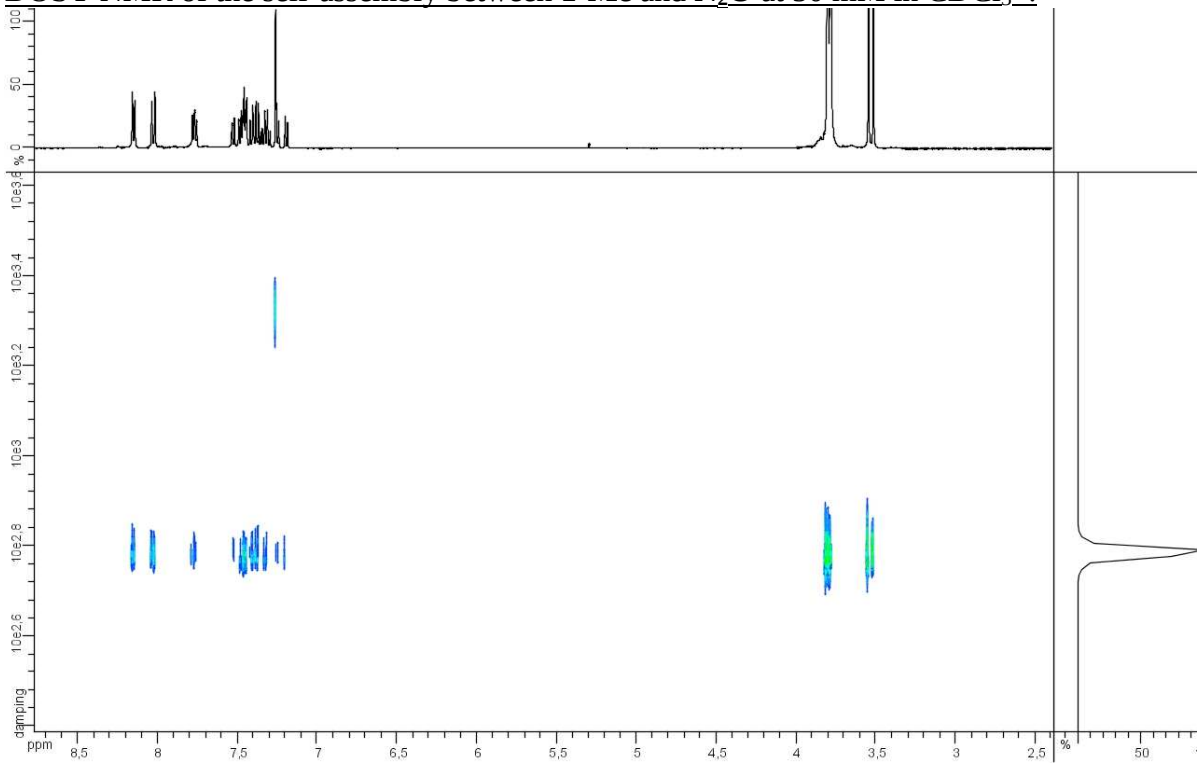

DOSY NMR of the self-assembly between **Zn.2$_2$** and **N_2C_3'** at 5 mM in $CDCl_3$*/CD_3CN: 6/4:

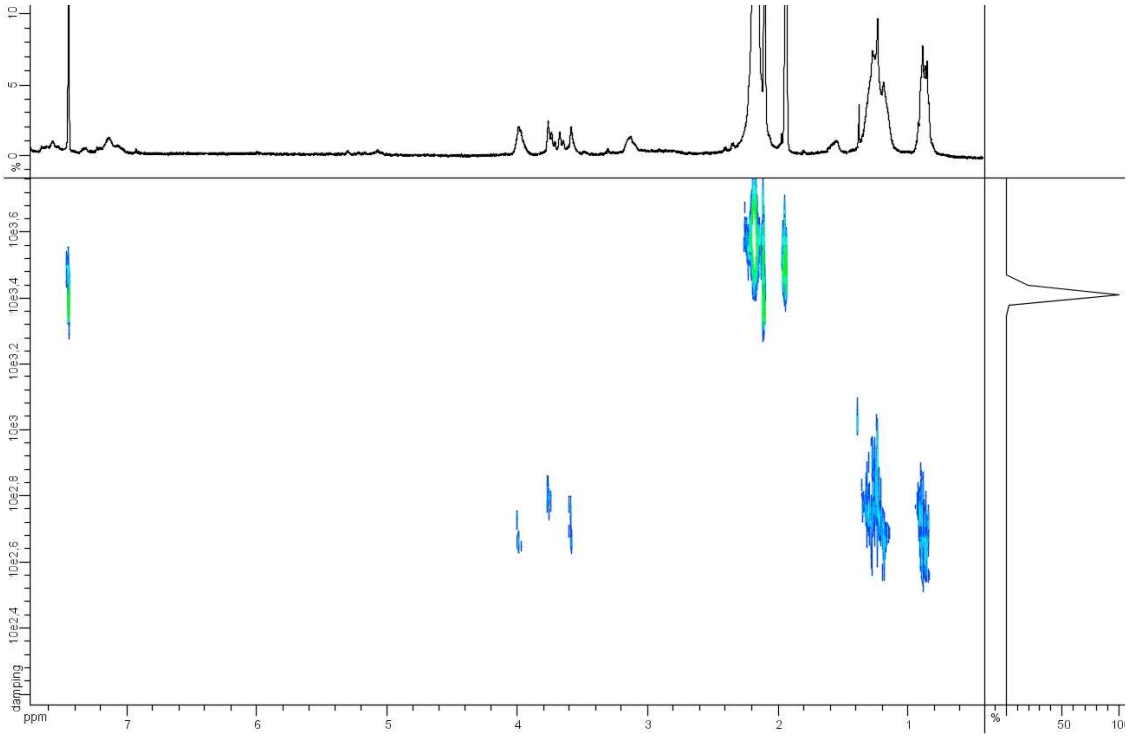

DOSY NMR of the self-assembly between **Zn.2**$_2$ and **N$_2$C$_3$'** at 50 mM in $CDCl_3$*/CD_3CN: 6/4:

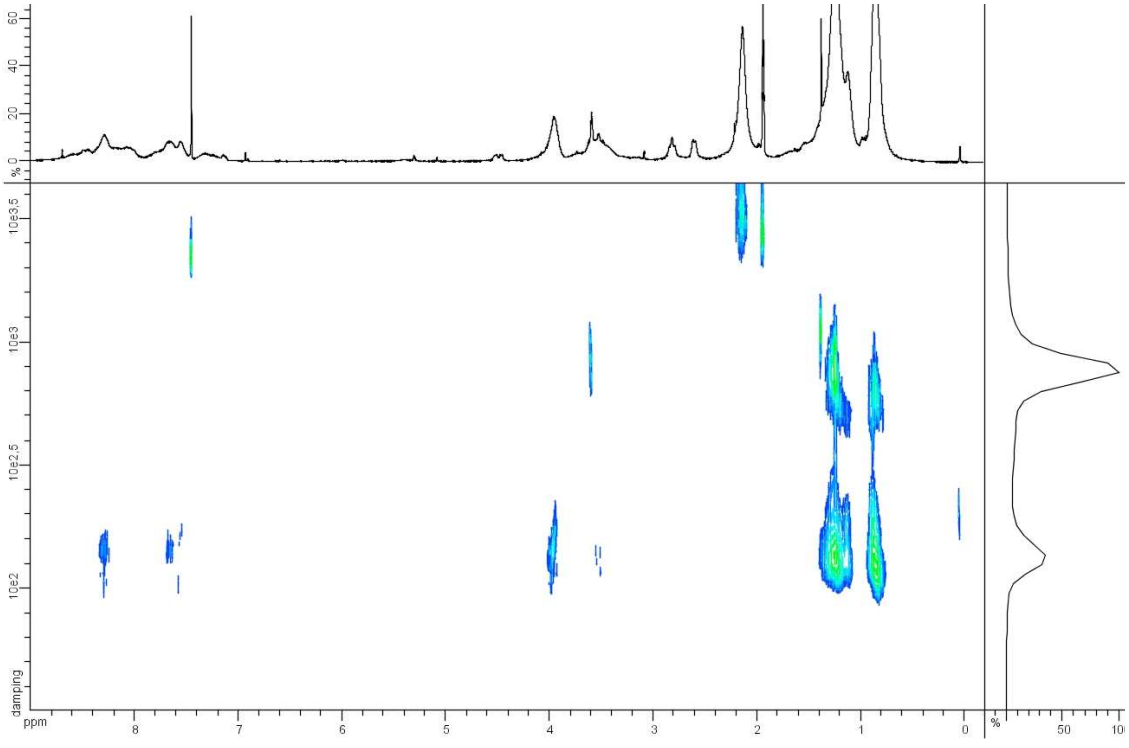

Macrocycle-macrocycle interconversion:

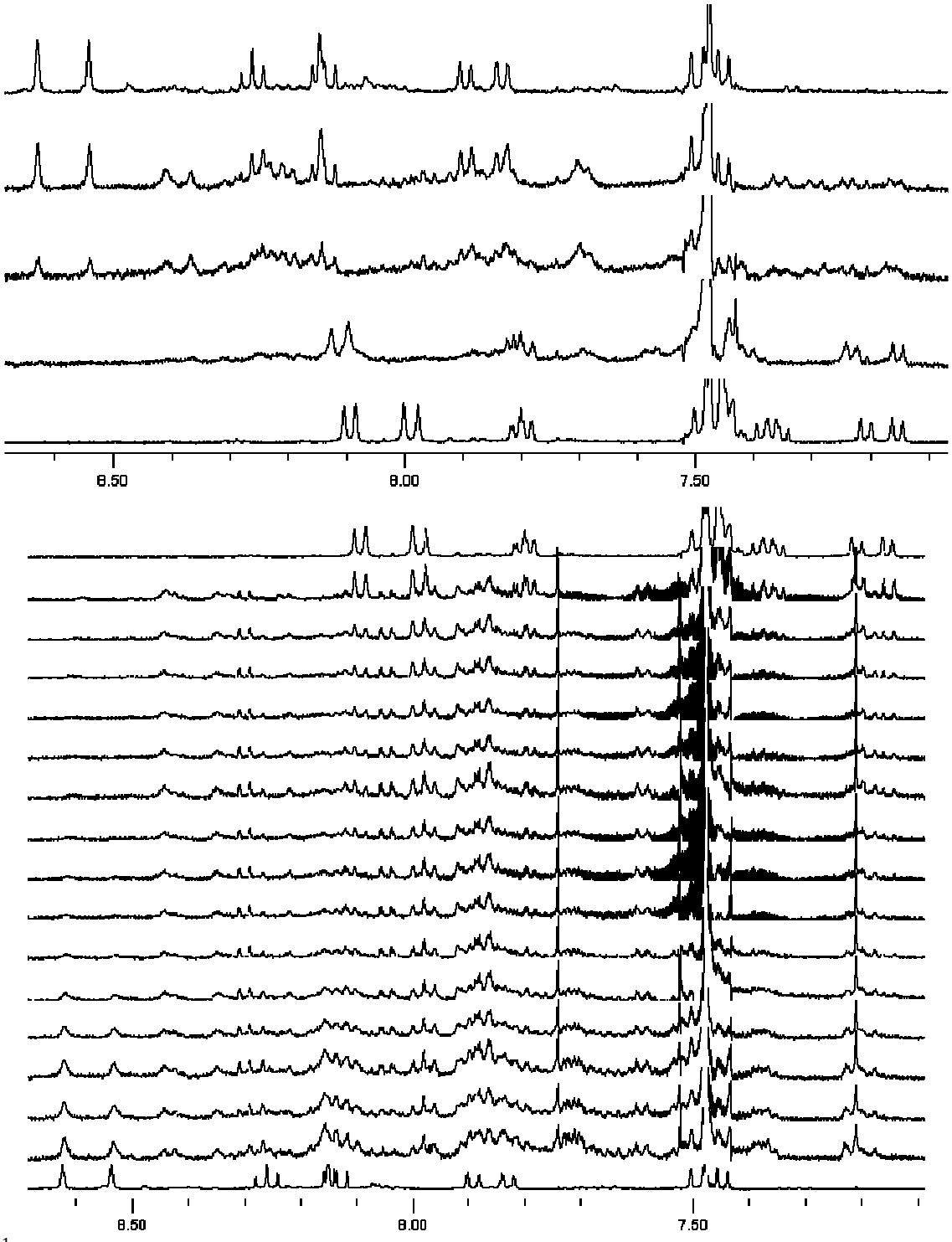

^{1}H NMR spectra showing the reversible constitutional conversion between the [2+2] macrocycle $\mathbf{1_2.(N_2O)_2}$ and the [1+1] metallo-macrocycles $\mathbf{Zn.1.N_2O}$ at 5 mM of each starting material in $CDCl_3/CD_3CN$: 6/4. Top: [2+2] macrocycle (bottom), then after addition of 0.3, 0.5, 0.7 and 1.0 equivalent of zinc triflate. NMR spectra were taken immediately after the addition ; bottom: [1+1] metallo-macrocycle (bottom), then after addition of 1.0 equivalent of hexacyclen, then a spectrum was recorded every 3 minutes, the last but one was recorded one day after the addition of hexacyclen and the last spectrum is a reference of the [2+2] macrocycle prepared from its components. Conversion is incomplete in the time frame due to the low concentration used.